Electronic Supplementary Material (ESI) for ChemComm.


# Contents

## General information

### NMR

Routine NMR spectra were recorded on a 400 MHz ($^1$H resonance frequency, Bruker AVANCE III HD, BBFO probe), 500 MHz ($^1$H resonance frequency, Bruker AVANCE III, BBFO), 600 MHz ($^1$H resonance frequency, Bruker AVANCE III, TBI) or 700 MHz ($^1$H resonance frequency, Bruker AVANCE III HD, QCI cryo probe) spectrometer.
Perfect-CLIP-HSQC-spectra[1] were recorded on a 700 MHz ($^1$H resonance frequency, Bruker AVANCE III HD, QCI cryo probe) spectrometer with a total of 8 k data point in F2 and 1 k data point in F1 (NS = 4, DS = 32). For processing the data was zero filled to 16 K points in F2 and 2 k points in F1.
Coupling constants were extracted from rows of the perfect-CLIP-HSQC-spectra. RDCs were calculated from the extracted total coupling in the anisotropic phases and the isotropic scalar coupling constants of the analyte ($^1T_{CH} = {}^1J_{CH} + 2\ {}^1D_{CH}$). The calculated $^1D_{CH}$ for methyl groups were converted to the corresponding $^1D_{CC}$ according to literature.[2] Errors for the $^1D_{CH}$ values were estimated via a literature procedure.[3] RDC data was evaluated using the software RDC@hotFCHT.[4] SECONDA[5]-based evaluation of the acquired RDC data was carried out using back-calculated RDCs ($D^{calc}$) from fit of experimental RDCs ($D^{exp}$) to the structural model of IPC using the software RDC@hotFCHT.

### Size exclusion chromatography

Chromatography was carried out with one pre-column and three main columns ($10^3$ Å, $10^5$ Å, $10^7$ Å). SEC was performed with a flow rate of 0.25 mL/min with a mobile phase of $CHCl_3$ (0.3 % tetrabutylammoniumbromid, TBAB) at 25 °C using a Jasco UV-2075 plus detector. Polymers were dissolved in $CHCl_3$ (0.5 mg/mL) with 0.1 % toluene as internal standard and a volume of 75 µL was injected. For calibration polystyrene standards were used. Thus values given in table S1 are only for comparison within this series.

### Circular dichroism spectroscopy

CD spectra were recorded on a Jasco-1500 high performance CD spectrometer with temperature unit (PTC-510). The polymers were dissolved in THF or $CDCl_3$ with a concentration of approximately 2.3 g/L and measured in 1 mm quartz glass cuvettes.

### Polarized Optical Microscopy (POM)

The optical textures of the mesophases were studied between crossed polarizers with a Nikon Eclipse LV100Pol optical polarizing microscope equipped with a Linkam LTS420 heating stage and a Linkam T95-HS system controller. The lyotropic LLC samples were prepared in square capillaries (HILGENBERG; outside: 2 ± 0.1 x 1 ± 0.1 mm; inside 1.78 ± 0.1 x 0.78 ± 0.1 mm; wall thickness: 0.11 ± 0.05 mm).

### Chemicals

Solvents and reagents were obtained from commercial sources and used without further purification unless indicated otherwise.

### Polymerization

The syntheses of the polymers were performed under argon atmosphere with flame dried glassware. $THF_{abs.}$ was degassed via the freeze-pump-thaw procedure before dissolving the NCA monomer **11** with a concentration of 0.1 M in $THF_{abs}$ in a glovebox under argon atmosphere. The corresponding amount of DMEA/TEA (DMEA M:I 400:1; TEA 10 µL) was added quickly and the suspension was stirred at room temperature for several days. Polymerization progress was monitored via IR-spectroscopy (characteristic band of NCA at around 1800 $cm^{-1}$ decreases). The resulting polymer solution was added dropwise to acidic MeOH (1 % conc. HCl) and stirred for 30 minutes. The precipitate was filtrated, washed with MeOH and dried in high vacuum. After dissolving the dry polymer in $CHCl_3$ the resulting solution was added dropwise to *n*-hexane. Again, the precipitated polymer was filtrated and dried in high vacuum.[6]

**IR-data:** An exemplary set of IR-spectra used for monitoring the polymerization progression is displayed in Figure S1 (recorded on a BRUKER ALPHA IR with Platinum-ATR unit).

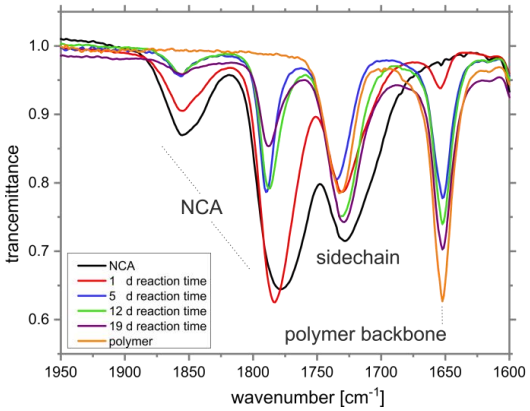


**Figure S1.** Exemplary IR-spectra obtained for monitoring the progress of the polymerization of the corresponding NCA (leading to the polymer $PBPM^3LG$ [DS-PG-11]) with DMEA in THF at 25 °C under argon atmosphere (glovebox).

**LLC phases**

**Preparation:** All LLC phases were prepared directly in 5 mm NMR-tubes. The corresponding polymer, analyte and capillary for locking purposes were weighed into the NMR tube and the solvent was added. The LLC phase was homogenized with a centrifuge or just by turning the tube. All phases contained a flame sealed capillary with deuterated solvent for locking (acetone-$d_6$ for $CDCl_3$-based phases; TCE-$d_2$ for THF-$d_8$-based phases; DMSO-$d_6$ for TCE-$d_2$-based phases).

## List of Samples

A list of the LLC phases used in this manuscript is displayed in Table S1. Only one batch of TEA- and DMEA-initiated polymers was synthesized. For characterization of the polymers see syntheses part. Thus all samples containing TEA-initiated polymer, contain the same batch of polymer with the same polymer properties.

**Table S1.** LLC phases prepared and investigated for this study.

| Name | Solvent | Initiator | IPC | c(Polymer) [w%] |
|---|---|---|---|---|
| DS-P74 | $CDCl_3$ | TEA | none | 14.8 |
| DS-P74a | $CDCl_3$ | TEA | (-) | 14.8 |
| DS-P75 | $CDCl_3$ | TEA | (+) | 14.8 |
| DS-P76 | THF-$d_8$ | TEA | (-) | 27.8 |
| DS-P77 | THF-$d_8$ | TEA | (+) | 27.8 |
| DS-P78 | TCE-$d_2$ | DMEA | none | 14.8 |

The critical concentration of the TEA-initiated polymer is ~13 w% in $CDCl_3$ and ~25 w% in THF-$d_8$. Those critical concentrations are higher than that of the parent polymer without restricted rotation Poly-γ-*p*-biphenylmethyl-L-glutamate (PBPMLG)[6-7] and the polymers containing spacer groups poly-γ-*p*-biphenylethoxy-L-glutamate (PBPELG) and poly-γ-*p*-biphenylhexoxy-L-glutamate (PBPHLG)[8] of our previous investigations. Shorter polymer chains are obtained for $PBPM^3LG$ than for the aforementioned polymers. Due to the critical concentrations being a function of polymer chain length, this behavior is expected.[9]

## LLC phases

$^{2}$H NMR spectra, $^{13}$C NMR spectra and perfect-CLIP-HSQC spectra[1] have been acquired for samples shown above at different temperatures. In this section the NMR spectra are plotted and discussed.

**PBPM$^{3}$LG in Chloroform**

Figure S2 shows $^{2}$H NMR spectra of a PBPM$^{3}$LG/$CDCl_3$ (14.8 w%) LLC phase without analyte. Figure S3 shows the corresponding zoom of the $CDCl_3$ signals.

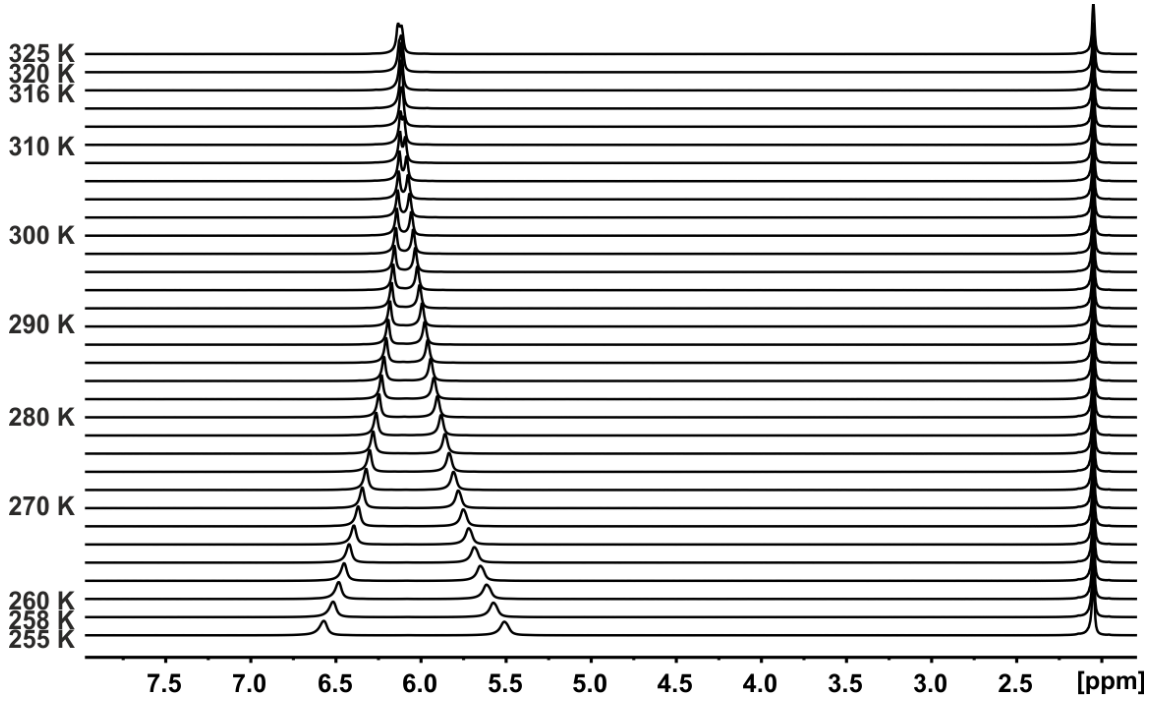


**Figure S2.** Temperature dependent $^{2}$H NMR spectra (107 MHz $^{2}$H-frequency) of a PBPM$^{3}$LG/$CDCl_3$ (14.8 w%). An acetone-$d_6$ capillary has been added for locking purposes. **[DS-P74]**

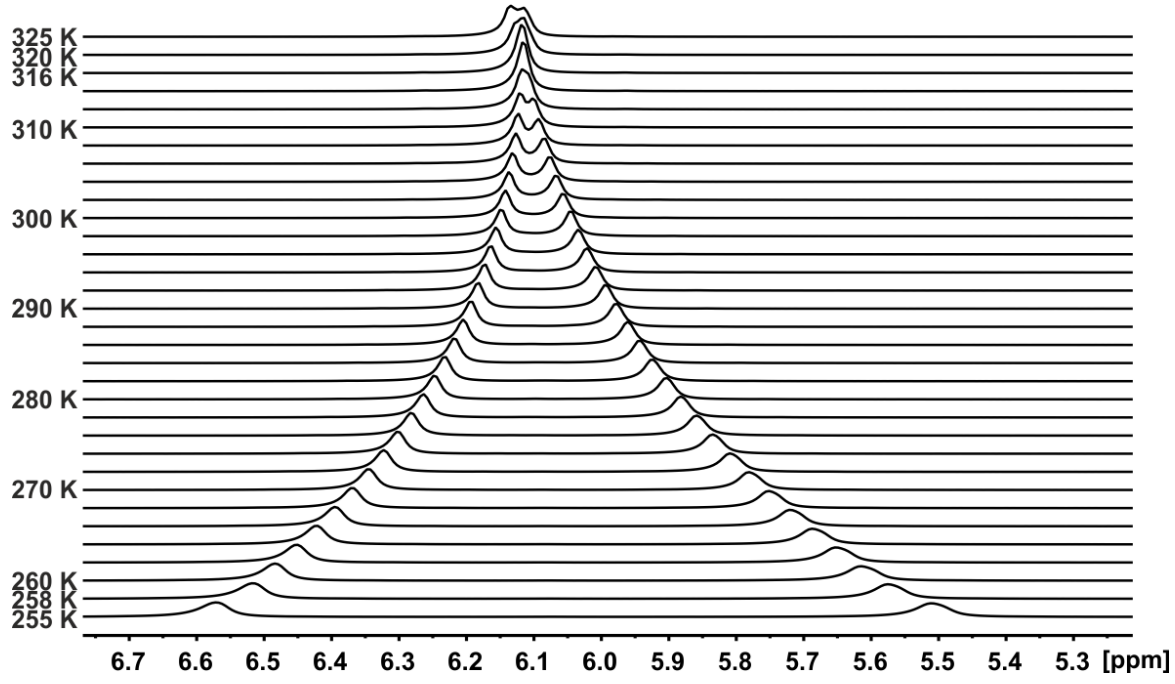


**Figure S3.** Section of temperature dependent $^{2}$H NMR spectra (107 MHz $^{2}$H-frequency) of a PBPM$^{3}$LG/$CDCl_3$ (14.8 w%). **[DS-P74]**

A temperature dependent change in quadrupolar splitting is observed. With lower temperature, the quadrupolar splitting becomes larger and the corresponding signals become broader. No *sudden* thermoresponsive change, comparable to the parent polymer PBPMLG, could be observed. Furthermore, the quadrupolar splitting does not follow a linear trend, as would be expected for a mere temperature dependent scaling.[10a, 6, 10b, 7] A zero-crossing of the quadrupolar splitting is visible at ~315 K. As RDCs at this temperature are non-zero in the corresponding samples with analyte ([DS-P74a] and [DS-P75]), isotropic conditions as reason for the zero-crossing of the quadrupolar splitting are ruled out. Thus, we interpret this as the result of the angle of the C-D-bond with respect to the external magnetic field crossing the magic angle (54.74°).

Figure S4 shows $^{13}$C NMR spectra of a PBPM$^3$LG/$CDCl_3$ (14.8 w%) LLC phase without analyte.

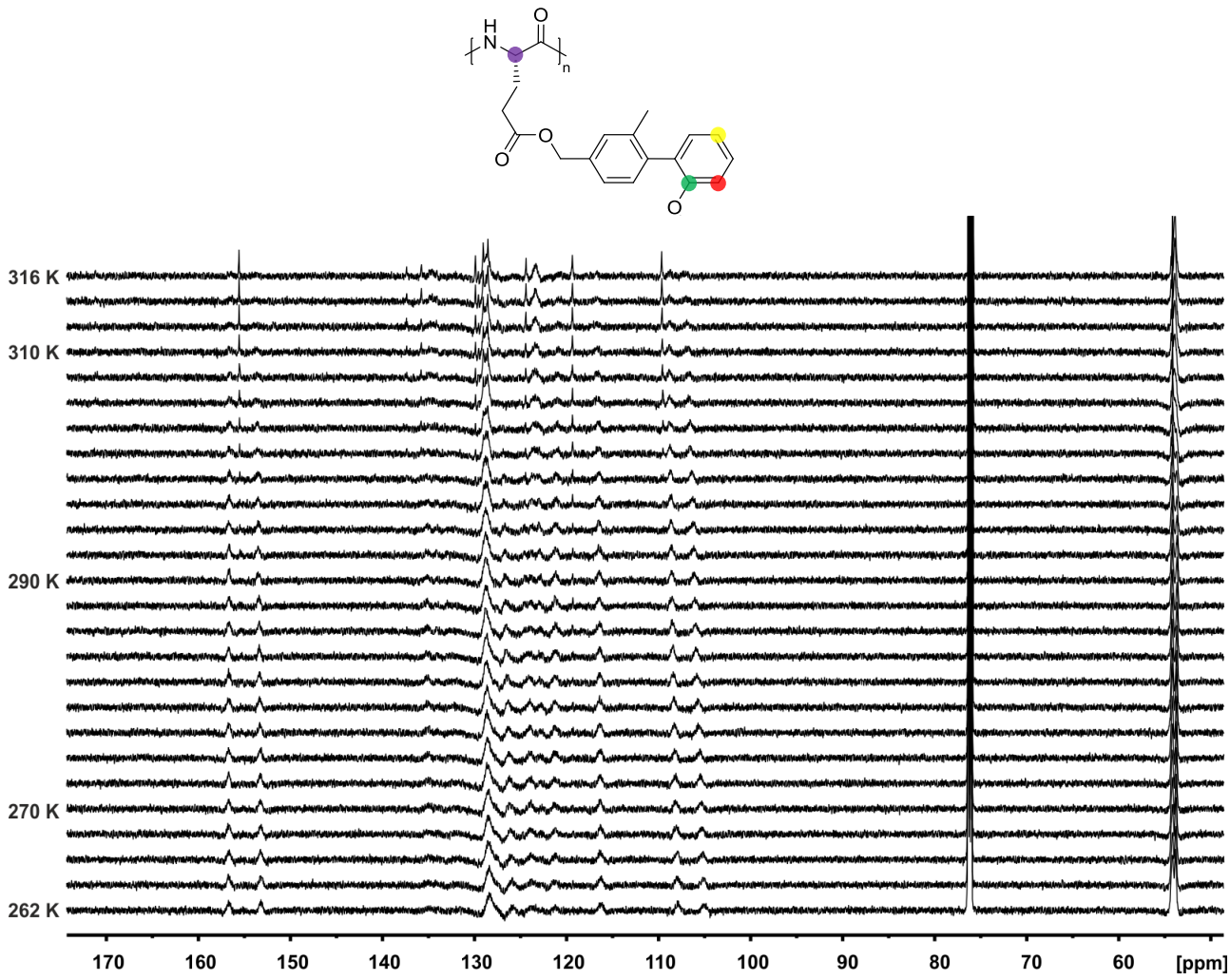


**Figure S4.** Temperature dependent $^{13}$C NMR spectra (176 MHz $^{13}$C-frequency) of a PBPM$^3$LG/$CDCl_3$ (14.8 w%) LLC phase with color coded signal assignment of characteristic $^{13}$C-atoms in PBPM$^3$LG. An acetone-$d_6$ capillary has been added for locking purposes (not shown). **[DS-P74]**

Figure S5 shows sections of the characteristic $^{13}$C NMR spectra.

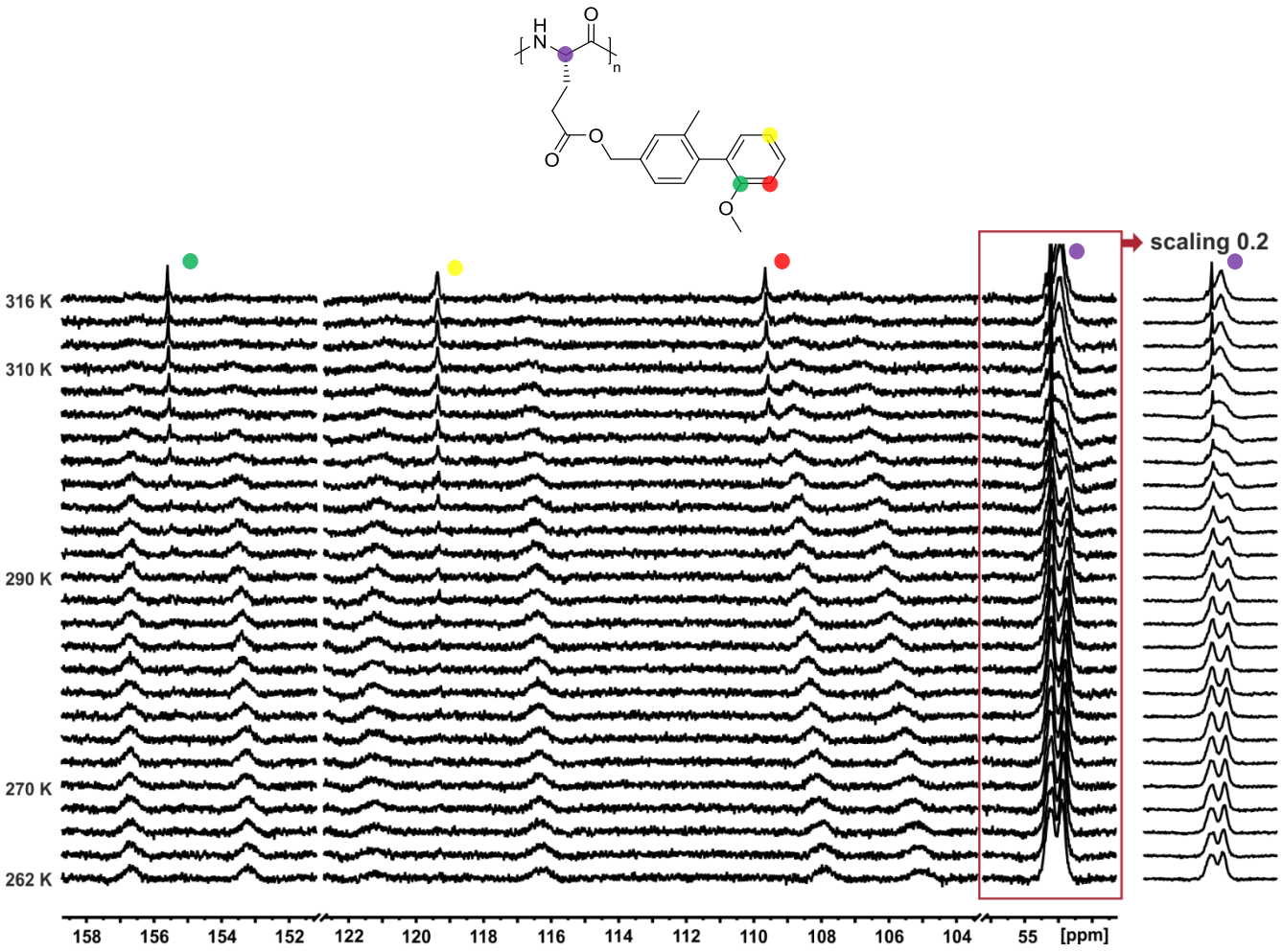


**Figure S5.** Sections of temperature dependent $^{13}$C NMR spectra (176 MHz $^{13}$C-frequency) of a PBPM$^{3}$LG/$CDCl_3$ (14.8 w%). Characteristic $^{13}$C-atoms in PBPM$^{3}$LG are color coded. An acetone-$d_6$ capillary has been added for locking purposes (not shown). **[DS-P74]**

The LLC phase was heated to 316 K for 1 hour prior to the NMR measurements, which have been conducted from 316 to 262 K via cooling the sample. As can be seen, two sets of signals are observed below 316 K. Due to the chirality of the backbone, diastereomeric polymers are obtained when rations is restricted (atropisomerism) leading to two signal sets. The $^{13}$C NMR signals thus confirm the presence of a temperature induced decrease of free rotation of the biphenyl axis below 316 K, which potentially translates into a thermoresponsive change in induced alignment.

Figure S6 shows temperature dependent $^{2}H$ NMR spectra of PBPM$^{3}$LG/$CDCl_3$ (14.8 w%) LLC phases with (+)-IPC and (-)-IPC as analytes and the corresponding RDCs.

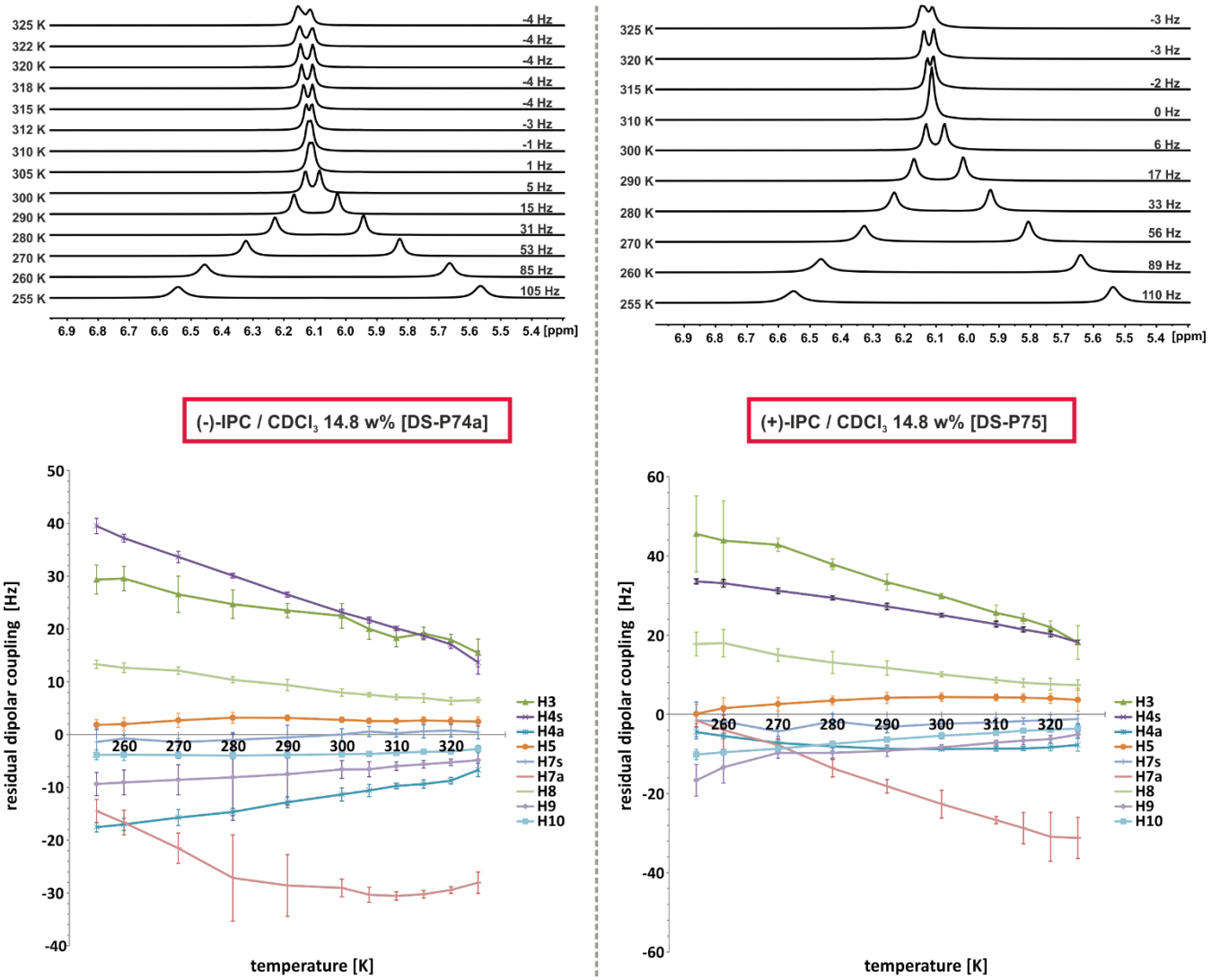


**Figure S6.** Temperature dependent $^{2}H$ NMR spectra (107 MHz $^{2}H$-frequency) and corresponding RDCs of (+) and (-)-IPC, respectively, in a PBPM$^{3}$LG/$CDCl_3$ LLC phase (14.8 w%).

The quadrupolar splitting (Figure S2, S3, S6) of the corresponding PBPM$^{3}$LG/$CDCl_3$ LLC phase crosses 0 Hz at approx. 310 K. The sign of the quadrupolar splittings has been determined via Q.E.COSY[11] NMR spectra (see corresponding section). At this zero-crossing, the LLC phase is not isotropic, as can be seen from the RDCs extracted (RDCs $\neq$ 0). We interpret this finding as a change in orientation of the C-D bond with respect to the external magnetic field of $CDCl_3$ crossing the magic angle. Furthermore, the temperature dependent change observed in quadrupolar splitting is not linear (Figure S7). These results show no deviation from the sample without analyte [DS-P74].

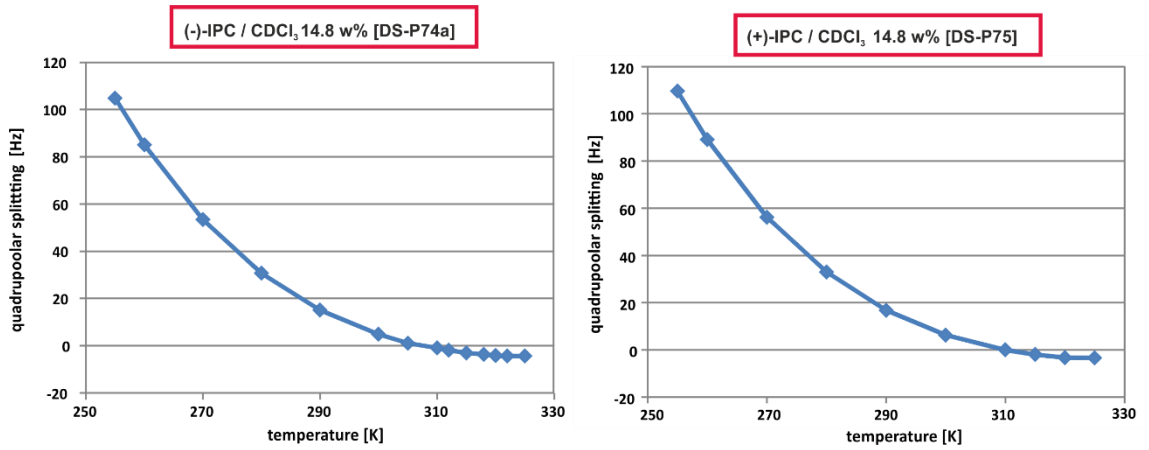


**Figure S7.** Plotted quadrupolar splitting from temperature dependent $^{2}$H NMR spectra of a PBPM$^{3}$LG/$CDCl_3$ LLC phase (14.8 w%) with (+)- and (-)-IPC, respectively.

Figure S8 shows temperature dependent $^{13}$C NMR spectra of a PBPM$^{3}$LG/$CDCl_3$ (14.8 w%) LLC phase with (+)-IPC.

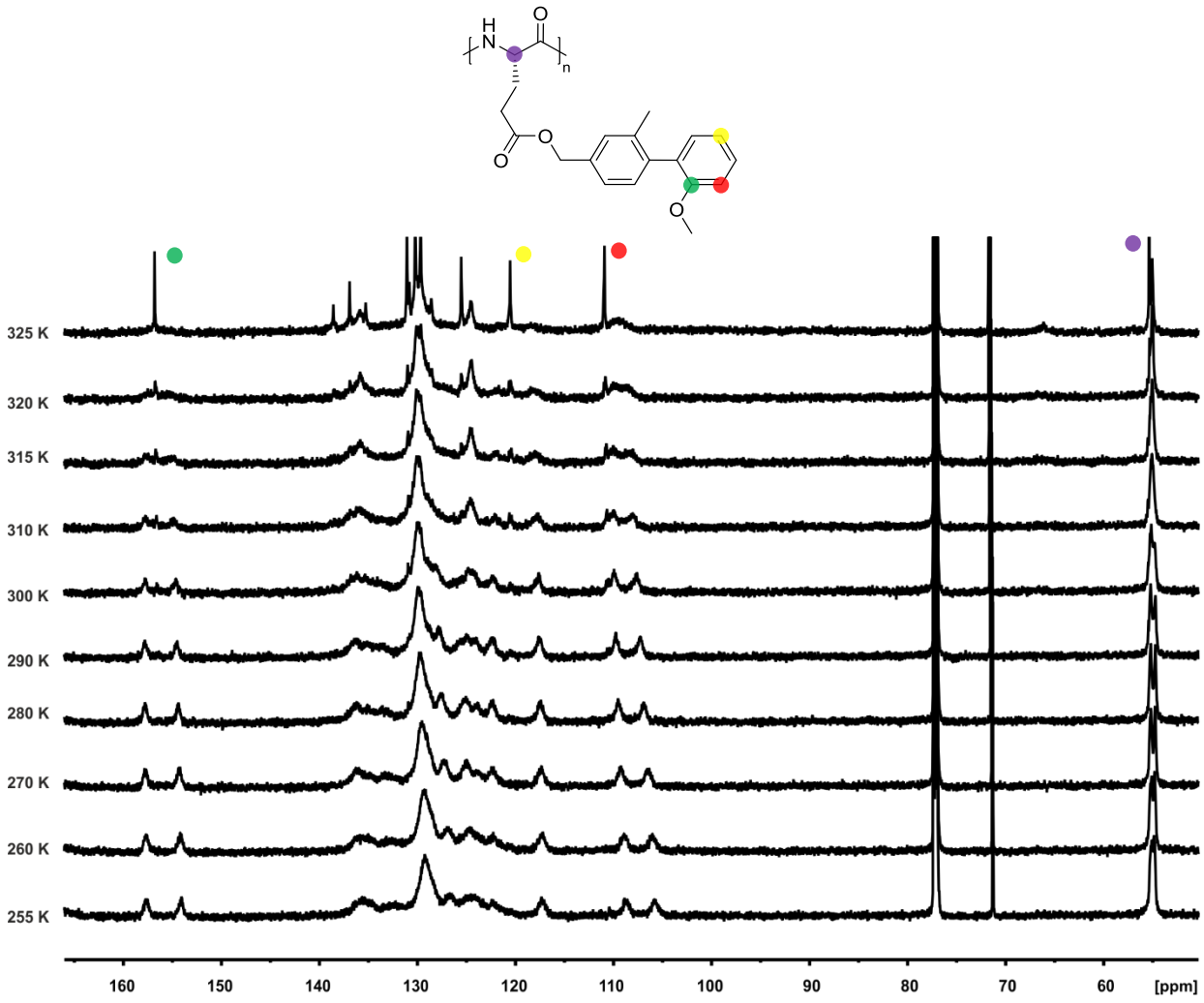


**Figure S8.** Temperature dependent $^{13}$C NMR spectra (176 MHz $^{13}$C-frequency) of a PBPM$^{3}$LG/$CDCl_3$ (14.8 w%) LLC phase with (+)-IPC as analyte with color coded signal assignment of characteristic $^{13}$C-atoms in PBPM$^{3}$LG. An acetone-$d_6$ capillary has been added for locking purposes (not shown). **[DS-P75]**

Figure S9 shows sections of the characteristic $^{13}$C NMR spectra.

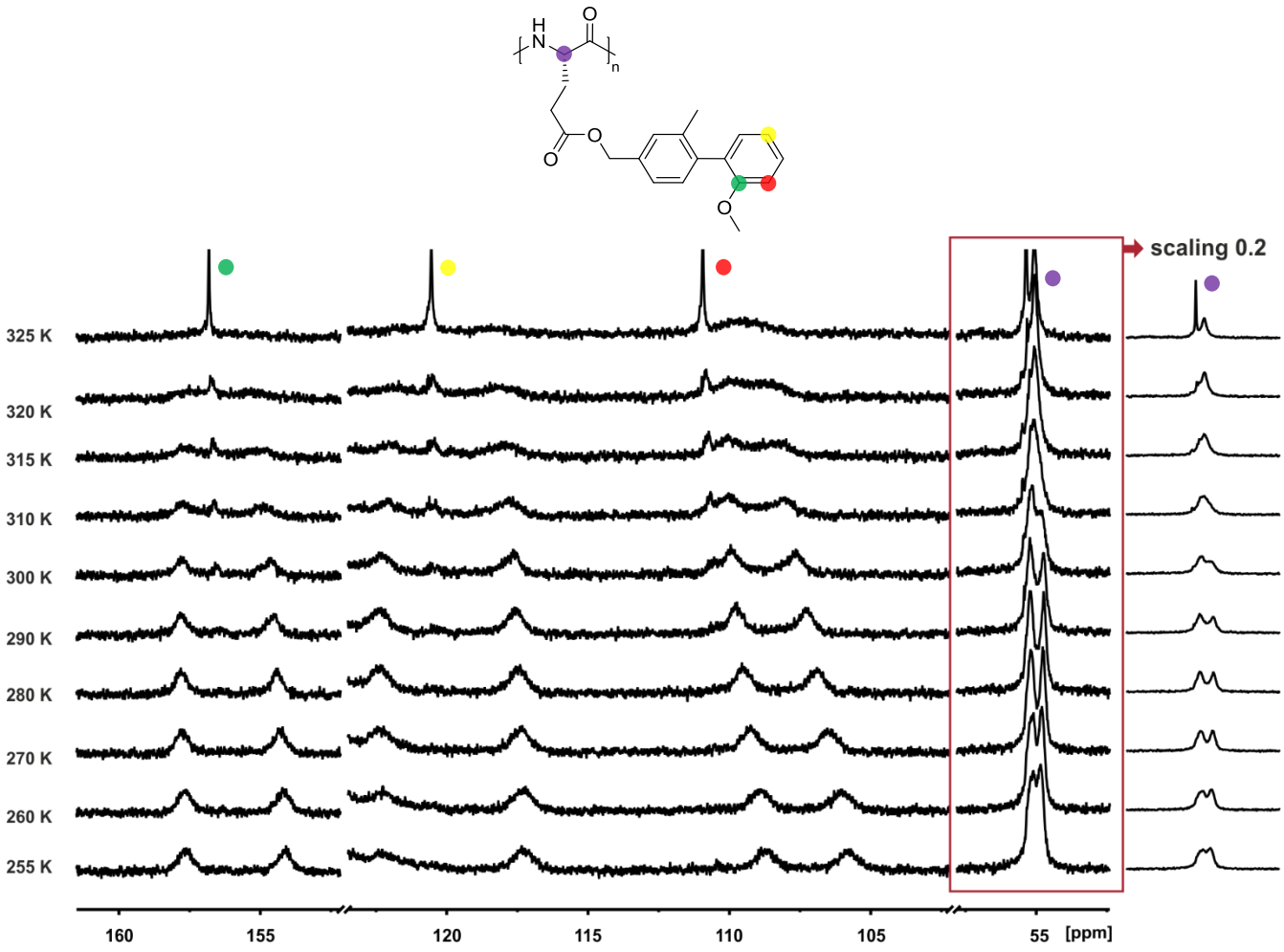


**Figure S9.** Sections of temperature dependent $^{13}$C NMR spectra (176 MHz $^{13}$C-frequency) of a PBPM$^3$LG/$CDCl_3$ (14.8 w%) LLC phase with (+)-IPC as analyte. Characteristic $^{13}$C-atoms in PBPM$^3$LG are color coded. An acetone-$d_6$ capillary has been added for locking purposes (not shown). **[DS-P75]**

The thermoresponsive restriction of the biphenyl rotation axis in the sample with (+)-IPC as analyte occurs at a similar temperature as for that without analyte (Figure S4 and S5). $^{13}$C NMR signals obtained in the region of restricted biphenyl rotation show 'similar' intensities. The chiral $\alpha$-helix does therefore not lead to the formation of a preferred rotamer; also confirmed by the CD-spectra.

**PBPM$^3$LG in THF**

Figure S10 shows temperature dependent $^2$H NMR spectra of a PBPM$^3$LG/THF-$d_8$ (27.8 w%) LLC phase with (-)-IPC as analyte.

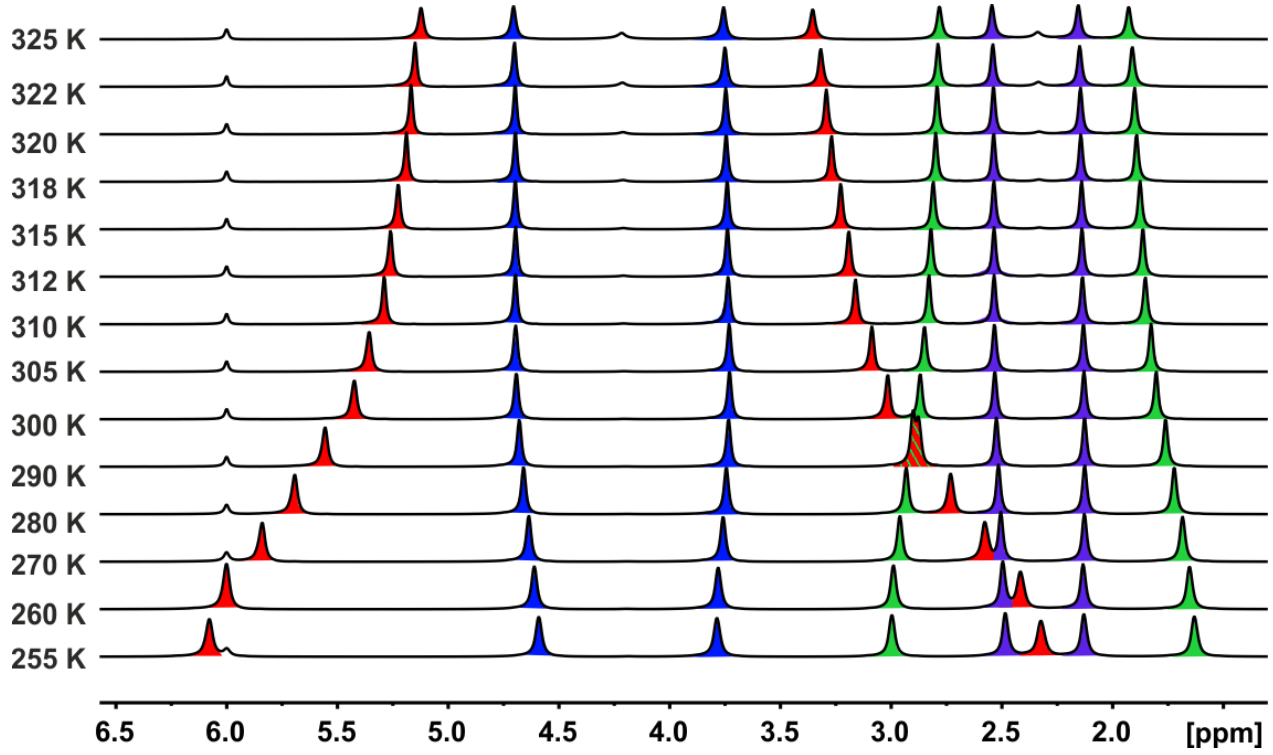


**Figure S10.** Temperature dependent $^2$H NMR spectra (107 MHz $^2$H-frequency) of a PBPM$^3$LG/THF-$d_8$ LLC phase with (-)-IPC (27.8 w%), color-coded for better visualization of the corresponding THF-$d_8$ signals. A TCE-$d_2$ capillary has been added for locking purposes. **[DS-P76]**

The quadrupolar splittings of the corresponding PBPM$^3$LG/THF-$d_8$ LLC phase also show a thermoresponsive change. Linear behavior is observed from 325 to ~310 K and nonlinear behavior below ~310 K. No zero-crossing, comparable to that in $CDCl_3$ (Figure S2, S3, S6) is observable. Small isotropic signals can be observed at higher temperatures.
Figure S11 shows temperature dependent $^{13}$C NMR spectra of a PBPM$^3$LG/THF-$d_8$ (27.8 w%) LLC phase with (-)-IPC.

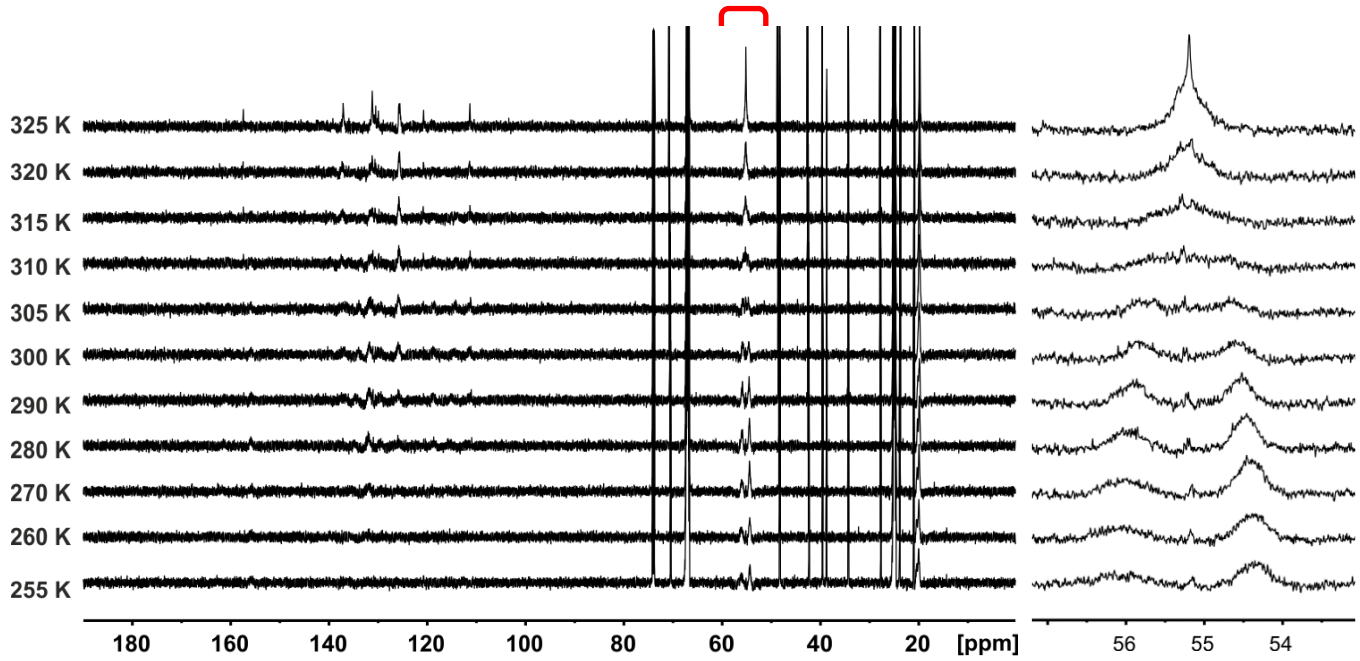


**Figure S11.** Temperature dependent $^{13}$C NMR spectra (176 MHz $^{13}$C-frequency) of a PBPM$^3$LG/THF-$d_8$ (27.8 w%) LLC phase. **Left**: Temperature dependent $^{13}$C NMR spectra. **Right:** Section of the $^{13}$C NMR signal of the α-C-atom (red box). A TCE-$d_2$ capillary has been added for locking purposes. **[DS-P76]**

A thermoresponsive restriction of the biphenyl rotation is visible (atropisomerism) in THF-$d_8$ as well and occurs in the same temperature region as in $CDCl_3$ (320 K to 290 K). $^{13}C$ NMR signals in the biphenyl region are broader compared to $CDCl_3$. Thus the restricted biphenyl rotation can only be verified in the $\alpha$-carbon in the polymer backbone.

Figure S12 shows temperature dependent $^2H$ NMR spectra of a PBPM$^3$LG/THF-$d_8$ (27.8 w%) LLC phases with (+)-IPC and (-)-IPC as analytes and the corresponding RDCs.

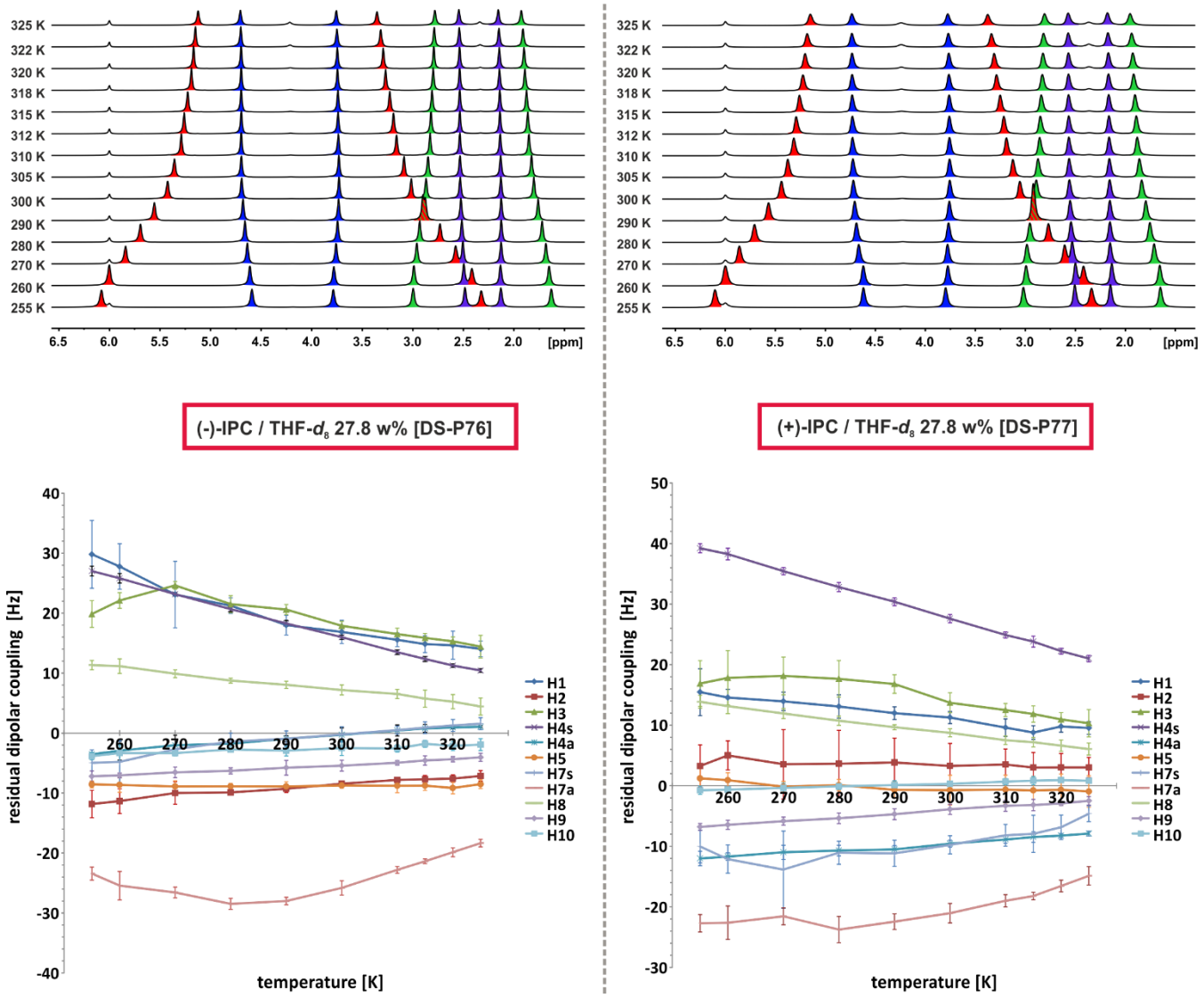


**Figure S12.** Temperature dependent $^2H$ NMR spectra (107 MHz $^2H$-frequency) and corresponding RDCs of (+) and (-)-IPC, respectively, in a PBPM$^3$LG/THF-$d_8$ LLC phase (27.8 w%).

The $^2H$ NMR signals of THF-$d_8$ are identical in both LLC phases with (+)-IPC and (-)-IPC. No *sudden* thermoresponsive change of the quadrupolar splitting nor the RDCs, comparable to that of the parent polymer PBPMLG[6-7], is observable. This is in contrast to our recent findings in PBPMLG and its derivates PBPHLG and PBPELG[8], where we observed sudden gelation of the LLC phase, leading to significant signal broadening in $^2H$ and $^{13}C$ NMR spectra and visible changes to the LLC phase. One might speculate that the conformation exhibited by the biphenyl side chain in PBPM$^3$LG inhibits gelation to some extent.

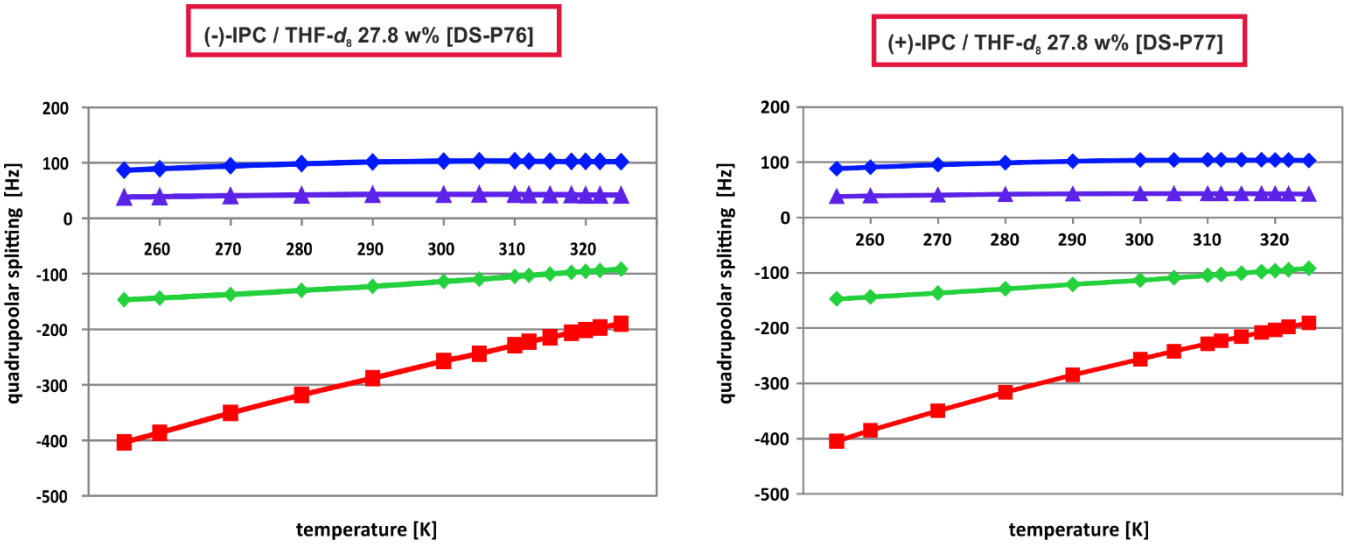


**Figure S13.** Plotted quadrupolar splitting from temperature dependent $^2$H NMR spectra of a PBPM$^3$LG/THF-$d_8$ LLC phase (27.8 w%) with (+) and (-)-IPC, respectively. The quadrupolar splitting are color coded corresponding to the $^2$H NMR spectra in Figure S9.

The signs of the quadrupolar splittings were determined via Q.E.COSY[11] NMR spectra (see corresponding section).

**PBPM$^3$LG in TCE**

Investigations into the behavior of PBPM$^3$LG in TCE-$d_2$ have been conducted to additionally screen the temperature region above 325 K, not accessible with THF-$d_8$ or $CDCl_3$. Figure S14 shows $^2$H NMR spectra of a PBPMLG/TCE-$d_2$ (14.8 w%) LLC phase.

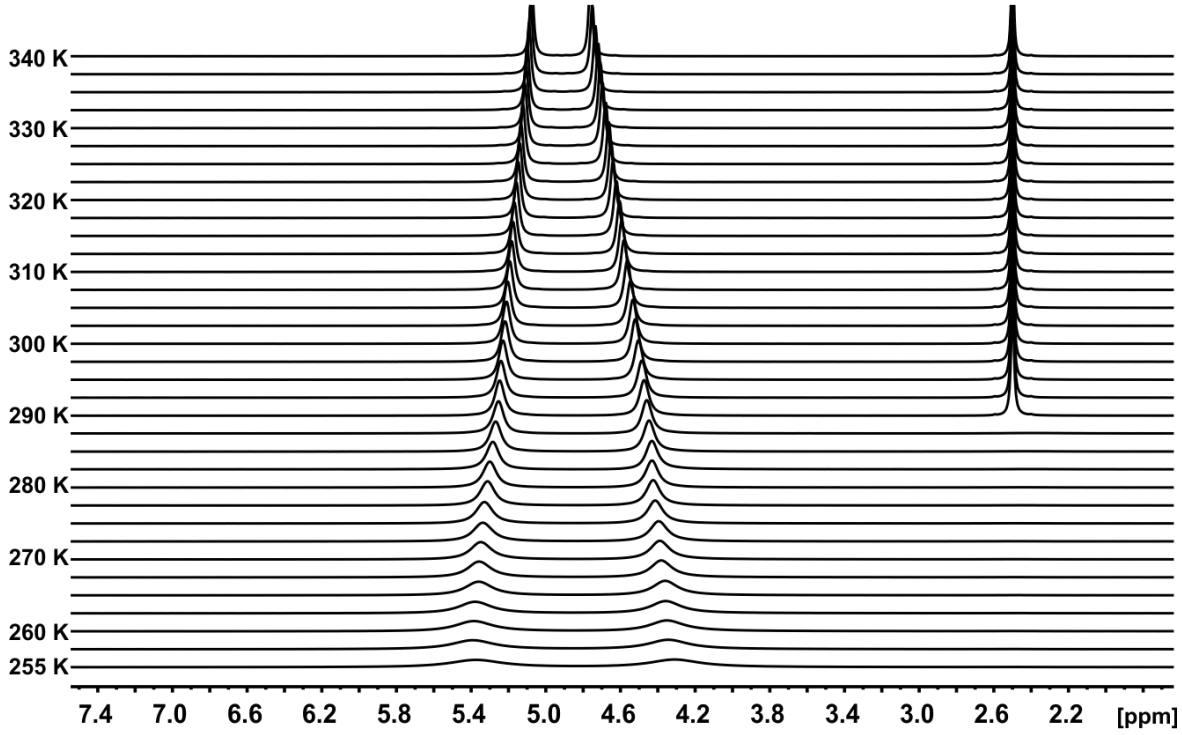


**Figure S14.** Temperature dependent $^2$H NMR spectra (107 MHz $^2$H-frequency) of a PBPM$^3$LG/TCE-$d_2$ LLC phase (14.8 w%) without analyte. A DMSO-$d_6$ capillary has been added for locking purposes, the signal of which was no longer observable at temperatures below 290 K. **[DS-P78]**

No significant change in quadrupolar splittings are observed, other than a temperature dependent change, as would be expected. Signal broadening is visible at lower temperatures, caused by the loss of the lock signal of DMSO-$d_6$. Figure S15 shows the corresponding section of the TCE-$d_2$ signals.

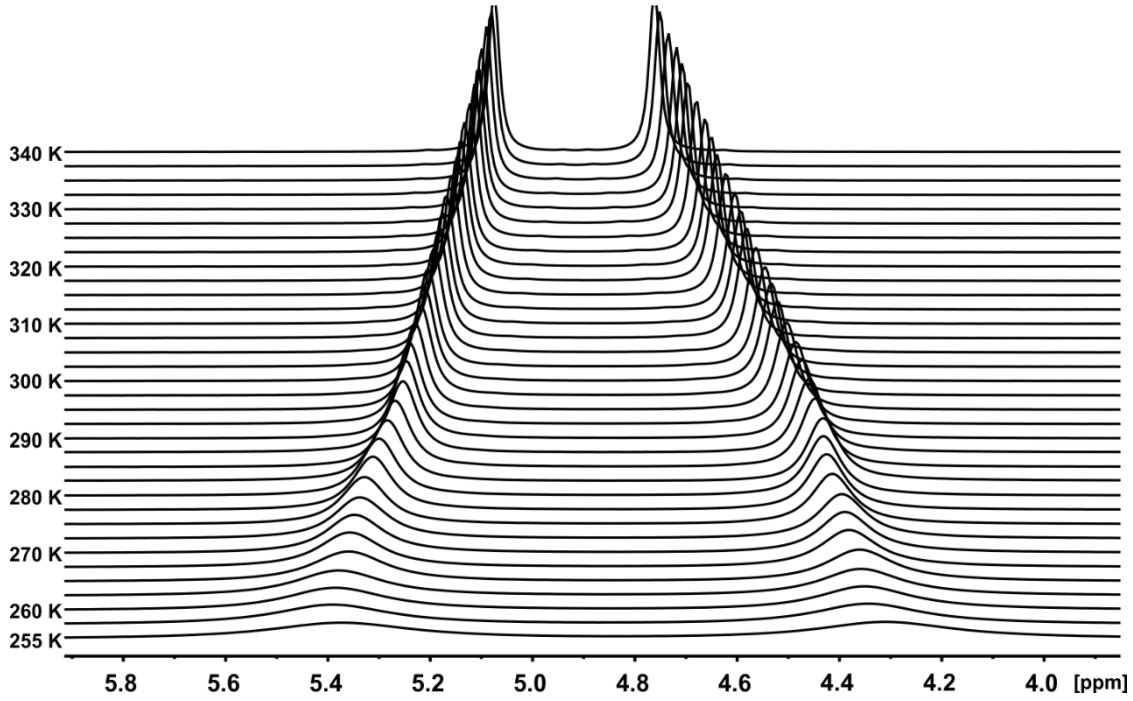


**Figure S15.** Section of the temperature dependent $^2$H NMR spectra (107 MHz $^2$H-frequency) of a PBPM$^3$LG/TCE-$d_2$ LLC phase (14.8 w%) without analyte. **[DS-P78]**

For other polymers (PBLG[12], PBLA[10b], PBPMLG[6]) one would expect a certain increase of quadrupolar splitting with decreasing temperature. This is also observed here. No additional significant change, which would indicate thermoresponsivity, was observed here.

Figure S16 shows temperature dependent $^{13}$C NMR spectra of a PBPM$^3$LG/TCE-$d_2$ (14.8 w%) LLC phase without analyte.

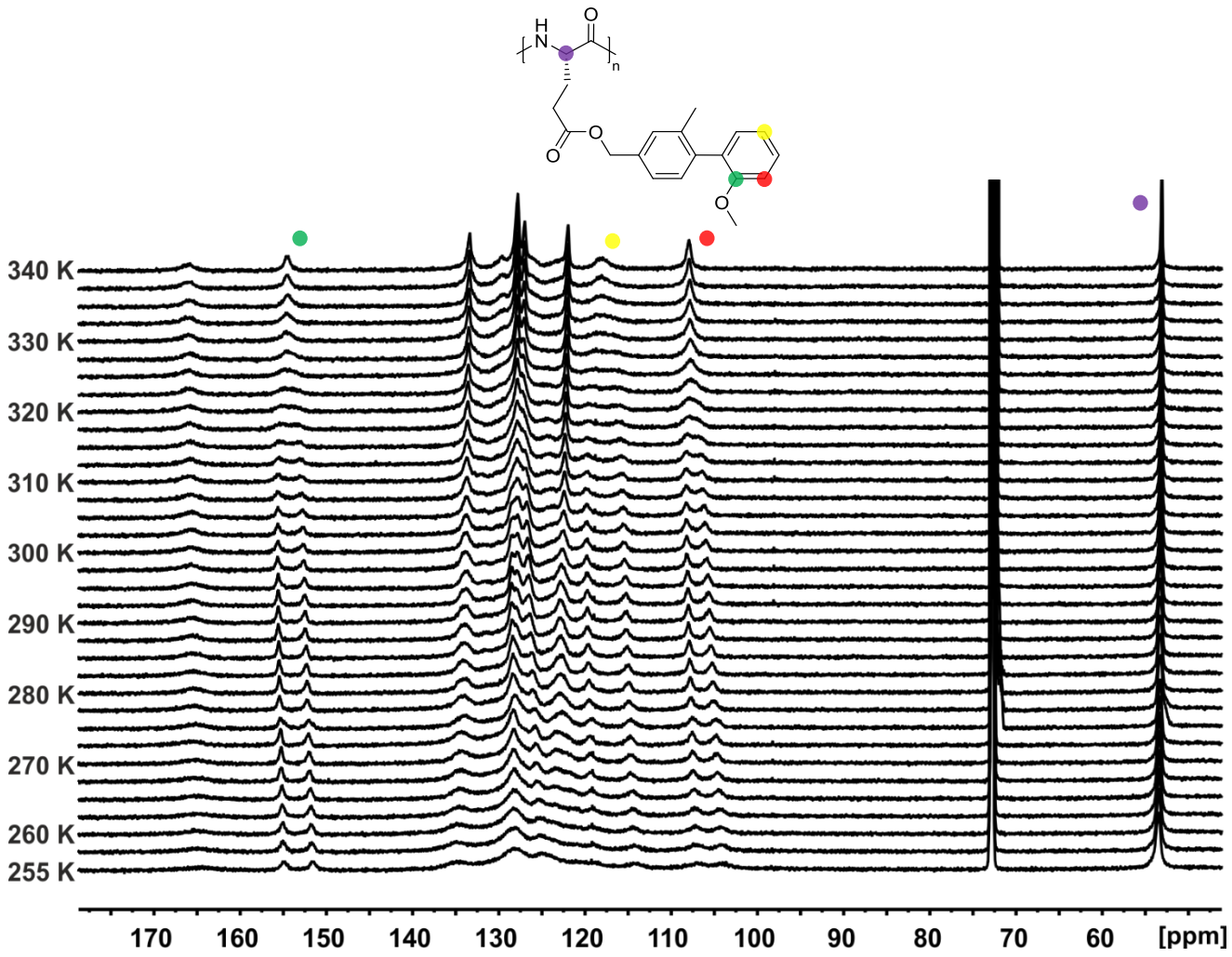


**Figure S16.** Temperature dependent $^{13}$C NMR spectra (176 MHz $^{13}$C-frequency) of a PBPM$^3$LG/TCE-$d_2$ (14.8 w%) LLC phase without analyte with color coded signal assignment of characteristic $^{13}$C-atoms in PBPM$^3$LG. An acetone-$d_6$ capillary has been added for locking purposes (not shown). **[DS-P78]**

Figure S17 shows the correspondent sections of the characteristic $^{13}$C-signals.

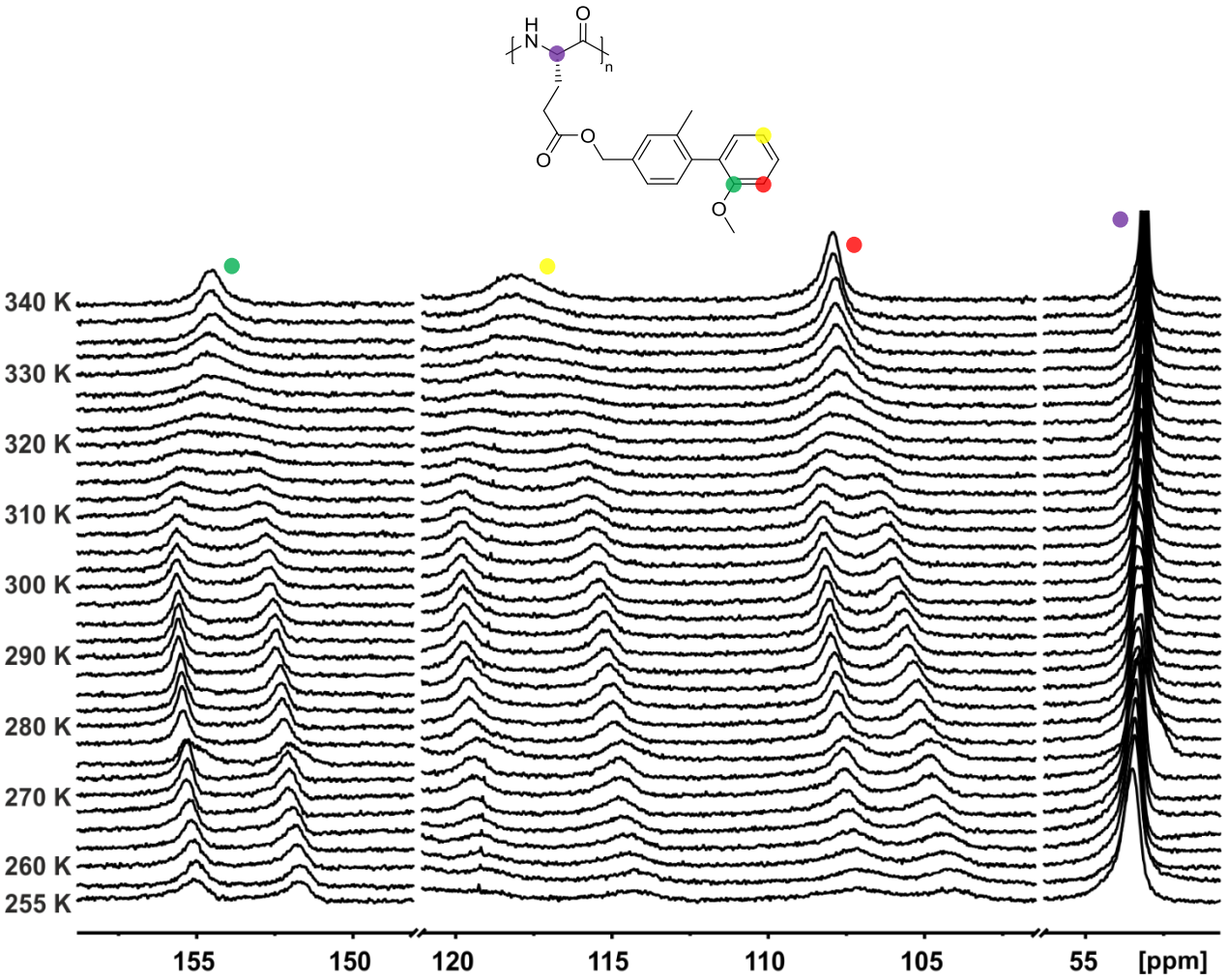


**Figure S17.** Sections of temperature dependent $^{13}$C NMR spectra (176 MHz $^{13}$C-frequency) of a PBPM$^3$LG/TCE-$d_2$ (14.8 w%) without analyte. Characteristic $^{13}$C-atoms in PBPM$^3$LG are color coded. An acetone-$d_6$ capillary has been added for locking purposes (not shown). **[DS-P75]**

Thermoresponsive restriction of the biphenyl rotation is also observed in TCE-$d_2$. No significant changes are observed below 290 K. Thermoresponsive restriction of the biphenyl rotation occurs in the same temperature region as in $CDCl_3$ and THF-$d_8$ (~320 K - 290 K). $^{13}$C NMR signals obtained in the region of restricted biphenyl rotation show 'similar' intensities. The chiral $\alpha$-helix does therefore not lead to the formation of a preferred rotamer; also confirmed by the CD-spectra.

**Q.E.COSY-spectra**

Sign determination of various quadrupolar couplings has been carried out using Q.E.COSY spectra.[11] Sign determination for various quadrupolar couplings at corresponding temperatures of a PBPM$^3$LG/CDCl$_3$ LLC phase with (-)-IPC **[DS-P74a]** is shown exemplary in Figure S18.

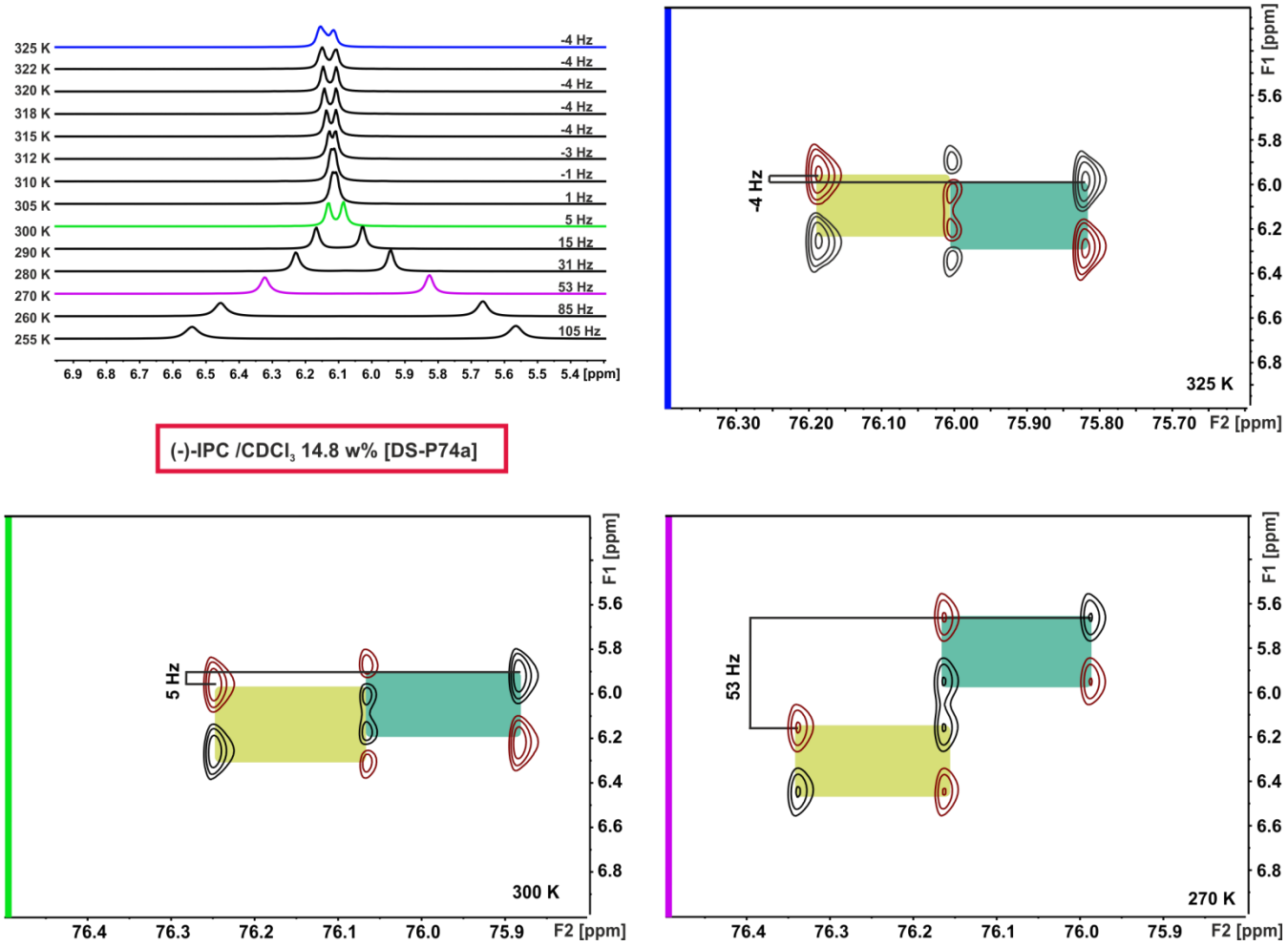


**Figure S18. Top left:** $^2$H NMR spectra (107 MHz $^2$H-frequency) of a PBPM$^3$LG/CDCl$_3$ LLC phase (14.8 w%) with (-)-IPC at various temperatures with the corresponding quadrupolar splittings $\Delta\nu_Q$. **Top right and bottom:** Q.E.COSY-spectra at 325 (blue), 300 (green) and 270 K (violet) for the sign determination; F2 corresponds to the $^{13}$C-frequency and F1 to $^2$H-frequency (107 MHz $^2$H-frequency, 176 MHz $^{13}$C-frequency). **[DS-P74a]**

## CD spectra

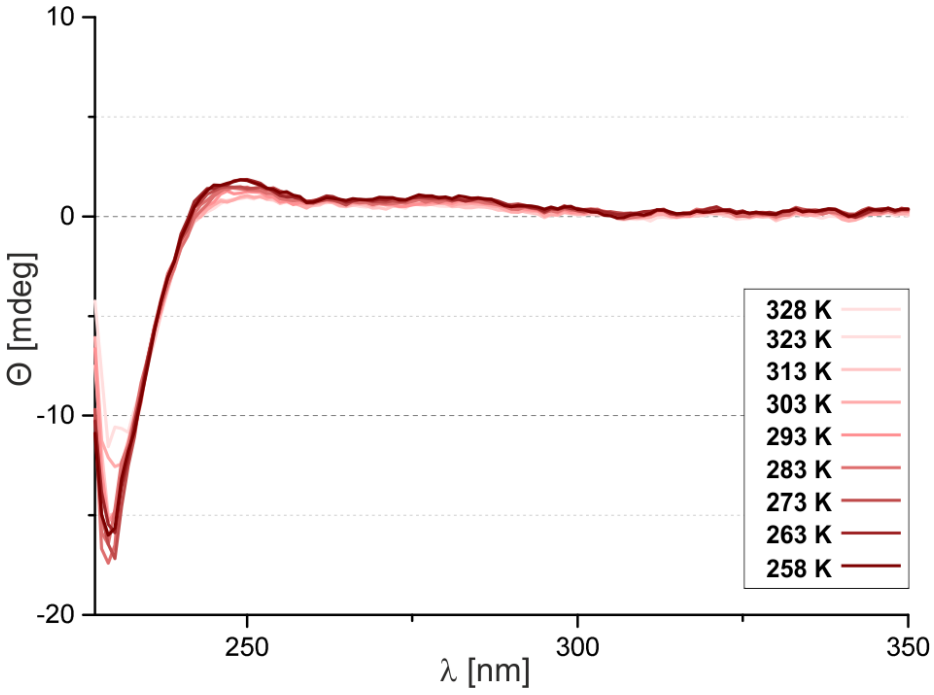


**Figure S19.** Temperature-dependent CD-spectra of PBPM$^3$LG in $CHCl_3$.

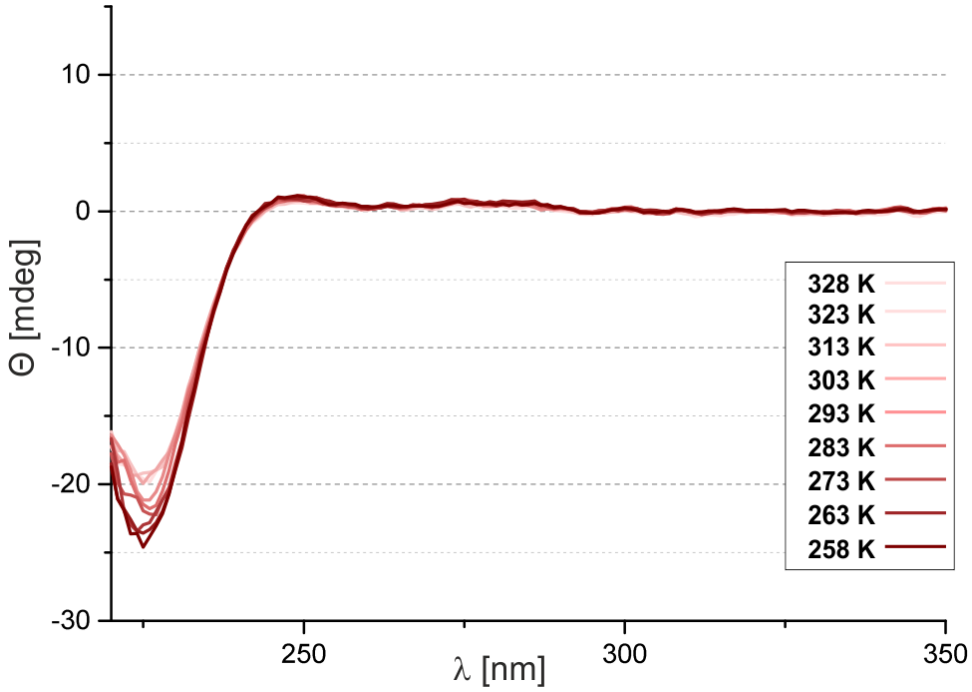


**Figure S20.** Temperature-dependent CD-spectra of PBPM$^3$LG in THF.

If the α-helix led do a preferential formation of one rotamer in the biphenyl side chain here (by annealing), one would expect a CD signal in the region of the biphenyl chromophore (at approximately 260 nm). This was previously observed for the parent polymer PBPMLG[6] and the C2-spacer polymer PBPELG[8]. Its absence confirms that no such chiral annealing takes place. This is in agreement with NMR data (see above).

The negative CD signal at ~220 nm is characteristic for the α-helix of L-polymers.[13] no 'chiral coupling', as was observed for PBPMLG[6] and PBPELG[8], is observed in the biphenyl region ~270 nm. This is in agreement with absent chiral annealing in the $^{13}$C NMR spectra (see section above).

## Polarized Optical Microscopy (POM)

A restriction of biphenyl rotation in the polymer sidechain could influence the morphology of the LLC phase as compared to the parent polymer without restricted rotation Poly-γ-*p*-biphenylmethyl-L-glutamate (PBPMLG)[6-7] and the polymers containing spacer groups poly-γ-*p*-biphenylethoxy-L-glutamate (PBPELG) and poly-γ-*p*-biphenylhexoxy-L-glutamate (PBPHLG)[8] of our previous investigations. Thus we conducted an investigation via POM to gain insights into the thermoresponsive phase morphology. To minimize reflections caused by the round glass surface of the capillaries (flame sealed capillaries prevent solvent evaporation, which is crucial for this application), we used square capillaries (HILGENBERG; 2 ± 0.1 x 1 ± 0.1 mm; inside 1.78 ± 0.1 x 0.78 ± 0.1 mm; wall thickness: 0.11 ± 0.05 mm). The preparation of the LLC phases was carried out in a 5 mm NMR-tube and after thorough homogenization the sample was transferred into the square capillaries (one end was flame sealed beforehand). After sample transfer is complete, the injection end of the capillary is flame sealed as well. Figure S21 shows the POM images of a LLC phase of PBPM$^3$LG (17.8 % w/w) in $CDCl_3$ at various temperatures.

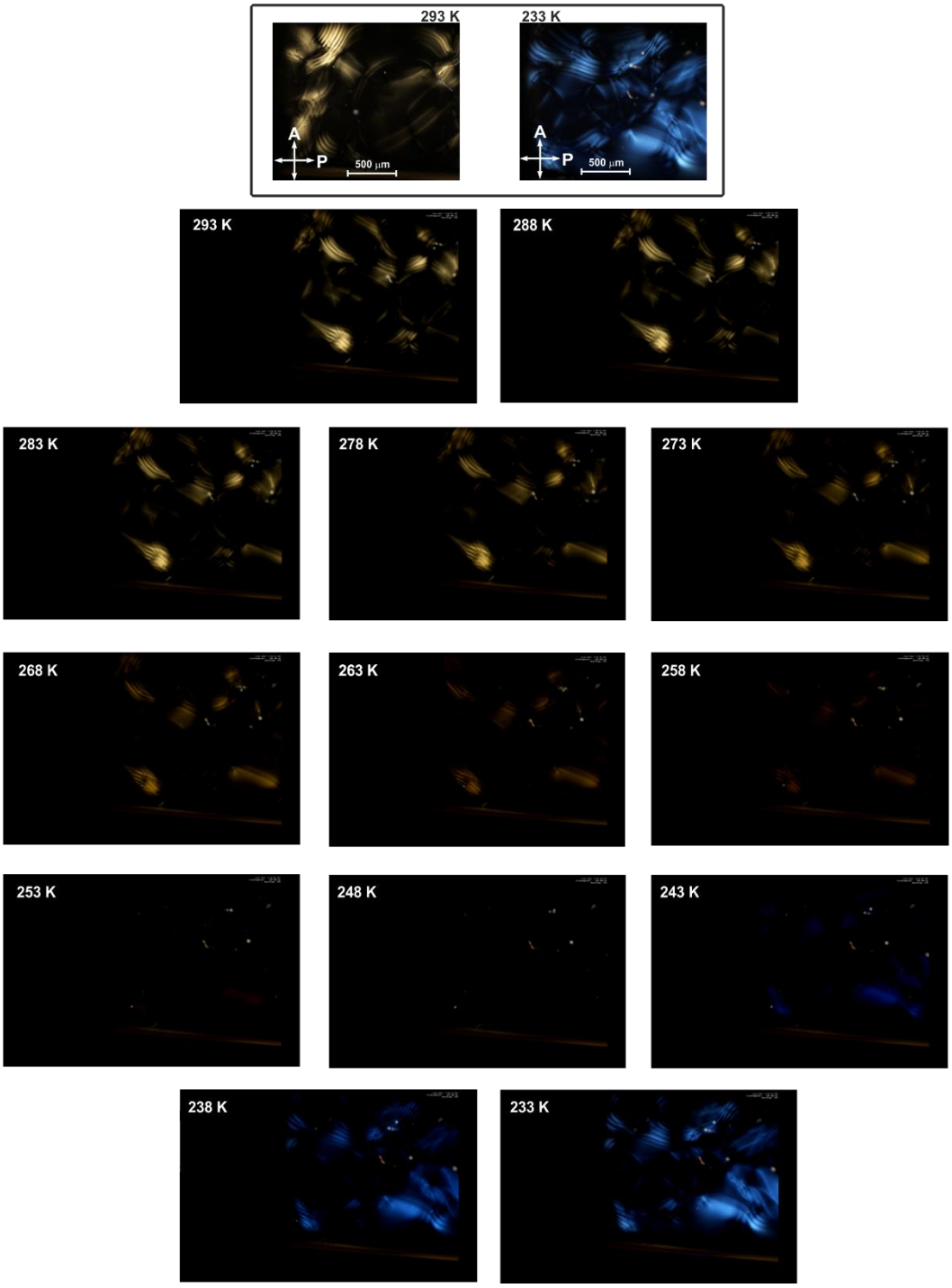


**Figure S21.** Polarized optical microscopy pictures of an LLC phase of PBPM$^3$LG (17.8 % w/w) in $CDCl_3$ at various temperatures. Rotation of the sample holder is 0° for all displayed images. The direction of the polarizer (P) and analyzer (A) are shown in the bottom of the pictures.

We interpret the temperature dependent color change, observed in the LLC-phases of PBPM$^3$LG in $CDCl_3$, as a result of a change in cholesteric pitch, which most certainly is the result of a gradual restriction of the biphenyl rotation in the polymer sidechain. Interestingly, PBPM$^3$LG in THF-$d_8$ does not show such a behavior (Figure S22). Neither the parent polymer PBPMLG[7] nor the polymers containing spacer groups PBPELG and PBPHLG[8] of our previous investigations exhibit a temperature dependent color change. Furthermore, no gelation was observed in the temperature range investigated.

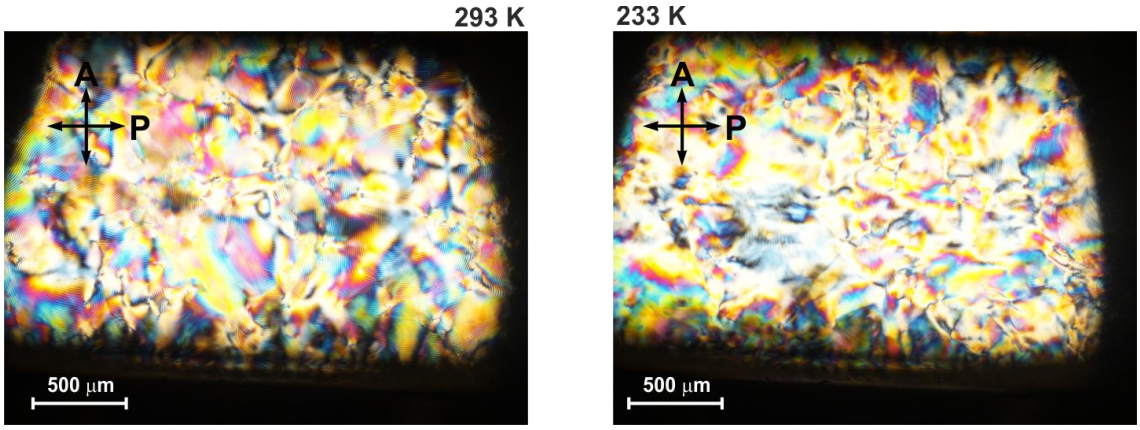


**Figure S22.** Polarized optical microscopy pictures of an LLC phase of PBPM$^3$LG (28.0 % w/w) in THF-$d_8$ at various temperatures. Rotation of the sample holder is 0° for the displayed images. The direction of the polarizer (P) and analyzer (A) are shown in the top left of the pictures.

As the cholesteric pitch of the LLC phase of PBPM$^3$LG is drastically different in THF-$d_8$ compared to $CDCl_3$, the colors observed are different. This can be explained by the relation of the observed spectral range $\Delta\lambda$ and the cholesteric pitch $P_0$ ($\Delta\lambda \sim P_0$).[14]
Figure S23 shows the cholesteric *fingerprint* texture in a magnified POM-image of the THF-$d_8$-based LLC phase of PBPM$^3$LG at room temperature.

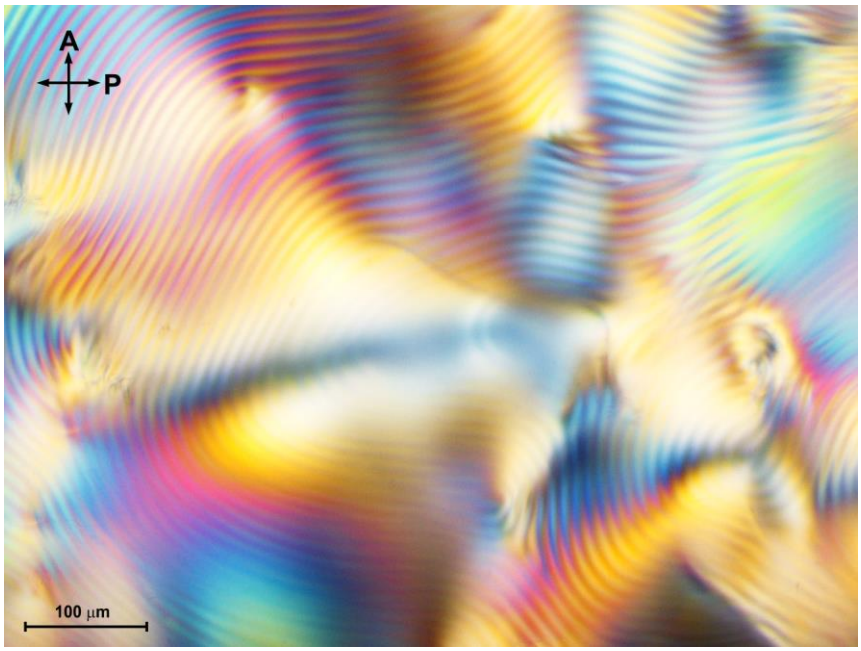


**Figure S23.** Magnified polarized optical microscopy picture of an LLC phase of PBPM$^3$LG (28.0 % w/w) in THF-$d_8$. Rotation of the sample holder is 0°. The direction of the polarizer (P) and analyzer (A) are shown in the top left of the pictures.

## IPC as analyte

The tables S2 and S3 below show one bond carbon proton coupling constants ($^1J_{CH}$) of IPC in THF-$d_8$ and $CDCl_3$ at various temperatures, which are needed to calculate the resulting dipolar couplings from the total couplings extracted (Figure S24 and S25) in anisotropic environments.

**Table S2.** $^1J_{CH}$ -values of (-)-IPC in THF-$d_8$ at various temperatures show no significant differences.

| $^1J_{CH}$ [Hz] | 320 K | | 310 K | | 300 K | |
|---|---|---|---|---|---|---|
| C1-H1 | **140.43** | ± 0.14 | **140.31** | ± 0.12 | **140.27** | ± 0.07 |
| C2-H2 | **127.24** | ± 0.13 | **127.13** | ± 0.11 | **127.31** | ± 0.11 |
| C3-H3 | **140.15** | ± 0.15 | **140.11** | ± 0.05 | **139.97** | ± 0.12 |
| C4-H4s | **125.74** | ± 0.10 | **125.69** | ± 0.09 | **125.59** | ± 0.16 |
| C4-H4a | **127.54** | ± 0.12 | **127.43** | ± 0.14 | **127.44** | ± 0.11 |
| C5-H5 | **140.81** | ± 0.17 | **140.55** | ± 0.11 | **140.62** | ± 0.06 |
| C7-H7s | **134.64** | ± 0.15 | **134.69** | ± 0.08 | **134.44** | ± 0.18 |
| C7-H7a | **137.37** | ± 0.06 | **137.39** | ± 0.06 | **137.34** | ± 0.11 |
| C8-H8 | **124.38** | ± 0.03 | **124.38** | ± 0.03 | **124.38** | ± 0.04 |
| C9H-9 | **123.55** | ± 0.04 | **123.55** | ± 0.04 | **123.54** | ± 0.05 |
| C10-H10 | **124.43** | ± 0.07 | **124.45** | ± 0.06 | **124.48** | ± 0.07 |

| $^1J_{CH}$ [Hz] | 290 K | | 280 K | | 270 K | | 260 K | |
|---|---|---|---|---|---|---|---|---|
| C1-H1 | **140.41** | ± 0.05 | **140.38** | ± 0.07 | **140.27** | ± 0.09 | **140.26** | ± 0.08 |
| C2-H2 | **127.15** | ± 0.14 | **127.17** | ± 0.14 | **127.15** | ± 0.13 | **127.15** | ± 0.12 |
| C3-H3 | **139.61** | ± 0.12 | **139.96** | ± 0.12 | **139.87** | ± 0.04 | **139.92** | ± 0.24 |
| C4-H4s | **125.57** | ± 0.12 | **125.67** | ± 0.24 | **125.53** | ± 0.22 | **125.55** | ± 0.22 |
| C4-H4a | **127.46** | ± 0.11 | **127.46** | ± 0.08 | **127.47** | ± 0.10 | **127.39** | ± 0.13 |
| C5-H5 | **140.50** | ± 0.13 | **140.47** | ± 0.10 | **140.53** | ± 0.09 | **140.58** | ± 0.09 |
| C7-H7s | **134.48** | ± 0.13 | **134.40** | ± 0.18 | **134.43** | ± 0.13 | **134.31** | ± 0.22 |
| C7-H7a | **137.32** | ± 0.07 | **137.25** | ± 0.12 | **137.24** | ± 0.03 | **137.22** | ± 0.15 |
| C8-H8 | **124.36** | ± 0.03 | **124.39** | ± 0.05 | **124.33** | ± 0.04 | **124.40** | ± 0.04 |
| C9H-9 | **123.54** | ± 0.03 | **123.52** | ± 0.06 | **123.49** | ± 0.05 | **123.53** | ± 0.11 |
| C10-H10 | **124.46** | ± 0.06 | **124.41** | ± 0.05 | **124.39** | ± 0.09 | **124.41** | ± 0.06 |

**Table S3.** $^1J_{CH}$ -values of (-)-IPC in $CDCl_3$ at 300 K.

| $^1J_{CH}$ [Hz] | 300 K | |
|---|---|---|
| C1-H1 | **141.37** | **± 0.16** |
| C2-H2 | **126.78** | **± 0.13** |
| C3-H3 | **142.49** | **± 0.09** |
| C4-H4s | **126.89** | **± 0.12** |
| C4-H4a | **127.10** | **± 0.07** |
| C5-H5 | **141.90** | **± 0.19** |
| C7-H7s | **135.36** | **± 0.12** |
| C7-H7a | **137.03** | **± 0.06** |
| C8-H8 | **124.71** | **± 0.02** |
| C9H-9 | **123.72** | **± 0.03** |
| C10-H10 | **124.97** | **± 0.05** |

In $CDCl_3$, $^1J_{CH}$ -values for IPC at 300 K were used for the calculation of the dipolar couplings at all measured temperatures. In our previous work[8] we showed that $^1J_{CH}$-values of IPC in THF-$d_8$ show no significant temperature dependent change. Nevertheless, the obtained values from this investigation at the respective temperatures have been used to calculate dipolar couplings in THF-based LLC phases, with the exception of temperatures below 260 K. These were calculated with the $^1J_{CH}$ -values for 260 K.

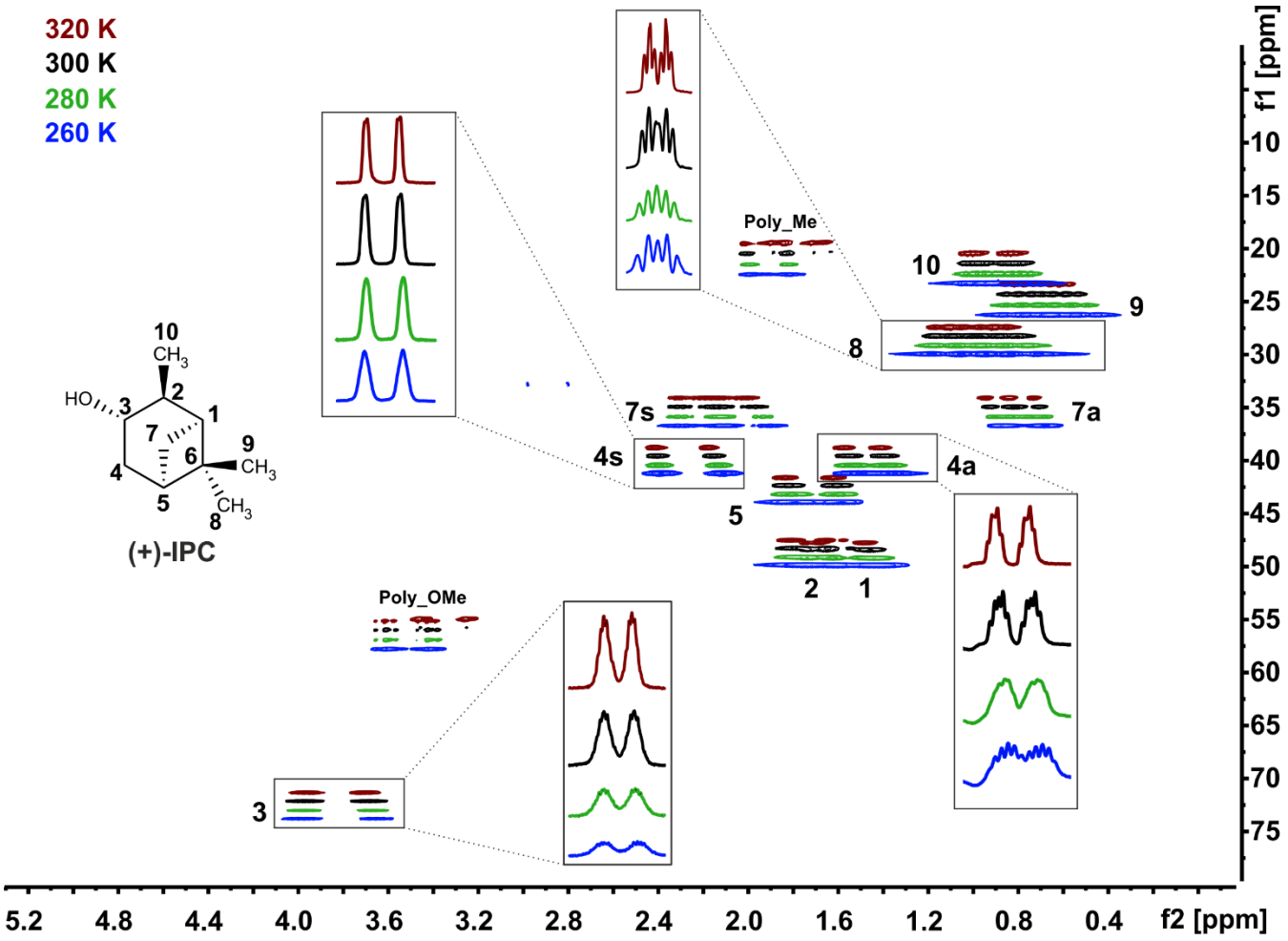


**Figure S24.** Perfect-CLIP-HSQC[1] spectra of (700 MHz $^1$H-frequency, 176 MHz $^{13}$C-frequency) (+)-IPC in PBPM$^3$LG (14.8 w%) with $CDCl_3$ as solvent **[DS-P75]** at various temperatures (red: 320 K, black: 300 K, green: 280 K and blue: 260 K). The displayed spectra are manually shifted in F1 for the sake of better visibility.

Spectral quality of (+)-IPC in PBPM$^3$LG-based LLC phases using $CDCl_3$ as solvent is excellent and does not decrease significantly with lower temperatures. The signals become negligibly broader, but without posing difficulties for analysis. RDCs C1H1 and C2H2 could not be extracted, due to overlap.

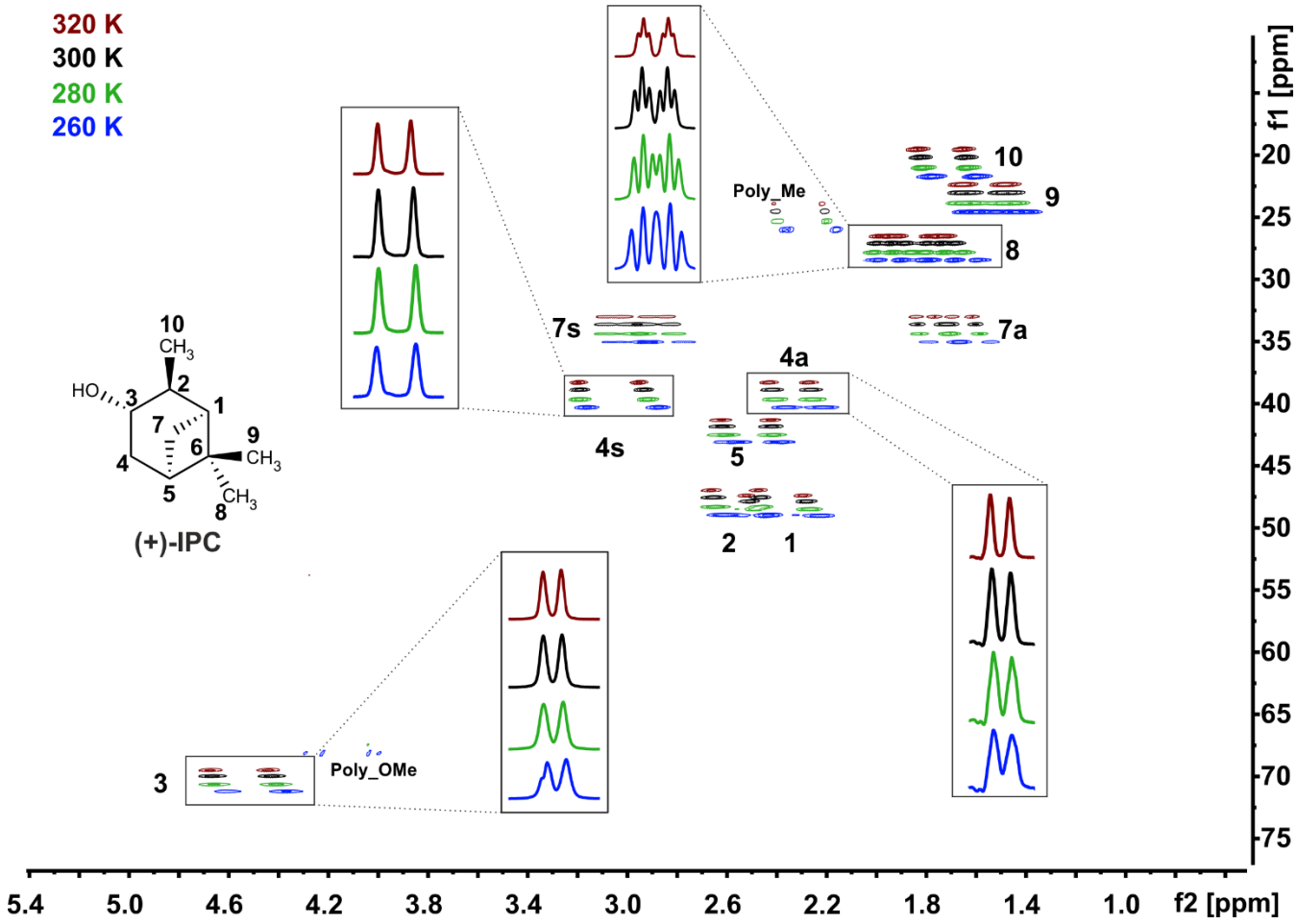


**Figure S25.** Perfect-CLIP-HSQC[1] spectra (700 MHz $^{1}$H-frequency, 176 MHz $^{13}$C-frequency) of (+)-IPC in PBPM$^{3}$LG (27.8 w%) with THF-$d_8$ as solvent **[DS-P77]** at various temperatures (red: 320 K, black: 300 K, green: 280 K and blue: 260 K). The displayed spectra are manually shifted in F1 for the sake of better visibility.

Spectral quality of (+)-IPC in PBPM$^{3}$LG-based LLC phases using THF-$d_8$ as solvent is excellent and also retained over the full temperature range.

## Temperature dependence of the enantiodiscrimination of IPC

Through the scalar product of the alignment tensors obtained an angle β is calculated. Ranging from 0° (equal orientations) to 90° (max. degree of linear independency), generalized |β|-angles thus provide insights into the difference in induced orientation of analytes.[15]

**Table S4.** Generalized angle |β| between (+) and (-)-IPC in LLC phases of PBPM$^3$LG in $CDCl_3$ and THF-$d_8$ at various temperatures.

| PBPM$^3$LG | $CDCl_3$ | THF-$d_8$ |
|---|---|---|
| T [K] | \|β\| [°] | \|β\| [°] |
| 325 | 5.3 | 41.6 |
| 320 | 7.4 | 41.2 |
| 315 | 12.6 | 39.7 |
| 310 | 19.8 | 38.3 |
| 300 | 22.0 | 35.2 |
| 290 | 29.1 | 33.7 |
| 280 | 34.3 | 32.2 |
| 270 | 32.1 | 32.6 |
| 260 | 27.0 | 32.9 |
| 255 | 28.1 | 31.9 |
| | DS-P74a<br>DS-P75 | DS-P76<br>DS-P77 |

In $CDCl_3$ enantiodiscrimination varies strongly with temperature; with ~35° β-angle being the highest value at 280 K. As we have established (see above and SECONDA analysis in manuscript), that PBPM$^3$LG in $CDCl_3$ thermoresponsively induces multiple alignments, this is not surprising. The parent polymer PBPMLG[6] has shown β-angles of up to ~25° in $CDCl_3$, while the spacer polymers have shown β-angles of up to ~15° (PBPELG)[8] and ~50° (PBPHLG)[8] in $CDCl_3$.

In THF-$d_8$ thermoresponsive changes in β-angles are also observable for PBPM$^3$LG, but smaller. Interestingly, β-angles in THF-$d_8$ show larger values at higher temperatures and smaller values at lower temperatures. Enantiodiscrimination usually is lower at high temperatures, as higher entropy causes the conditions compared to be more similar than at lower temperatures. β-angles of up to ~42° are observed for PBPM$^3$LG in THF-$d_8$, whereas the parent polymer PBPMLG[6] and the spacer polymers PBPELG and PBPHLG[8] have shown β-angles of up to ~90°.

## Temperature dependence of orientations within one sample

As discussed in the main text, multiple alignments are induced at different temperatures within the same sample. This effect is present in $CDCl_3$-based LLC phases of PBPM$^3$LG as can also be seen from β-angles calculated within one sample in this section. The investigation is performed for both enantiomers of IPC.

**Table S5.** β-angles in [°] between two orientations at corresponding temperatures of (-)-IPC in a PBPM$^3$LG/$CDCl_3$ LLC phase (14.8 w%) at various temperatures. **[Sample DS-P74a]**

| | 325 K | 320 K | 315 K | 310 K | 305 K | 300 K | 290 K | 280 K | 270 K | 260 K | 255 K |
|---|---|---|---|---|---|---|---|---|---|---|---|
| 325 K | x | 6.0 | 8.0 | 8.6 | 12.3 | 18.5 | 24.1 | 31.2 | 44.8 | 56.5 | 60.6 |
| 320 K | x | x | 2.1 | 3.6 | 6.4 | 12.6 | 18.2 | 25.3 | 38.9 | 50.6 | 54.6 |
| 315 K | x | x | x | 2.8 | 4.4 | 10.6 | 16.1 | 23.2 | 36.8 | 48.5 | 52.6 |
| 310 K | x | x | x | x | 4.3 | 11.2 | 16.3 | 23.2 | 36.9 | 48.7 | 52.7 |
| 305 K | x | x | x | x | x | 7.0 | 12.1 | 19.1 | 32.7 | 44.5 | 48.5 |
| 300 K | x | x | x | x | x | x | 5.7 | 12.9 | 26.3 | 37.9 | 42.0 |
| 290 K | x | x | x | x | x | x | x | 7.2 | 20.7 | 32.5 | 36.5 |
| 280 K | x | x | x | x | x | x | x | x | 13.7 | 25.6 | 29.5 |
| 270 K | x | x | x | x | x | x | x | x | x | 12.0 | 15.9 |
| 260 K | x | x | x | x | x | x | x | x | x | x | 4.4 |
| 255 K | x | x | x | x | x | x | x | x | x | x | x |

**Table S6.** β-angles in [°] between two orientations at corresponding temperatures of (+)-IPC in a PBPM$^3$LG/$CDCl_3$ LLC phase (14.8 w%) at various temperatures. **[Sample DS-P75]**

| | 325 K | 320 K | 315 K | 310 K | 300 K | 290 K | 280 K | 270 K | 260 K | 255 K |
|---|---|---|---|---|---|---|---|---|---|---|
| 325 K | x | 7.8 | 15.2 | 21.2 | 34.4 | 45.7 | 55.9 | 64.8 | 69.4 | 71.9 |
| 320 K | x | x | 7.4 | 13.5 | 26.7 | 38.0 | 48.2 | 57.0 | 61.7 | 64.2 |
| 315 K | x | x | x | 6.1 | 19.2 | 30.5 | 40.8 | 49.1 | 54.3 | 56.8 |
| 310 K | x | x | x | x | 13.2 | 24.5 | 34.7 | 43.6 | 48.3 | 50.8 |
| 300 K | x | x | x | x | x | 11.3 | 21.6 | 30.4 | 35.1 | 37.7 |
| 290 K | x | x | x | x | x | x | 11.4 | 19.2 | 23.9 | 26.6 |
| 280 K | x | x | x | x | x | x | x | 9.0 | 13.6 | 16.3 |
| 270 K | x | x | x | x | x | x | x | x | 5.1 | 7.8 |
| 260 K | x | x | x | x | x | x | x | x | x | 2.8 |
| 255 K | x | x | x | x | x | x | x | x | x | x |

**Table S7.** β-angles in [°] between two orientations at corresponding temperatures of (-)-IPC in a PBPM$^3$LG/THF-$d_8$ LLC phase (27.8 w%) at various temperatures. **[Sample DS-P76]**

| | 325 K | 320 K | 315 K | 310 K | 300 K | 290 K | 280 K | 270 K | 260 K | 255 K |
|---|---|---|---|---|---|---|---|---|---|---|
| 325 K | x | 0.7 | 2.9 | 4.3 | 6.9 | 8.5 | 9.3 | 10.5 | 14.1 | 16.9 |
| 320 K | x | x | 2.2 | 3.6 | 6.2 | 7.8 | 8.7 | 9.8 | 13.6 | 16.6 |
| 315 K | x | x | x | 1.5 | 4.1 | 5.7 | 6.9 | 8.2 | 12.6 | 15.9 |
| 310 K | x | x | x | x | 2.6 | 4.2 | 5.4 | 6.8 | 11.5 | 15.0 |
| 300 K | x | x | x | x | x | 1.8 | 3.1 | 4.8 | 10.1 | 13.9 |
| 290 K | x | x | x | x | x | x | 2.8 | 4.3 | 10.2 | 14.2 |
| 280 K | x | x | x | x | x | x | x | 2.3 | 7.4 | 11.4 |
| 270 K | x | x | x | x | x | x | x | x | 6.5 | 10.6 |
| 260 K | x | x | x | x | x | x | x | x | x | 4.2 |
| 255 K | x | x | x | x | x | x | x | x | x | x |

**Table S8.** β-angles in [°] between two orientations at corresponding temperatures of (+)-IPC in a PBPM$^3$LG/THF-$d_8$ LLC phase (27.8 w%) at various temperatures. **[Sample DS-P77]**

| | 325 K | 320 K | 315 K | 310 K | 300 K | 290 K | 280 K | 270 K | 260 K | 255 K |
|---|---|---|---|---|---|---|---|---|---|---|
| 325 K | x | 3.5 | 5.5 | 5.3 | 5.9 | 6.9 | 6.9 | 7.3 | 6.0 | 3.9 |
| 320 K | x | x | 2.5 | 2.3 | 2.4 | 3.8 | 3.7 | 4.2 | 3.6 | 2.5 |
| 315 K | x | x | x | 0.3 | 1.6 | 1.9 | 1.8 | 3.5 | 3.6 | 4.0 |
| 310 K | x | x | x | x | 1.5 | 2.0 | 1.9 | 3.4 | 3.4 | 3.7 |
| 300 K | x | x | x | x | x | 1.8 | 1.4 | 2.9 | 3.7 | 4.2 |
| 290 K | x | x | x | x | x | x | 0.5 | 3.0 | 4.3 | 5.4 |
| 280 K | x | x | x | x | x | x | x | 3.3 | 4.5 | 5.4 |
| 270 K | x | x | x | x | x | x | x | x | 2.8 | 4.6 |
| 260 K | x | x | x | x | x | x | x | x | x | 2.6 |
| 255 K | x | x | x | x | x | x | x | x | x | x |

In $CDCl_3$ the β-angles (Table S5, S6) indicate a thermoresponsive change in induced alignment, which is, however, different for the enantiomers of IPC. (+)-IPC shows higher values (up to ~25° at 325 K *vs.* 300 K) in calculated β-angles than (-)-IPC, when comparing the alignment tensors of 325 K with all other temperatures. Similar results were obtained in the investigation[10b] of poly-benzyl-L-aspartate PBLA in $CDCl_3$ showing difference in β-angels (IPC) within the same sample of up to 5°. These differences are more significant and parallel those of our previous investigations in PBPMLG[6] (up to ~25°). This effect can also be seen in our investigation of poly-γ-*p*-biphenylethoxy-L-glutamate (PBPELG) and poly-γ-*p*-biphenylhexoxy-L-glutamate (PBPHLG)[8]. Here differences in β-angle up to ~15° within one sample can be seen in PBPHLG/$CDCl_3$ as well as in PBPHDG/$CDCl_3$. These differences are practically nonexistent in PBPELG or PBPEDG when using THF-$d_8$ as solvent for both polymers. PBPM$^3$LG, however, shows this behavior in THF-$d_8$ (Table S7, S8). Again, comparing 325 K with every temperature within the same sample yields larger β-angles for (-)-IPC. A systematic trend in this *matched*/*mismatched* behavior of enantiomer orientation is not yet observable.

Figure S26 shows alignment tensors of (+)-IPC in a PBPM$^3$LG-based LLC phase in $CDCl_3$ at various temperatures (see table S6).

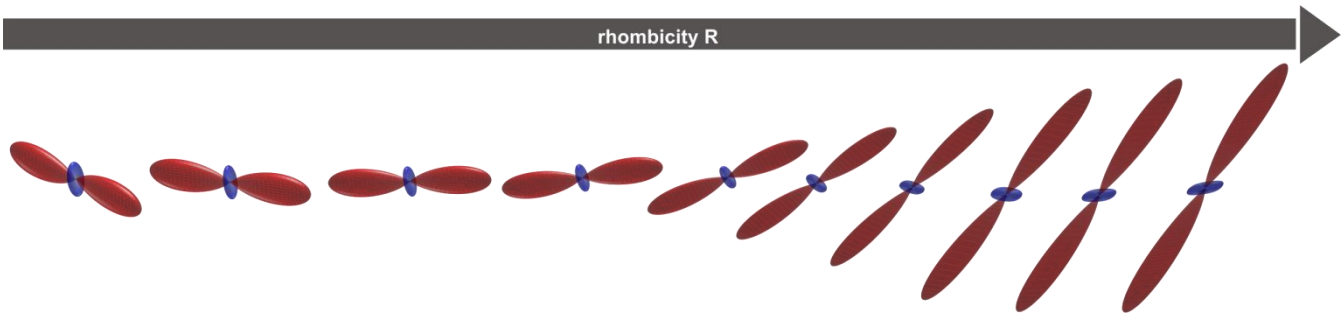


| temperature | 325 K | 320 K | 315 K | 310 K | 300 K | 290 K | 280 K | 270 K | 260 K | 255 K |
|---|---|---|---|---|---|---|---|---|---|---|
| β-angle between 325 K and *X*, ° | 0 | 7.8 | 15.2 | 21.2 | 34.4 | 45.7 | 55.9 | 64.8 | 69.4 | **71.9** |

**Figure S26.** Graphical representation of the alignment tensors of (+)-IPC at various temperatures (from 325 K on the left to 255 K on the right) in a PBPM$^3$LG-based LLC phase ($CDCl_3$, 14.8 % *w/w*, TEA initiated **[DS-P75]**). The alignment tensors are displayed in a fixed molecular frame. Below the tensors, β-angles[15] between the alignment tensors at 325 K and at the corresponding other temperature are shown.

The alignment tensors of (+)-IPC show a temperature dependent change in orientation as well as anisotropy/rhombicity (for Euler angles and rhombicity values, see below). This translates into a temperature dependent change in the alignment induced. The change in the alignment induced is confirmed here by a notable change in β-angle for (+)-IPC in the same sample at various temperatures.

## RDC Data

In this section RDCs for all LLC phases and associated data is presented. The standard deviation σ was used as error for the RDCs extracted. The errors describe a positive and negative deviation (±). Euler angles within the tables carry the unit [°]. The condition number given here is the condition number of the coefficient matrix.

**Table S9a.** RDCs ($^1D_{CH}$) and orientation properties extracted of (-)-IPC in a PBPM$^3$LG/$CDCl_3$ LLC phase (14.8 w%) at various temperatures. **[Sample DS-P74a]**

| **RDC [Hz]** | **$^1D_{CH}$** | **σ** | **$^1D_{CH}$** | **σ** | **$^1D_{CH}$** | **σ** | **$^1D_{CH}$** | **σ** | **$^1D_{CH}$** | **σ** | **$^1D_{CH}$** | **σ** |
|---|---|---|---|---|---|---|---|---|---|---|---|---|
| **Temp.** | **325 K** | | **320 K** | | **315 K** | | **310 K** | | **305 K** | | **300 K** | |
| C1-H1 | **-** | - | **-** | - | **-** | - | **-** | - | **-** | - | **-** | - |
| C2-H2 | **-** | - | **-** | - | **-** | - | **-** | - | **-** | - | **-** | - |
| C3-H3 | **15.46** | 2.62 | **17.96** | 1.03 | **19.14** | 1.20 | **18.31** | 1.67 | **20.01** | 1.99 | **22.48** | 2.32 |
| C4-H4s | **13.66** | 2.20 | **17.08** | 0.75 | **18.72** | 0.60 | **20.12** | 0.38 | **21.70** | 0.60 | **23.16** | 0.59 |
| C4-H4a | **-6.70** | 1.27 | **-8.73** | 0.63 | **-9.37** | 0.81 | **-9.72** | 0.55 | **-10.59** | 1.16 | **-11.34** | 1.24 |
| C5-H5 | **2.47** | 0.93 | **2.58** | 0.74 | **2.68** | 0.69 | **2.55** | 0.48 | **2.58** | 0.53 | **2.80** | 0.52 |
| C7-H7s | **0.44** | 1.25 | **0.76** | 1.19 | **0.62** | 1.24 | **0.26** | 0.75 | **0.58** | 0.95 | **0.02** | 1.11 |
| C7-H7a | **-28.06** | 2.03 | **-29.44** | 0.63 | **-30.25** | 0.74 | **-30.56** | 0.80 | **-30.34** | 1.43 | **-29.05** | 1.68 |
| C8-H8 | **6.53** | 0.98 | **6.36** | 1.13 | **6.92** | 1.18 | **7.09** | 0.87 | **7.55** | 1.39 | **7.95** | 0.86 |
| C9-H9 | **-4.86** | 0.47 | **-5.26** | 0.67 | **-5.63** | 0.81 | **-5.98** | 0.51 | **-6.57** | 0.39 | **-6.60** | 0.68 |
| C10-H10 | **-2.72** | 0.69 | **-3.21** | 0.46 | **-3.25** | 0.36 | **-3.47** | 0.27 | **-3.67** | 0.28 | **-3.72** | 0.43 |
| Quality factor Q | 0.023 | | 0.017 | | 0.014 | | 0.002 | | 0.001 | | 0.011 | |
| RMSD [Hz] | 0.272 | | 0.224 | | 0.192 | | 0.033 | | 0.018 | | 0.170 | |
| Condition number | 2.858 | | 2.858 | | 2.858 | | 2.858 | | 2.858 | | 2.858 | |
| GDO [$10^{-3}$] | 1.433 | | 1.522 | | 1.582 | | 1.604 | | 1.624 | | 1.636 | |
| $D_a$ [$10^{-4}$] | 7.129 | | 7.510 | | 7.778 | | 7.853 | | 7.897 | | 7.879 | |
| $D_r$ [$10^{-4}$] | 0.8271 | | 1.420 | | 1.651 | | 1.877 | | 2.187 | | 2.538 | |
| Rhombicity *R* | 0.116 | | 0.189 | | 0.212 | | 0.239 | | 0.277 | | 0.322 | |
| Euler angle α | 32.5 | | 31.5 | | 31.4 | | 31.7 | | 30.9 | | 29.9 | |
| Euler angle β | 85.5 | | 88.0 | | 88.9 | | 88.8 | | 90.7 | | 94.1 | |
| Euler angle γ | 110.3 | | 116.3 | | 116.9 | | 110.5 | | 115.2 | | 120.6 | |

**Table S9b.** RDCs ($^1D_{CH}$) and orientation properties extracted of (-)-IPC in a PBPM$^3$LG/$CDCl_3$ LLC phase (14.8 w%) at various temperatures. Continuation of table S9a. **[Sample DS-P74a]**

| **RDC [Hz]** | **$^1D_{CH}$** | **σ** | **$^1D_{CH}$** | **σ** | **$^1D_{CH}$** | **σ** | **$^1D_{CH}$** | **σ** | **$^1D_{CH}$** | **σ** |
|---|---|---|---|---|---|---|---|---|---|---|
| **Temp.** | **290 K** | | **280 K** | | **270 K** | | **260 K** | | **255 K** | |
| C1-H1 | **-** | - | **-** | - | **-** | - | **-** | - | **-** | - |
| C2-H2 | **-** | - | **-** | - | **-** | - | **-** | - | **-** | - |
| C3-H3 | **23.51** | 1.34 | **24.70** | 2.71 | **26.57** | 3.44 | **29.57** | 2.30 | **29.35** | 2.76 |
| C4-H4s | **26.52** | 0.49 | **30.09** | 0.44 | **33.65** | 1.07 | **37.20** | 0.74 | **39.50** | 1.47 |
| C4-H4a | **-12.82** | 1.01 | **-14.65** | 0.70 | **-15.71** | 1.52 | **-17.01** | 1.15 | **-17.55** | 0.90 |
| C5-H5 | **3.17** | 0.56 | **3.19** | 1.03 | **2.70** | 1.32 | **1.96** | 1.24 | **1.85** | 0.96 |
| C7-H7s | **-0.54** | 2.32 | **-1.00** | 1.36 | **-1.42** | 0.65 | **-0.74** | 0.63 | **-1.40** | 2.48 |
| C7-H7a | **-28.58** | 5.85 | **-27.15** | 8.16 | **-21.52** | 2.87 | **-16.65** | 2.36 | **-14.48** | 2.20 |
| C8-H8 | **9.39** | 1.80 | **10.38** | 0.77 | **12.11** | 1.80 | **12.65** | 1.13 | **13.33** | 2.30 |
| C9-H9 | **-7.50** | 1.08 | **-8.09** | 0.57 | **-8.56** | 0.69 | **-9.06** | 0.91 | **-9.36** | 0.78 |
| C10-H10 | **-3.87** | 0.65 | **-3.97** | 0.64 | **-3.88** | 0.69 | **-3.81** | 1.08 | **-3.85** | 0.93 |
| Quality factor Q | 0.010 | | 0.018 | | 0.034 | | 0.044 | | 0.054 | |
| RMSD [Hz] | 0.165 | | 0.293 | | 0.572 | | 0.784 | | 0.981 | |
| Condition number | 2.858 | | 2.858 | | 2.858 | | 2.858 | | 2.858 | |
| GDO [$10^{-3}$] | 1.697 | | 1.756 | | 1.797 | | 1.955 | | 2.027 | |
| $D_a$ [$10^{-4}$] | 8.052 | | 8.138 | | 7.981 | | -8.474 | | -8.896 | |
| $D_r$ [$10^{-4}$] | 3.081 | | 3.801 | | 4.764 | | -5.632 | | -5.607 | |
| Rhombicity *R* | 0.383 | | 0.467 | | 0.597 | | 0.665 | | 0.630 | |
| Euler angle α | 28.7 | | 26.7 | | 21.8 | | 151.2 | | 156.2 | |
| Euler angle β | 96.8 | | 100.3 | | 107.7 | | 147.7 | | 148.3 | |
| Euler angle γ | 118.1 | | 116.0 | | 114.5 | | 50.9 | | 57.8 | |

**Table S10a.** RDCs ($^1D_{CH}$) and orientation properties extracted of (+)-IPC in a PBPM$^3$LG/$CDCl_3$ LLC phase (14.8 w%) at various temperatures. **[Sample DS-P75]**

| **RDC [Hz]** | **$^1D_{CH}$** | **σ** | **$^1D_{CH}$** | **σ** | **$^1D_{CH}$** | **σ** | **$^1D_{CH}$** | **σ** | **$^1D_{CH}$** | **σ** |
|---|---|---|---|---|---|---|---|---|---|---|
| **Temp.** | **325 K** | | **320 K** | | **315 K** | | **310 K** | | **300 K** | |
| C1-H1 | **-** | - | **-** | - | **-** | - | **-** | - | **-** | - |
| C2-H2 | **-** | - | **-** | - | **-** | - | **-** | - | **-** | - |
| C3-H3 | **18.15** | 4.25 | **21.97** | 1.61 | **24.16** | 1.28 | **25.63** | 1.99 | **29.85** | 0.65 |
| C4-H4s | **18.20** | 0.55 | **20.27** | 0.74 | **21.44** | 0.63 | **22.79** | 0.77 | **25.05** | 0.46 |
| C4-H4a | **-7.72** | 1.58 | **-8.31** | 0.93 | **-8.64** | 0.53 | **-8.67** | 0.61 | **-8.77** | 0.36 |
| C5-H5 | **3.66** | 2.90 | **4.06** | 1.24 | **4.20** | 1.07 | **4.29** | 0.83 | **4.36** | 1.05 |
| C7-H7s | **-1.18** | 1.17 | **-1.45** | 1.35 | **-1.67** | 0.82 | **-2.03** | 1.11 | **-2.37** | 0.78 |
| C7-H7a | **-31.20** | 5.18 | **-30.92** | 6.17 | **-28.73** | 3.95 | **-26.71** | 0.93 | **-22.65** | 3.53 |
| C8-H8 | **7.40** | 1.32 | **7.63** | 1.49 | **8.00** | 1.05 | **8.67** | 0.72 | **10.10** | 0.60 |
| C9-H9 | **-5.11** | 0.79 | **-6.24** | 0.92 | **-6.63** | 1.02 | **-7.13** | 0.56 | **-8.34** | 0.71 |
| C10-H10 | **-3.55** | 0.93 | **-3.89** | 0.52 | **-4.12** | 0.55 | **-4.66** | 0.33 | **-5.40** | 0.80 |
| Quality factor Q | 0.010 | | 0.012 | | 0.013 | | 0.009 | | 0.016 | |
| RMSD [Hz] | 0.139 | | 0.178 | | 0.194 | | 0.138 | | 0.239 | |
| Condition number | 2.858 | | 2.858 | | 2.858 | | 2.858 | | 2.858 | |
| GDO [$10^{-3}$] | 1.638 | | 1.691 | | 1.668 | | 1.665 | | 1.743 | |
| $D_a$ [$10^{-4}$] | 8.126 | | 8.349 | | 8.141 | | 8.030 | | 8.155 | |
| $D_r$ [$10^{-4}$] | 1.158 | | 1.545 | | 2.087 | | 2.530 | | 3.546 | |
| Rhombicity *R* | 0.143 | | 0.185 | | 0.256 | | 0.315 | | 0.435 | |
| Euler angle α | 32.8 | | 32.2 | | 31.2 | | 30.4 | | 27.5 | |
| Euler angle β | 88.2 | | 91.6 | | 95.3 | | 98.5 | | 106.1 | |
| Euler angle γ | 108.7 | | 124.8 | | 130.6 | | 131.6 | | 133.2 | |

**Table S10b.** RDCs ($^1D_{CH}$) and orientation properties extracted of (+)-IPC in a PBPM$^3$LG/$CDCl_3$ LLC phase (14.8 w%) at various temperatures. Continuation of table S10a. **[Sample DS-P75]**

| **RDC [Hz]** | **$^1D_{CH}$** | **σ** | **$^1D_{CH}$** | **σ** | **$^1D_{CH}$** | **σ** | **$^1D_{CH}$** | **σ** | **$^1D_{CH}$** | **σ** |
|---|---|---|---|---|---|---|---|---|---|---|
| **Temp.** | **290 K** | | **280 K** | | **270 K** | | **260 K** | | **255 K** | |
| C1-H1 | **-** | - | **-** | - | **-** | - | **-** | - | **-** | - |
| C2-H2 | **-** | - | **-** | - | **-** | - | **-** | - | **-** | - |
| C3-H3 | **33.38** | 2.06 | **37.89** | 1.33 | **42.82** | 1.66 | **43.88** | 10.06 | **45.57** | 9.60 |
| C4-H4s | **27.26** | 0.83 | **29.43** | 0.50 | **31.22** | 0.77 | **33.12** | 1.01 | **33.57** | 0.66 |
| C4-H4a | **-8.69** | 0.44 | **-8.06** | 1.14 | **-7.20** | 0.83 | **-5.47** | 0.69 | **-4.47** | 1.12 |
| C5-H5 | **4.16** | 1.43 | **3.49** | 1.15 | **2.60** | 1.71 | **1.57** | 2.64 | **0.12** | 2.46 |
| C7-H7s | **-3.20** | 1.50 | **-1.77** | 1.92 | **-4.32** | 1.26 | **-1.77** | 1.49 | **-1.52** | 4.69 |
| C7-H7a | **-18.16** | 1.73 | **-13.61** | 2.21 | **-7.75** | 1.63 | **-3.99** | 4.84 | **-1.56** | 1.53 |
| C8-H8 | **11.72** | 1.79 | **13.10** | 2.75 | **14.96** | 1.60 | **18.00** | 3.50 | **17.77** | 3.00 |
| C9-H9 | **-9.19** | 1.43 | **-9.71** | 1.34 | **-9.73** | 1.38 | **-13.37** | 3.99 | **-16.65** | 4.02 |
| C10-H10 | **-6.37** | 0.64 | **-7.43** | 0.53 | **-8.66** | 0.71 | **-9.57** | 0.57 | **-10.16** | 1.29 |
| Quality factor Q | 0.027 | | 0.042 | | 0.050 | | 0.077 | | 0.078 | |
| RMSD [Hz] | 0.430 | | 0.715 | | 0.911 | | 1.425 | | 1.489 | |
| Condition number | 2.858 | | 2.858 | | 2.858 | | 2.858 | | 2.858 | |
| GDO [$10^{-3}$] | 1.872 | | 2.078 | | 2.377 | | 2.482 | | 2.575 | |
| $D_a$ [$10^{-4}$] | 8.569 | | 9.330 | | 10.667 | | 11.047 | | 11.385 | |
| $D_r$ [$10^{-4}$] | 4.352 | | 5.284 | | 6.070 | | 6.529 | | 6.940 | |
| Rhombicity *R* | 0.508 | | 0.566 | | 0.560 | | 0.591 | | 0.610 | |
| Euler angle α | 24.1 | | 19.1 | | 16.0 | | 12.0 | | 10.2 | |
| Euler angle β | 113.3 | | 120.1 | | 125.9 | | 128.8 | | 130.4 | |
| Euler angle γ | 130.8 | | 128.4 | | 123.9 | | 120.4 | | 118.8 | |

**Table S11a.** RDCs ($^1D_{CH}$) and orientation properties extracted of (-)-IPC in a PBPM$^3$LG/THF-$d_8$ LLC phase (27.7 w%) at various temperatures. **[Sample DS-P76]**

| **RDC [Hz]** | **$^1D_{CH}$** | **σ** | **$^1D_{CH}$** | **σ** | **$^1D_{CH}$** | **σ** | **$^1D_{CH}$** | **σ** | **$^1D_{CH}$** | **σ** |
|---|---|---|---|---|---|---|---|---|---|---|
| **Temp.** | **325 K** | | **320 K** | | **315 K** | | **310 K** | | **300 K** | |
| C1-H1 | **14.04** | 1.31 | **14.65** | 2.35 | **14.83** | 1.40 | **15.56** | 1.14 | **16.87** | 1.94 |
| C2-H2 | **-7.15** | 0.90 | **-7.59** | 0.63 | **-7.70** | 0.63 | **-7.81** | 0.43 | **-8.44** | 0.42 |
| C3-H3 | **14.42** | 1.89 | **15.31** | 0.73 | **15.87** | 0.74 | **16.51** | 1.00 | **17.89** | 0.75 |
| C4-H4s | **10.43** | 0.31 | **11.26** | 0.27 | **12.35** | 0.43 | **13.49** | 0.38 | **15.98** | 0.36 |
| C4-H4a | **1.06** | 0.51 | **0.93** | 0.18 | **0.78** | 0.20 | **0.44** | 0.67 | **-0.29** | 0.93 |
| C5-H5 | **-8.52** | 0.73 | **-9.15** | 0.97 | **-8.76** | 0.79 | **-8.78** | 1.16 | **-8.73** | 0.45 |
| C7-H7s | **1.56** | 1.00 | **1.27** | 1.00 | **0.90** | 0.96 | **0.49** | 0.67 | **-0.22** | 1.27 |
| C7-H7a | **-18.35** | 0.63 | **-19.87** | 0.74 | **-21.38** | 0.38 | **-22.81** | 0.58 | **-25.82** | 1.19 |
| C8-H8 | **4.43** | 1.42 | **5.24** | 1.18 | **5.74** | 1.42 | **6.52** | 0.76 | **7.18** | 0.83 |
| C9-H9 | **-4.04** | 0.67 | **-4.36** | 0.43 | **-4.56** | 0.77 | **-4.96** | 0.38 | **-5.44** | 0.90 |
| C10-H10 | **-1.91** | 0.99 | **-2.14** | 0.73 | **-1.79** | 0.57 | **-2.56** | 0.57 | **-2.49** | 1.25 |
| Quality factor Q | 0.018 | | 0.027 | | 0.031 | | 0.034 | | 0.040 | |
| RMSD [Hz] | 0.171 | | 0.273 | | 0.327 | | 0.375 | | 0.491 | |
| Condition number | 1.661 | | 1.661 | | 1.661 | | 1.661 | | 1.661 | |
| GDO [$10^{-3}$] | 1.202 | | 1.284 | | 1.343 | | 1.413 | | 1.563 | |
| $D_a$ [$10^{-4}$] | 5.899 | | 6.301 | | 6.595 | | 6.940 | | 7.668 | |
| $D_r$ [$10^{-4}$] | 1.333 | | 1.416 | | 1.444 | | 1.541 | | 1.751 | |
| Rhombicity *R* | 0.226 | | 0.225 | | 0.219 | | 0.222 | | 0.228 | |
| Euler angle α | 44.2 | | 44.1 | | 43.4 | | 43.0 | | 42.3 | |
| Euler angle β | 76.0 | | 76.4 | | 77.5 | | 78.3 | | 79.6 | |
| Euler angle γ | 111.0 | | 111.3 | | 112.0 | | 111.1 | | 109.8 | |

**Table S11b.** RDCs ($^1D_{CH}$) and orientation properties extracted of (-)-IPC in a PBPM[3]LG/THF-$d_8$ LLC phase (27.7 w%) at various temperatures. Continuation of table S11a. **[Sample DS-P76]**

| RDC [Hz] | $^1D_{CH}$ | σ | $^1D_{CH}$ | σ | $^1D_{CH}$ | σ | $^1D_{CH}$ | σ | $^1D_{CH}$ | σ |
|---|---|---|---|---|---|---|---|---|---|---|
| **Temp.** | **290 K** | | **280 K** | | **270 K** | | **260 K** | | **255 K** | |
| C1-H1 | **18.01** | 1.66 | **21.24** | 1.30 | **23.10** | 5.54 | **27.77** | 3.80 | **29.81** | 5.66 |
| C2-H2 | **-9.28** | 0.63 | **-9.90** | 0.40 | **-9.99** | 1.87 | **-11.35** | 2.06 | **-11.83** | 2.29 |
| C3-H3 | **20.60** | 0.84 | **21.50** | 1.40 | **24.62** | 0.64 | **22.10** | 1.31 | **19.86** | 2.24 |
| C4-H4s | **18.28** | 0.50 | **20.66** | 0.43 | **23.15** | 0.30 | **25.81** | 0.80 | **27.01** | 0.82 |
| C4-H4a | **-0.94** | 1.14 | **-1.76** | 0.50 | **-2.02** | 0.76 | **-2.94** | 1.66 | **-3.54** | 1.58 |
| C5-H5 | **-8.90** | 0.79 | **-8.88** | 0.48 | **-8.89** | 0.92 | **-8.65** | 1.23 | **-8.55** | 0.56 |
| C7-H7s | **-0.95** | 1.29 | **-1.41** | 1.42 | **-2.70** | 0.77 | **-4.80** | 3.53 | **-4.96** | 2.16 |
| C7-H7a | **-28.01** | 0.62 | **-28.48** | 0.92 | **-26.58** | 0.91 | **-25.44** | 2.38 | **-23.44** | 1.09 |
| C8-H8 | **8.05** | 0.60 | **8.75** | 0.41 | **9.90** | 0.65 | **11.15** | 1.22 | **11.33** | 0.76 |
| C9-H9 | **-5.77** | 1.23 | **-6.29** | 0.52 | **-6.54** | 0.87 | **-7.04** | 0.41 | **-7.21** | 0.91 |
| C10-H10 | **-2.93** | 0.87 | **-2.73** | 0.29 | **-3.34** | 0.45 | **-3.33** | 1.38 | **-3.84** | 0.62 |
| Quality factor Q | 0.037 | | 0.036 | | 0.099 | | 0.133 | | 0.158 | |
| RMSD [Hz] | 0.504 | | 0.518 | | 1.512 | | 2.124 | | 2.537 | |
| Condition number | 1.661 | | 1.661 | | 1.661 | | 1.661 | | 1.661 | |
| GDO [$10^{-3}$] | 1.725 | | 1.831 | | 1.920 | | 1.977 | | 1.948 | |
| $D_a$ [$10^{-4}$] | 8.459 | | 8.931 | | 9.335 | | 9.465 | | 9.143 | |
| $D_r$ [$10^{-4}$] | 1.931 | | 2.327 | | 2.578 | | 3.290 | | 3.885 | |
| Rhombicity *R* | 0.228 | | 0.261 | | 0.276 | | 0.348 | | 0.425 | |
| Euler angle α | 41.9 | | 42.4 | | 43.5 | | 44.7 | | 45.8 | |
| Euler angle β | 80.5 | | 80.8 | | 81.4 | | 81.7 | | 81.5 | |
| Euler angle γ | 111.5 | | 106.0 | | 106.3 | | 96.0 | | 92.6 | |

**Table S12a.** RDCs ($^1D_{CH}$) and orientation properties extracted of (+)-IPC in a PBPM$^3$LG/THF-$d_8$ LLC phase (27.7 w%) at various temperatures. **[Sample DS-P77]**

| **RDC [Hz]** | **$^1D_{CH}$** | **σ** | **$^1D_{CH}$** | **σ** | **$^1D_{CH}$** | **σ** | **$^1D_{CH}$** | **σ** | **$^1D_{CH}$** | **σ** |
|---|---|---|---|---|---|---|---|---|---|---|
| **Temp.** | **325 K** | | **320 K** | | **315 K** | | **310 K** | | **300 K** | |
| C1-H1 | **9.53** | 1.04 | **9.78** | 0.93 | **8.78** | 1.13 | **9.60** | 1.44 | **11.27** | 1.00 |
| C2-H2 | **3.02** | 1.66 | **3.03** | 2.29 | **3.01** | 2.46 | **3.51** | 2.56 | **3.27** | 3.70 |
| C3-H3 | **10.32** | 2.27 | **10.95** | 1.14 | **11.84** | 1.36 | **12.50** | 1.09 | **13.70** | 1.65 |
| C4-H4s | **20.99** | 0.53 | **22.23** | 0.48 | **23.80** | 0.90 | **24.89** | 0.52 | **27.59** | 0.68 |
| C4-H4a | **-7.91** | 0.40 | **-8.24** | 0.35 | **-8.47** | 0.88 | **-8.88** | 0.61 | **-9.58** | 0.55 |
| C5-H5 | **-0.94** | 2.61 | **-0.66** | 2.60 | **-0.77** | 2.30 | **-0.64** | 2.39 | **-0.72** | 2.44 |
| C7-H7s | **-4.62** | 1.32 | **-6.85** | 2.02 | **-7.94** | 3.06 | **-8.18** | 1.80 | **-9.76** | 1.49 |
| C7-H7a | **-14.88** | 1.53 | **-16.56** | 0.97 | **-18.20** | 0.61 | **-18.99** | 1.02 | **-21.05** | 1.59 |
| C8-H8 | **6.06** | 0.99 | **6.62** | 0.93 | **7.19** | 0.78 | **7.51** | 0.70 | **8.74** | 0.67 |
| C9-H9 | **-2.49** | 0.71 | **-2.93** | 0.33 | **-3.18** | 0.95 | **-3.31** | 0.91 | **-3.90** | 0.84 |
| C10-H10 | **0.83** | 0.15 | **0.93** | 0.43 | **0.84** | 0.69 | **0.68** | 0.52 | **0.31** | 0.27 |
| Quality factor Q | 0.024 | | 0.037 | | 0.071 | | 0.056 | | 0.062 | |
| RMSD [Hz] | 0.222 | | 0.374 | | 0.764 | | 0.634 | | 0.773 | |
| Condition number | 1.661 | | 1.661 | | 1.661 | | 1.661 | | 1.661 | |
| GDO [$10^{-3}$] | 1.075 | | 1.176 | | 1.260 | | 1.323 | | 1.479 | |
| $D_a$ [$10^{-4}$] | -4.733 | | 5.145 | | 5.607 | | 5.875 | | 6.602 | |
| $D_r$ [$10^{-4}$] | -2.946 | | 3.293 | | 3.316 | | 3.508 | | 3.848 | |
| Rhombicity *R* | 0.622 | | 0.640 | | 0.591 | | 0.597 | | 0.583 | |
| Euler angle α | 150.6 | | 37.5 | | 37.1 | | 37.2 | | 38.0 | |
| Euler angle β | 168.0 | | 95.6 | | 96.3 | | 96.3 | | 96.0 | |
| Euler angle γ | 24.4 | | 99.6 | | 100.4 | | 100.3 | | 99.4 | |

**Table S12b.** RDCs ($^1D_{CH}$) and orientation properties extracted of (+)-IPC in a PBPM[3]LG/THF-$d_8$ LLC phase (27.7 w%) at various temperatures. Continuation of table S12a. **[Sample DS-P77]**

| **RDC [Hz]** | **$^1D_{CH}$** | **σ** | **$^1D_{CH}$** | **σ** | **$^1D_{CH}$** | **σ** | **$^1D_{CH}$** | **σ** | **$^1D_{CH}$** | **σ** |
|---|---|---|---|---|---|---|---|---|---|---|
| **Temp.** | **290 K** | | **280 K** | | **270 K** | | **260 K** | | **255 K** | |
| C1-H1 | **11.98** | 1.05 | **13.08** | 1.93 | **13.93** | 1.52 | **14.56** | 1.36 | **15.46** | 3.87 |
| C2-H2 | **3.84** | 4.02 | **3.64** | 5.50 | **3.55** | 5.72 | **5.01** | 2.39 | **3.25** | 3.49 |
| C3-H3 | **16.80** | 1.54 | **17.65** | 3.02 | **18.14** | 3.13 | **17.82** | 4.48 | **16.88** | 3.78 |
| C4-H4s | **30.39** | 0.65 | **32.79** | 0.76 | **35.43** | 0.60 | **38.25** | 0.96 | **39.21** | 0.75 |
| C4-H4a | **-10.51** | 0.63 | **-10.70** | 0.89 | **-10.99** | 1.17 | **-11.70** | 0.62 | **-12.01** | 1.19 |
| C5-H5 | **-0.68** | 1.39 | **0.10** | 0.95 | **-0.16** | 0.88 | **0.92** | 1.21 | **1.22** | 1.88 |
| C7-H7s | **-11.16** | 2.15 | **-11.07** | 1.90 | **-13.84** | 6.38 | **-12.11** | 2.34 | **-10.04** | 2.69 |
| C7-H7a | **-22.44** | 1.30 | **-23.76** | 2.16 | **-21.57** | 1.39 | **-22.62** | 2.75 | **-22.72** | 1.45 |
| C8-H8 | **9.66** | 0.42 | **10.73** | 0.76 | **11.94** | 0.83 | **13.14** | 1.25 | **13.86** | 1.07 |
| C9-H9 | **-4.70** | 0.90 | **-5.37** | 0.87 | **-5.85** | 0.66 | **-6.45** | 0.75 | **-6.80** | 0.57 |
| C10-H10 | **0.11** | 0.73 | **-0.10** | 0.51 | **-0.36** | 0.81 | **-0.63** | 0.33 | **-0.74** | 0.68 |
| Quality factor Q | 0.064 | | 0.057 | | 0.105 | | 0.089 | | 0.117 | |
| RMSD [Hz] | 0.884 | | 0.843 | | 1.606 | | 1.420 | | 1.882 | |
| Condition number | 1.661 | | 1.661 | | 1.661 | | 1.661 | | 1.661 | |
| GDO [$10^{-3}$] | 1.643 | | 1.746 | | 1.811 | | 1.878 | | 1.865 | |
| $D_a$ [$10^{-4}$] | 7.399 | | 7.873 | | 8.052 | | 8.176 | | -8.140 | |
| $D_r$ [$10^{-4}$] | 4.123 | | 4.358 | | 4.787 | | 5.333 | | -5.249 | |
| Rhombicity *R* | 0.557 | | 0.554 | | 0.594 | | 0.652 | | 0.644 | |
| Euler angle α | 38.2 | | 37.9 | | 39.9 | | 38.4 | | 162.5 | |
| Euler angle β | 96.3 | | 96.2 | | 96.7 | | 97.2 | | 269.0 | |
| Euler angle γ | 100.9 | | 100.5 | | 99.6 | | 99.6 | | 35.6 | |

## Experimental Procedures

PBPM$^3$LG was synthesized via an eight step protocol (Scheme S1).
The reaction protocol starts with the synthesis of the boronic acid[16] **5**, which is afterwards used for a cross-coupling reaction with *p*-bromo-*m*-methylbenzoic acid methyl ester **4** to form biphenyl **6**.[17] After reduction[18] of **6** to the substituted biphenyl methanol **7**, an APPEL-reaction[19] yields the halogenated biphenyl **8**. Key step in this reaction protocol is the esterification[20] of copper(II)-protected L-glutamic acid **9** with **8** to form L-glutamic acid ester **10**. A reaction[21, 6] of **10** with phosgene yields NCA **11**, which is polymerized to PBPM$^3$LG with the corresponding initiator triethylamine (TEA) or diethylmethanolamine (DMEA).[22] As the polymerization is sensitive to even minor impurities, the requirements for the purity of the employed monomer (*N*-carboxyanhydride, NCA) are relatively high.[23] Diffusion-driven crystallization[9] could not be utilized to purify this NCA, hence, column chromatography under inert conditions was carried out.[24]

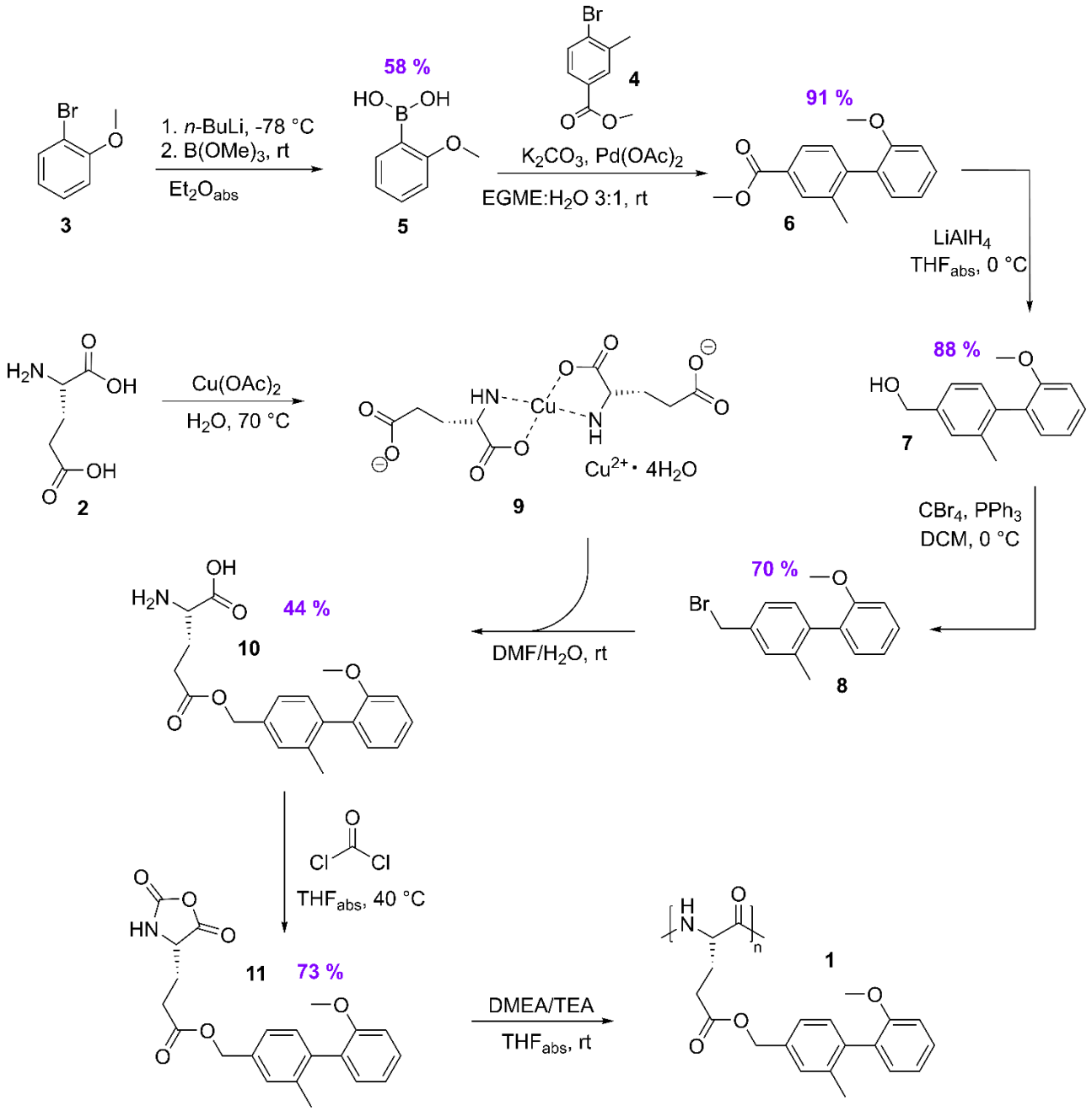


**Scheme S1.** Eight step protocol to synthesize PBPM$^3$LG. EGME = 2-methoxyethanol.

Atom assignment in the NMR spectra was carried out using 2D-NMR-spectroscopy. Characteristic IR bands were extracted and assigned to the respective resonances, excluding -C-H and C=C-H stretching bands, which are existent in every compound. As ATR-IR spectra were recorded, the resulting intensities of the bands might be unexpected.

To assure stereochemical purity in our starting materials and analytes, the specific rotation of the enantiomers of IPC (after sublimation) and glutamic acid have been measured:

**L-glutamic acid** $[\alpha]_{589}^{20°C}$ 31.9° (β = 1.003·10$^{-3}$ g/mL. 6N HCl)

**(+)-IPC** $[\alpha]_{589}^{20°C}$ 40.9° (β = 1.113·10$^{-3}$ g/mL. EtOH)

**(-)-IPC** $[\alpha]_{589}^{20°C}$ -41.5° (β = 1.085·10$^{-3}$ g/mL. EtOH)

**(+)-IPC** $[\alpha]_{589}^{20°C}$ 33.6° (β = 1.510·10$^{-3}$ g/mL. $CDCl_3$)

**(-)-IPC** $[\alpha]_{589}^{20°C}$ -31.2° (β = 1.571·10$^{-3}$ g/mL. $CDCl_3$)

The measurements are in good agreement with the literature.[25]

**Synthesis of *o*-methoxybenzeneboronic acid (5)**
IUPAC: (2-methoxyphenyl)boronic acid

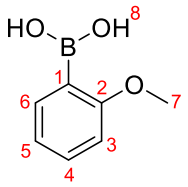


According to a literature procedure[16], 75.0 g (389 mmol, 1 equiv.) 2-bromoanisole **3** were dissolved in 250 mL dry diethyl ether in a Schlenk flask under argon atmosphere. The solution was cooled to -78 °C and 171 mL (428 mmol, 1.1 equiv.) *n*-buthyllithium (2.5 M in *n*-hexane) were added dropwise. The reaction mixture was stirred for 2 h, followed by the addition of 45 mL (389 mmol, 1.0 equiv.) $B(OMe)_3$. The reaction mixture was stirred overnight at room temperature. After the addition of 100 mL HCl (2 N) the product was extracted in 5 portions of diethyl ether (150 mL). The resulting organic mixture was dried over magnesium sulfate and concentrated under reduced pressure. The crude product was recrystallized from *n*-hexane.
**[DS-02-65]** [DS-02-74] [DS-PG-01-01]

**Product yield, properties:** 34.3 g (58 %), colorless crystal.

***R*F** 0.81 [V(ethyl acetate):V(cyclohexane) = 1:1]

**$^1$H-NMR**($CDCl_3$, 500 MHz, 300 K) δ/ppm = 7.90 (dd, *J* = 7.15, 1.3 Hz, $1H_6$), 7.48 - 7.44 (m, $1H_4$), 7.05 (φt, *J* = 7.34Hz, $1H_5$), 6.92 (d, *J* = 8.31 Hz, $1H_3$), 6.67 (s, 2B-$OH_8$), 3.92 (s, $3H_7$).

**$^{13}$C-NMR**($CDCl_3$, 125 MHz, 300 K) δ/ppm = 164.63 ($C_2$), 136.99 ($C_6$), 132.94 ($C_4$), 121.36 ($C_5$), 118.63 (bs, $C_1$), 110.08 ($C_3$), 55.56 ($C_7$).

The obtained NMR spectra for **5** are in agreement with the NMR spectra of *o*-methoxybenzeneboronic acid[16].

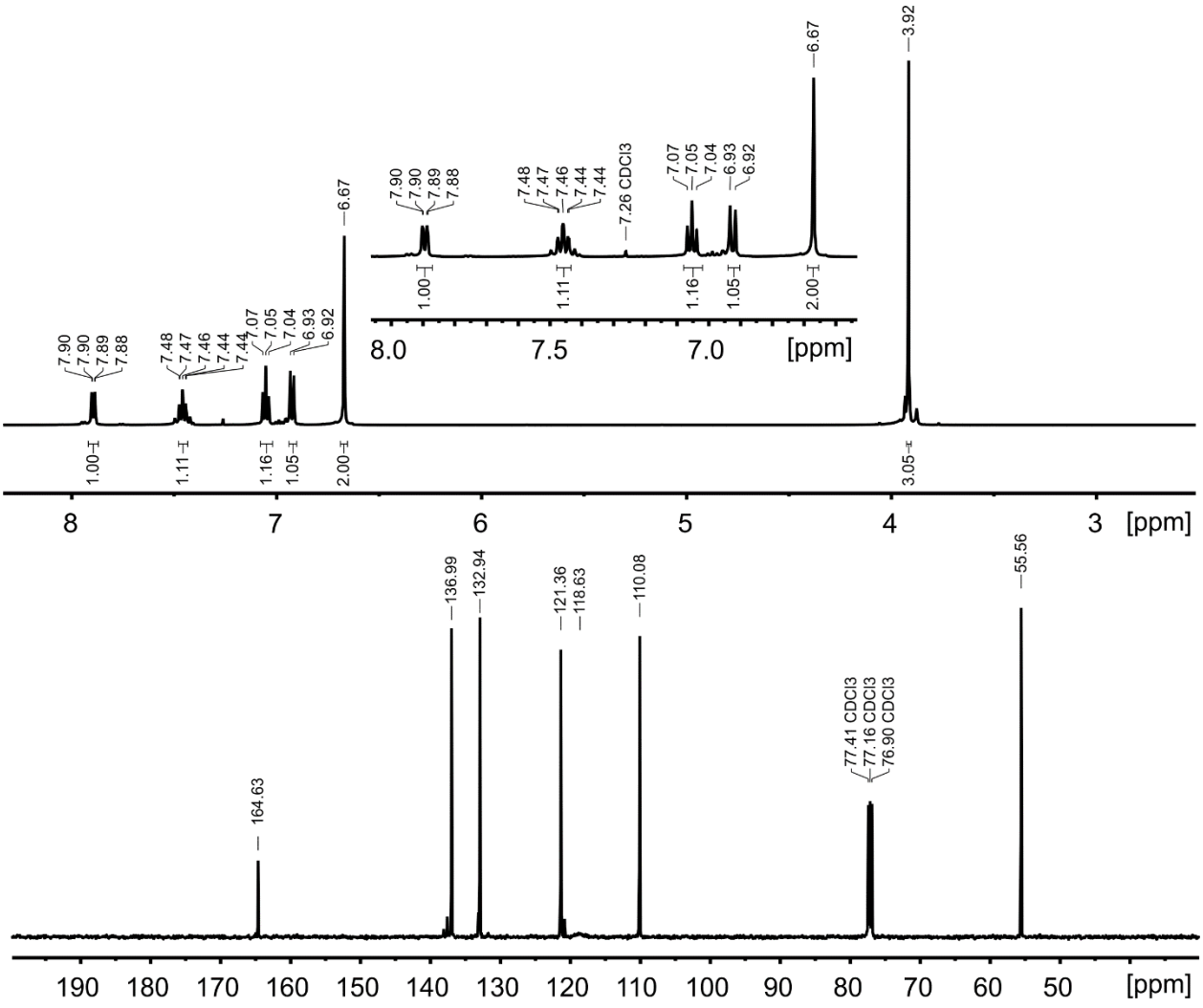

**EI-MS:** Theory: m/z: 152 $[M]^{+\cdot}$

Experimental: m/z: 152 $[M]^{+\cdot}$, 134 ($[M]^{+\cdot}$-$H_2O$), 108 ($[M]^{+\cdot}$-$B(OH)_2$)

**HR EI-MS:** Theory: m/z: 152.0641 $[M]^{+\cdot}$

Experimental: m/z: 152.0641 $[M]^{+\cdot}$

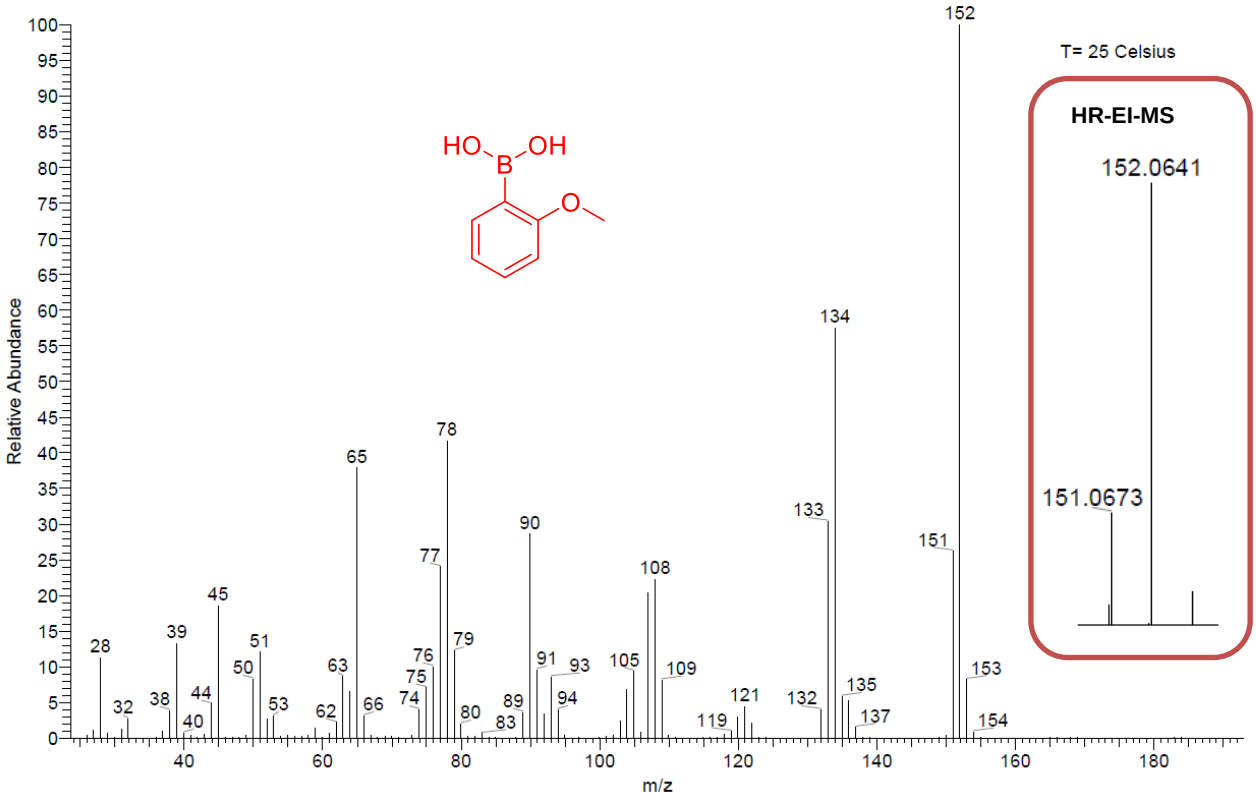


**IR** $\tilde{\nu}$ / $cm^{-1}$ 3350 (br) -O-H stretching

750 (vs) =C-H bending (1,2 disubstituted benzene)

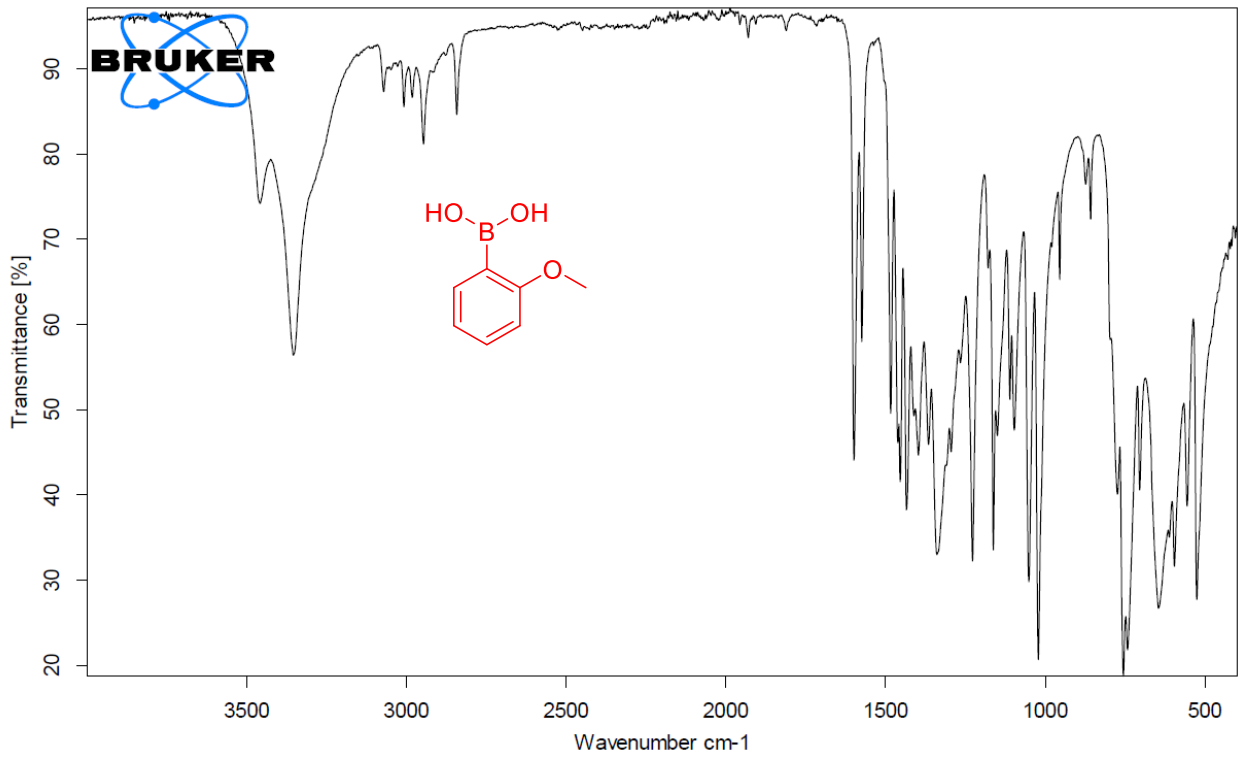

**Synthesis of *m*-methyl-*p*-(*o*-methoxyphenyl) benzoic acid methyl ester (6)**
IUPAC: methyl 2'-methoxy-2-methyl-[1,1'-biphenyl]-4-carboxylate

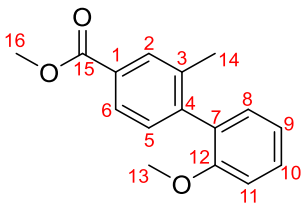


According to a literature procedure[17], 27.0 g (118 mmol, 1 equiv.) *p*-bromo-*m*-methylbenzoic acid methyl ester **4**, 19.5 g (141 mmol, 1.2 equiv.) potassium carbonate and 19.7 g (130 mmol, 1.1 equiv.) *o*-methoxybenzeneboronic acid **5** were dissolved in a mixture 2-methoxyethanol (EGME) : water (400 mL, 3:1). After adding 25 mg palladium(II) acetate, the reaction mixture was stirred overnight. After filtration over celite, the product was extracted with dichloromethane (300 mL), dried over magnesium sulfate and concentrated under reduced pressure. Purification was carried out using column chromatography [V(dichloromethane):V(cyclohexane) = 2:1].
**[DS-02-86]** [DS-02-75] [DS-02-66] [DS-02-59] [DS-PG-01-02]

**Product yield, properties:** 27.5 g (91 %), maroon oil.

***R*F** 0.69 [V(ethyl acetate):V(cyclohexane) = 1:2]

**$^{1}$H-NMR**($CDCl_3$, 400 MHz, 300 K) δ/ppm = 7.94 (s, $1H_2$), 7.90 (dd, *J* = 7.9, 1.5 Hz, $1H_6$), 7.39 - 7.35 (m, $1H_{10}$), 7.26 (d, *J* = 7.9 Hz, $1H_5$), 7.13 (dd, *J* = 7.42, 1.78 Hz, $1H_8$), 7.03 (φtd, 7.42, 1.78 Hz, $1H_9$), 6.98 (d, *J* = 8.3 Hz, $1H_{11}$), 3.93 (s, $3H_{16}$), 3.76 (s, $3H_{13}$), 2.19 (s, $3H_{14}$).

**$^{13}$C-NMR**($CDCl_3$, 100 MHz, 300 K) δ/ppm = 167.42 ($C_{15}$), 156.51 ($C_{12}$), 143.81 ($C_4$), 137.38 ($C_3$), 130.88 ($C_2$), 130.70 ($C_8$), 130.33 ($C_5$), 130.05 ($C_7$), 129.23 ($C_{10}$), 129.11 ($C_1$), 126.84 ($C_6$), 120.70 ($C_9$), 110.91 ($C_{11}$), 55.55 ($C_{13}$), 52.15 ($C_{16}$), 20.10 ($C_{14}$).

**$^{1}$H-NMR**

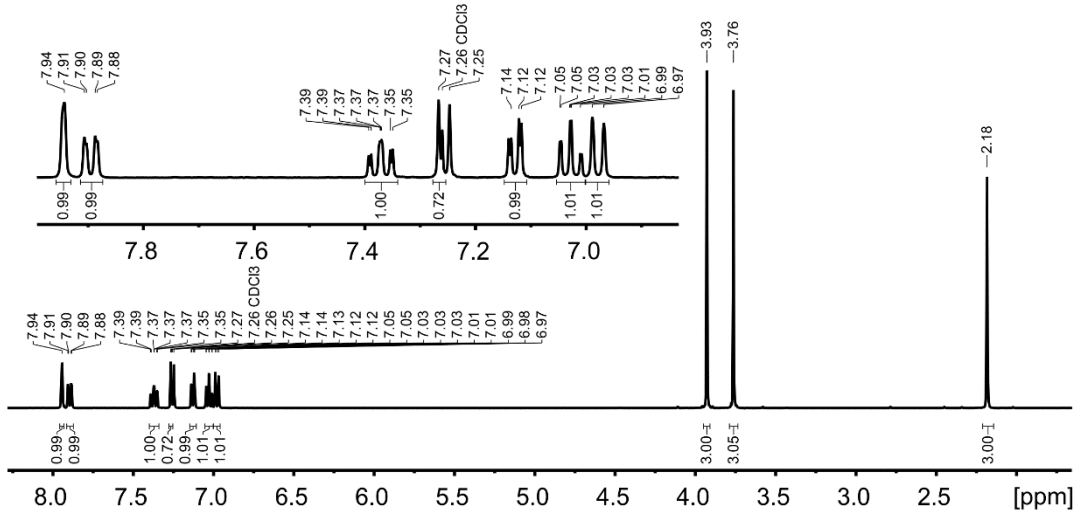


**$^{13}$C-NMR**

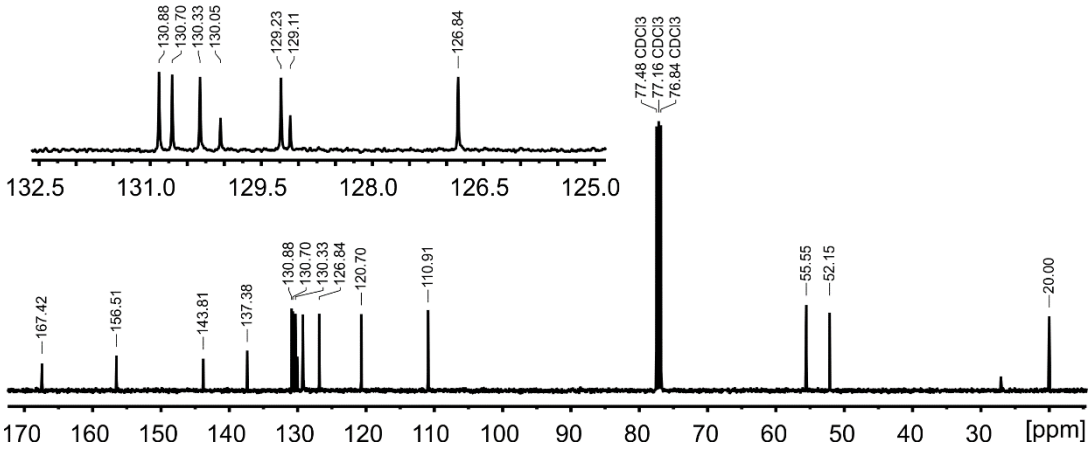

**EI-MS:** Theory: m/z: 256 $[M]^{+\cdot}$

Experimental: m/z: 256 $(M]^{+\cdot}$, 226 ($[M]^{+\cdot}$-OMe)

**HR EI-MS:** Theory: m/z: 256.1094 $[M]^{+\cdot}$

Experimental: m/z: 256.1093 $[M]^{+\cdot}$

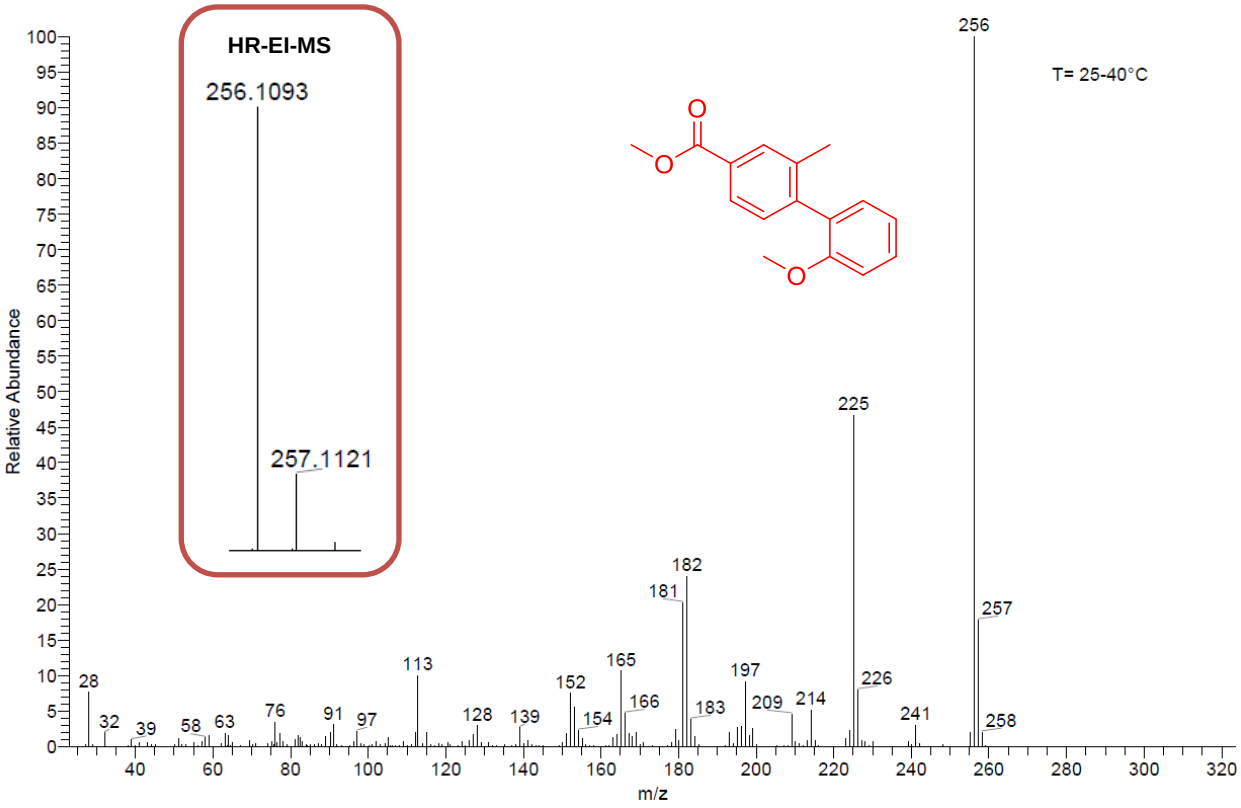


**IR** $\tilde{\nu}$ / $cm^{-1}$

| | |
|---|---|
| 2915 (vs) | -C-H stretching |
| 1720 (vs) | -C=O stretching (ester) |
| 740 (m) | =C-H bending (1,2 disubstituted benzene) |

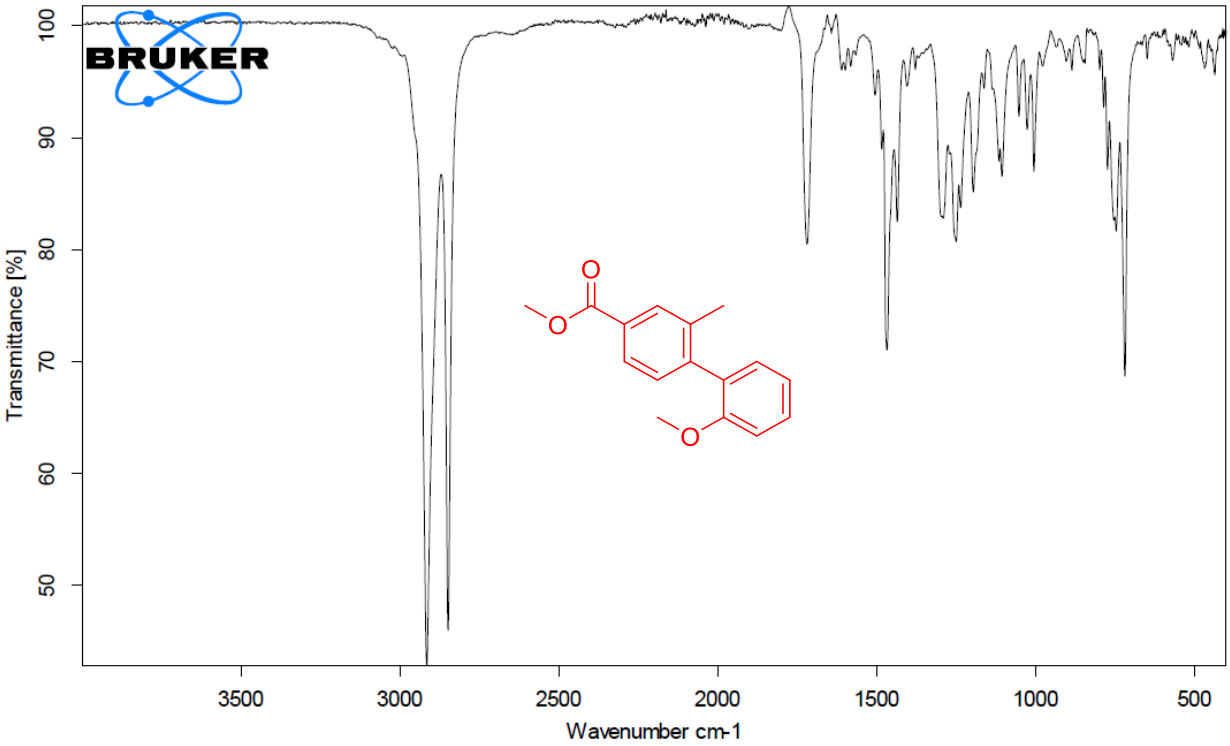

**Synthesis of *m*-methyl-*p*-(*o*-methoxyphenyl) benzyl alcohol (7)**
IUPAC: (2'-methoxy-2-methyl-[1,1'-biphenyl]-4-yl)methanol

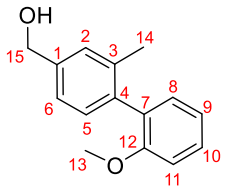


According to a literature procedure[18], 30.0 g (117 mmol, 1 equiv.) *m*-methyl-*p*-(*o*-methoxyphenyl) benzoic acid methyl ester **6** were dissolved in 250 mL dry THF under argon atmosphere and cooled to 0 °C. Lithium aluminum hydride (3.51 g, 88 mmol, 0.75 equiv.) was added portionwise and the resulting mixture was stirred at room temperature overnight. 1 M HCl (100 mL) was added slowly and the remaining solid was removed by filtration and washed with dichloromethane. The aqueous layer containing the product was extracted with dichloromethane and the combined organic layers were dried over magnesium sulfate and concentrated under vacuum. **[DS-02-88]** [DS-02-76][DS-02-67] [DS-02-60] [DS-PG-01-03]

**Product yield, properties:** 23.6 g (88 %), colorless oil.

***R*F** 0.10 [V(ethyl acetate):V(cyclohexane) = 1:5]

**$^1$H-NMR**($CDCl_3$, 400 MHz, 300 K) δ/ppm = 7.35 (φtd, *J* = 7.4, 1.5 Hz, $1H_{10}$), 7.27 (s, $1H_2$), 7.24 (d, *J* = 7.8 Hz, $1H_6$), 7.19 (d, *J* = 7.8 Hz, $1H_5$), 7.14 (dd, *J* = 7.4, 1.8 Hz, $1H_8$), 7.02 (φtd, *J* = 7.4, 1.0 Hz, $1H_9$), 6.97 (d, *J* = 8.3 Hz, $1H_{11}$), 4.71 (s, $2H_{15}$), 3.77 (s, $3H_{13}$), 2.16 (s, $3H_{14}$).

**$^{13}$C-NMR**($CDCl_3$, 100 MHz, 300 K) δ/ppm = 156.76 ($C_{12}$), 139.94 ($C_1$), 138.28 ($C_4$), 137.32 ($C_3$), 131.13 ($C_8$), 130.64 ($C_7$), 130.42 ($C_5$), 128.78 ($C_{10}$), 128.51 ($C_2$), 124.30 ($C_6$), 120.61 ($C_9$), 110.81 ($C_{11}$), 65.52 ($C_{15}$), 55.54 ($C_{13}$), 20.05 ($C_{14}$).

**$^1$H-NMR**

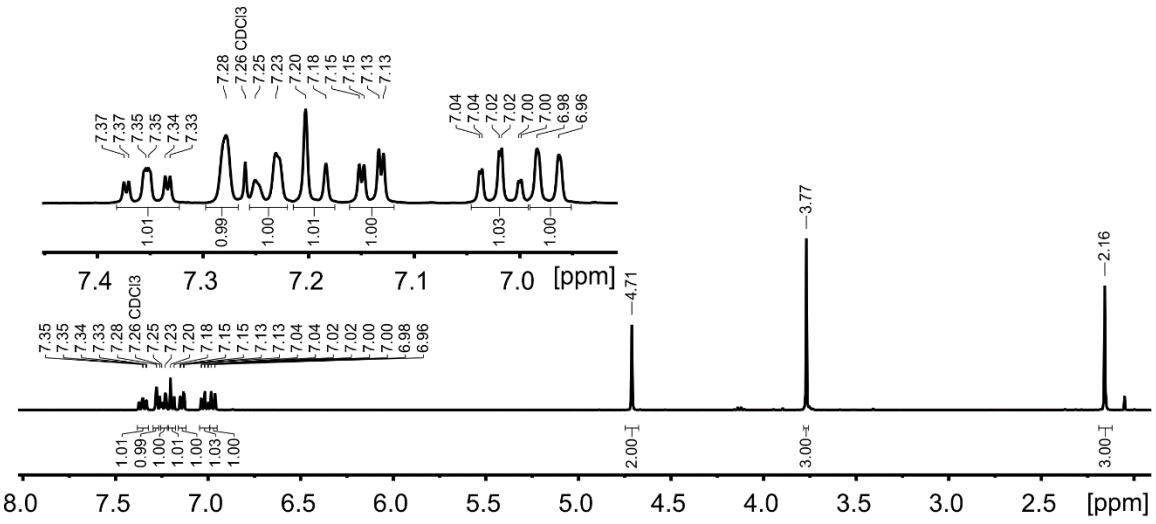


**$^{13}$C-NMR**

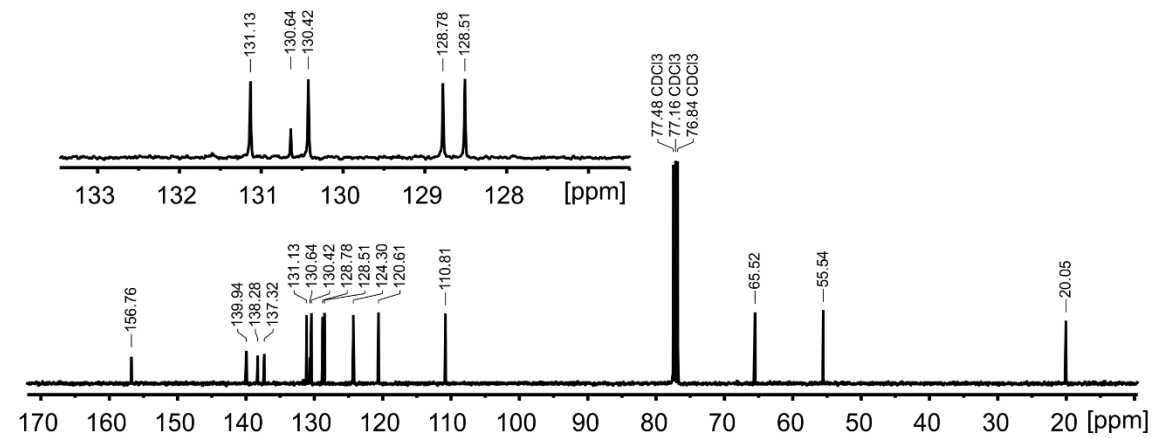

**EI-MS:** Theory: m/z: 228 $[M]^{+\cdot}$
Experimental: m/z: 228 $[M]^{+\cdot}$

**HR EI-MS:** Theory: m/z: 228.1145 $[M]^{+\cdot}$
Experimental: m/z: 228.1145 $[M]^{+\cdot}$

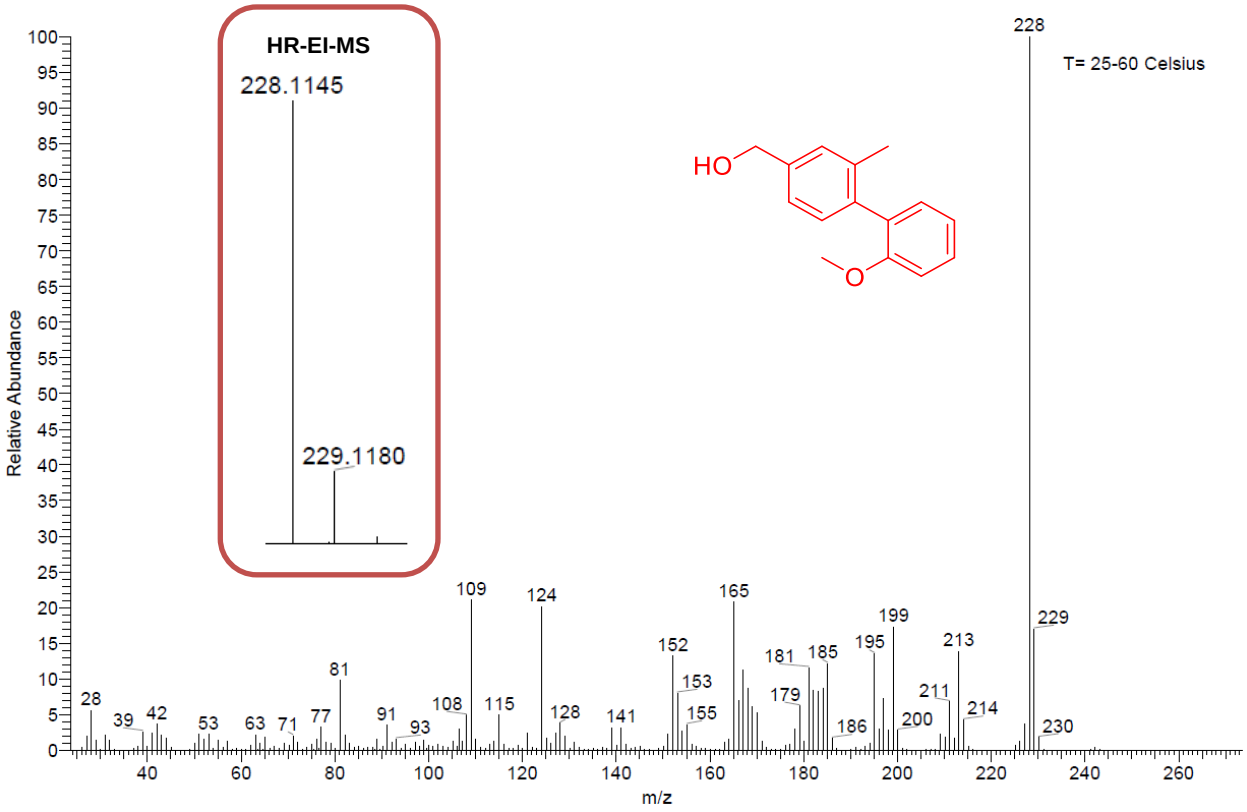


**IR** $\tilde{\nu}$ / $cm^{-1}$ 3340 (br) -O-H stretching
750 (vs) =C-H bending (1,2 disubstituted benzene)

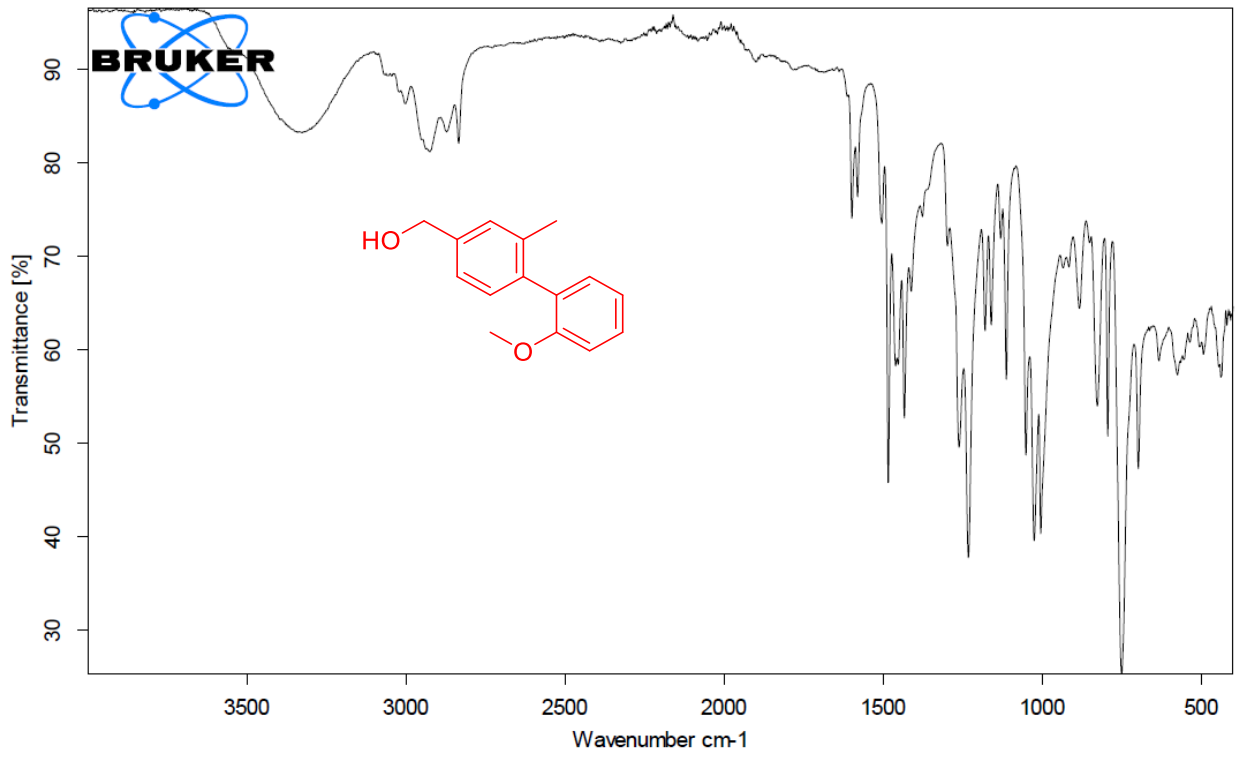

**Synthesis of *m*-methyl-*p*-(*o*-methoxyphenyl) benzyl bromide (8)**
IUPAC: 4-(bromomethyl)-2'-methoxy-2-methyl-1,1'-biphenyl

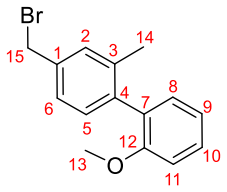


According to a literature procedure[19b], 33.5 g (147 mmol, 1 equiv.) of *m*-methyl-*p*-(*o*-methoxyphenyl) benzyl alcohol **7** and 54.6 g (161 mmol, 1.1 equiv.) tetrabromomethane were dissolved in 300 mL dry dichloromethane and cooled to 0 °C. 42.8 g (161 mmol, 1.1 equiv.) triphenylphosphine were added under vigorous stirring. The reaction mixture was stirred for 3 hours at room temperature, followed by concentration under reduced pressure. Purification was carried out by column chromatography with *n*-hexane.
**[DS-02-92]** [DS-02-68] [DS-02-62] [DS-02-61] [DS-PG-01-04]

**Product yield, properties:** 30.0 g (70 %), colorless crystal.

$R_F$ 0.77 [V(ethyl acetate):V(cyclohexane) = 1:2]

**$^1$H-NMR**($CDCl_3$, 400 MHz, 300 K) δ/ppm = 7.35 (φtd, *J* = 8.2, 1.8 Hz, $1H_{10}$), 7.29 (s, $1H_2$), 7.24 (dd, *J* = 7.8, 1.4 Hz, $1H_6$), 7.19 (d, *J* = 7.7 Hz, $1H_5$), 7.14 (dd, *J* = 7.4, 1.8 Hz, $1H_8$), 7.02 (φtd, *J* = 7.4, 1.0 Hz, $1H_9$), 6.97 (d, *J* = 8.3 Hz, $1H_{11}$), 4.53 (s, $2H_{15}$), 3.77 (s, $3H_{13}$), 2.14 (s, $3H_{14}$).

**$^{13}$C-NMR**($CDCl_3$, 100 MHz, 300 K) δ/ppm = 156.71 ($C_{12}$), 139.15 ($C_1$), 137.62 ($C_4$), 136.63 ($C_3$), 131.07 ($C_8$), 130.66 ($C_5$), 130.45 ($C_2$), 130.30 ($C_7$), 128.93 ($C_{10}$), 126.29 ($C_6$), 120.64 ($C_9$), 110.82 ($C_{11}$), 55.53 ($C_{15}$), 33.97 ($C_{13}$), 20.01 ($C_{14}$).

**$^1$H-NMR**

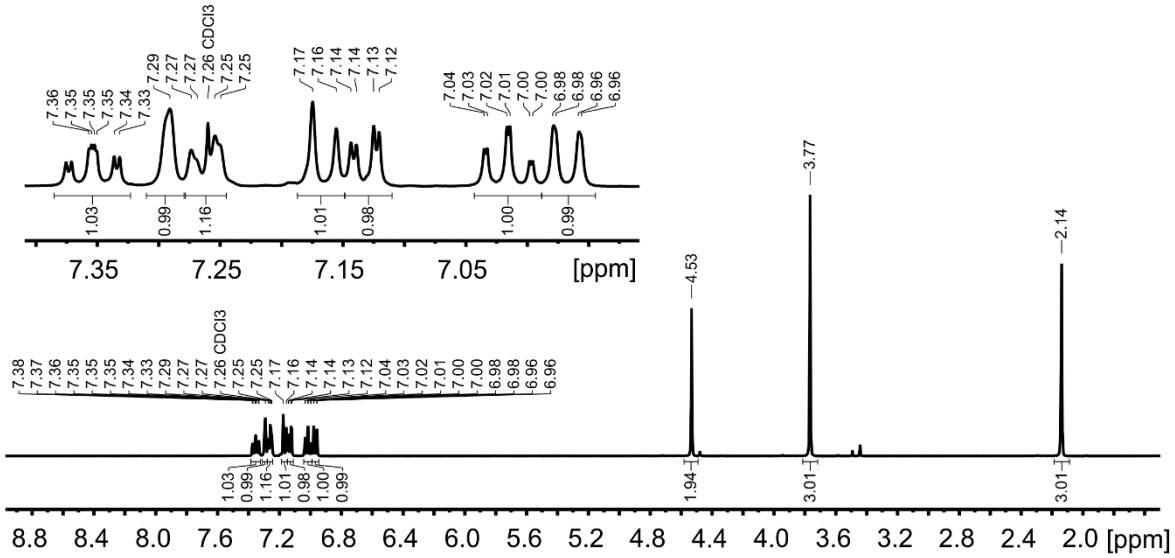


**$^{13}$C-NMR**

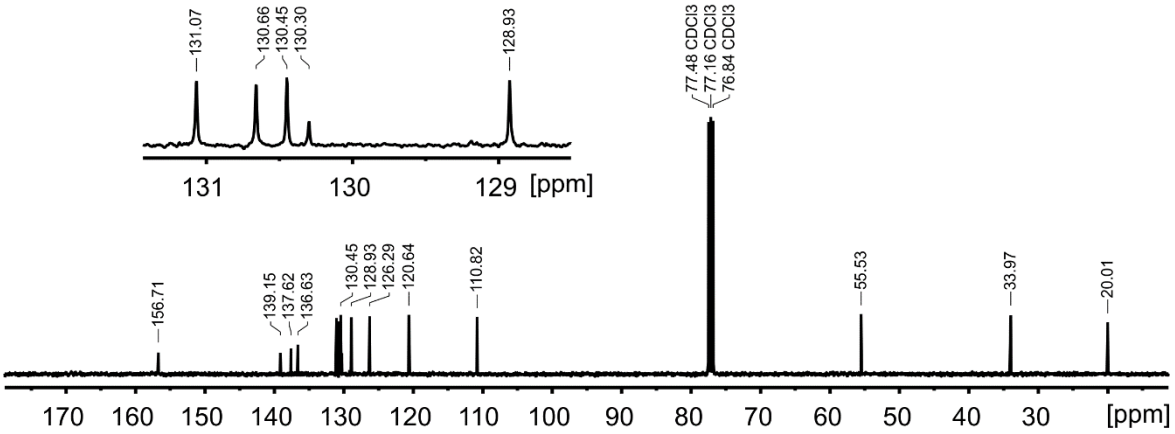

**EI-MS:** Theory: m/z: 290 $[M]^{+\cdot}$
Experimental: m/z: 290 ($[M]^{+\cdot}$), 211 ($[M]^{+\cdot}$-$Br^{\cdot}$)

**HR EI-MS:** Theory: m/z: 290.0301 $[M]^{+\cdot}$
Experimental: m/z: 290.0300 $[M]^{+\cdot}$

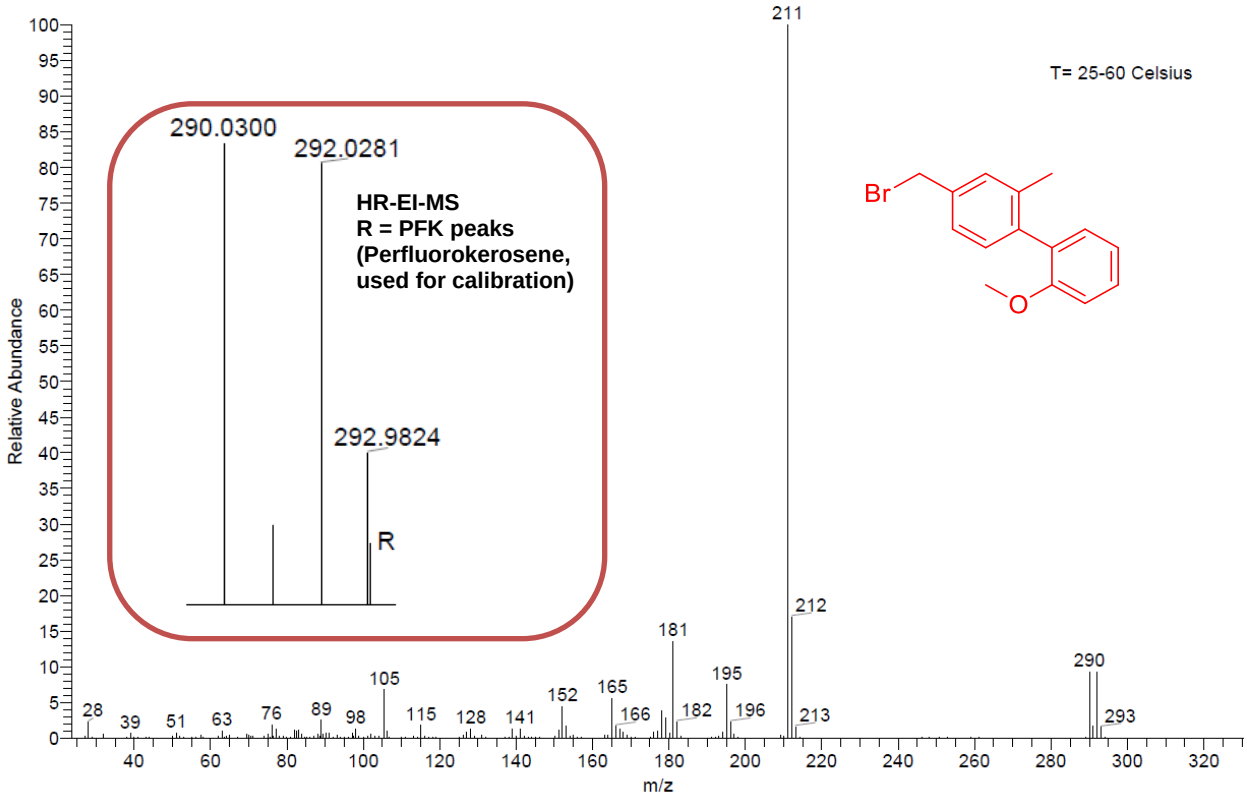


**IR** $\tilde{\nu}$ / $cm^{-1}$ 760 (vs) =C-H bending (1,2 disubstituted benzene)
625 (s) -C-Br stretching

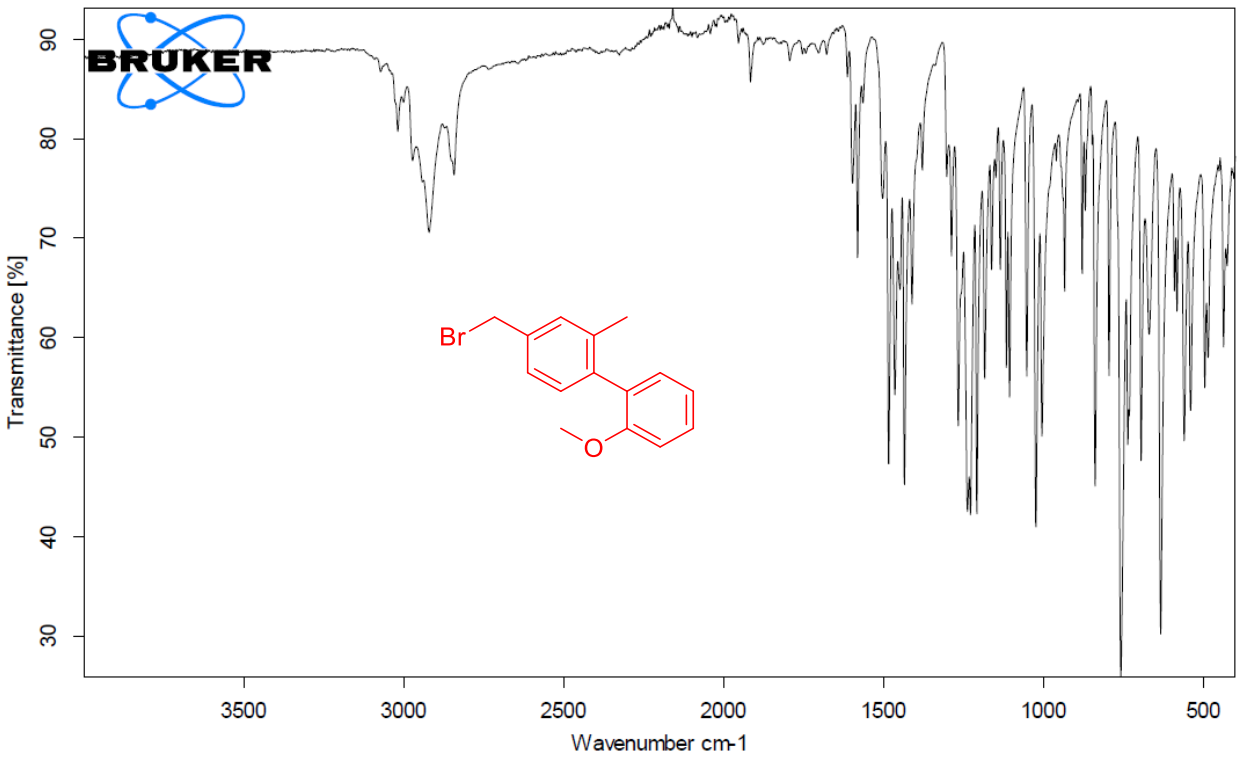

**Synthesis of L-glutamic acid γ-p-biphenylmethyl ester (*m*-methyl-*p*-(*o*-methoxyphenyl) (10)**
IUPAC: (S)-2-amino-5-((2'-methoxy-2-methyl-[1,1'-biphenyl]-4-yl)methoxy)-5-oxopentanoic acid

Following literature procedures[20], 29.4 g (198 mmol, 1.0 equiv) glutamic acid **2** was suspended in 750 mL of water. A solution of 41.5 g (208 mmol, 1.05 equiv) copper(II) acetate monohydrate in 750 mL water was added dropwise to this suspension at 70 °C. After addition, the solution was allowed to cool to room temperature. After filtration, the crude product was washed with water, ethanol and diethyl ether and dried in high vacuum. The L-glutamic acid copper(II) complex **9** obtained was used in the synthesis of **10** without further purification or characterization.

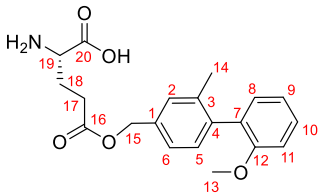

The L-glutamic acid copper(II) complex **9** (6.4 g, 15 mmol, 0.28 equiv.) and L-glutamic acid **2** (4.9 g, 33 mmol, 0.6 equiv.) were suspended in water (4.5 mL). 7 mL 1,1,3,3-tetramethylguanidine (55 mmol, 1 equiv.) were added and the reaction mixture was stirred for 2 hours until a homogenous solution was formed. 16 g (55 mmol, 1 equiv.) *m*-methyl-*p*-(*o*-methoxyphenyl) benzyl bromide **9** in 40 mL DMF was added, and the reaction mixture was stirred for 2 days at room temperature. After the addition of 250 mL acetone, the precipitant was filtered, washed with 200 mL acetone and vigorously stirred in 500 mL EDTA solution (3.6 g EDTA, 2.1 g $NaHCO_3$) for 3 hours. The product was extracted with chloroform, dried over magnesium sulfate and additionally dried in high vacuum.
**[DS-PG-01-08]** [DS-PG-01-06] [DS-PG-01-05] [DS-02-73] [DS-02-72]

**Product yield, properties:** 8.6 g (44 %), light blue solid.

***R*F** 0.15 [V(dichloromethane):V(cyclohexane) = 1:2]

**$^1$H-NMR**($CDCl_3$, 400 MHz, 300 K) δ/ppm = 7.28 (φtd, *J* = 7.6, 1.8 Hz, $1H_{10}$), 7.15 (s, $1H_2$), 7.11 (d, *J* = 7.8 Hz, $1H_6$), 7.01 - 6.97 (m, $3H_{5,8,11}$), 6.92 (φt, *J* = 7.32 Hz, $1H_9$), 5.01 (s, $2H_{15}$), 3.87 (φt, *J* = 6.6 Hz, $1H_{19}$), 3.61 (s, $3H_{13}$), 2.60 (ddd, *J* = 17.0, 9.1, 6.5 Hz, $1H_{17a}$), 2.50 - 2.45 (m, $1H_{17b}$), 2.10 - 2.00 (m, $2H_{18}$), 1.94 (s, $3H_{14}$).

**$^{13}$C-NMR**($CDCl_3$, 100 MHz, 300 K) δ/ppm = 172.30 ($C_{16}$), 170.65 ($C_{20}$), 156.69 ($C_{12}$), 138.88 ($C_4$), 136.91 ($C_3$), 135.31 ($C_1$), 131.00, 130.50 ($C_{5,8}$), 130.11 ($C_7$), 129.74 ($C_2$), 129.59 ($C_{10}$), 125.78 ($C_6$), 121.06 ($C_9$), 111.76 ($C_{11}$), 66.27 ($C_{15}$), 55.85 ($C_{13}$), 51.53 ($C_{19}$), 29.91 ($C_{17}$), 25.54 ($C_{18}$), 20.12 ($C_{14}$).

**$^1$H-NMR**

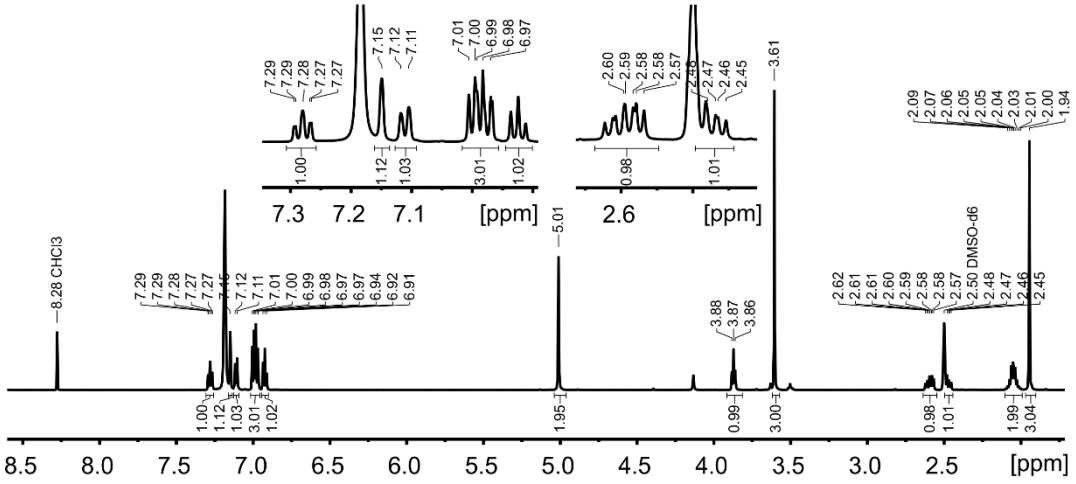


**$^{13}$C-NMR**

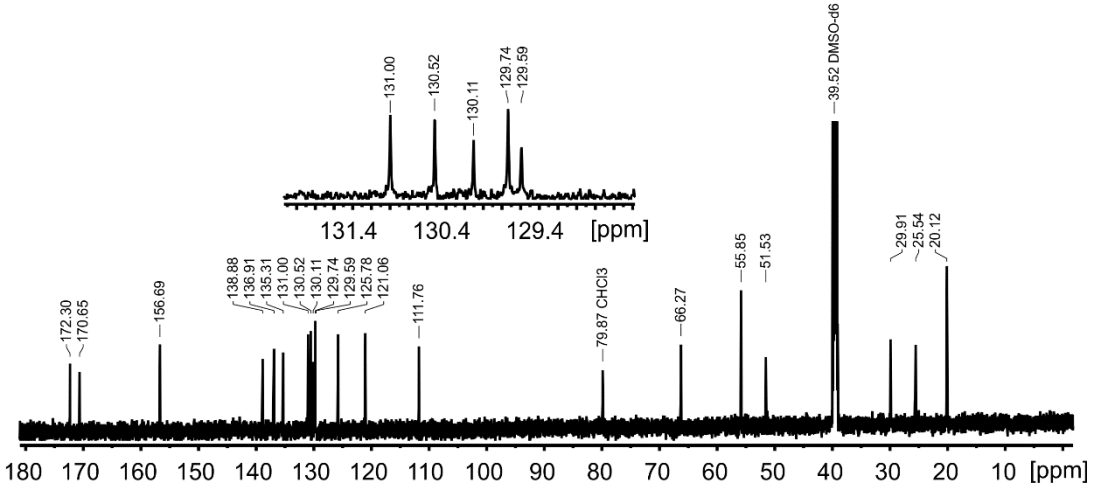

**EI-MS:** Theory: m/z: 357 $[M]^{+\cdot}$
Experimental: m/z: 357 $[M]^{+\cdot}$

**HR ESI-MS:** Theory: m/z: 358.16490 $[M+H]^{+}$
Experimental: m/z: 358.16495 $[M+H]^{+}$

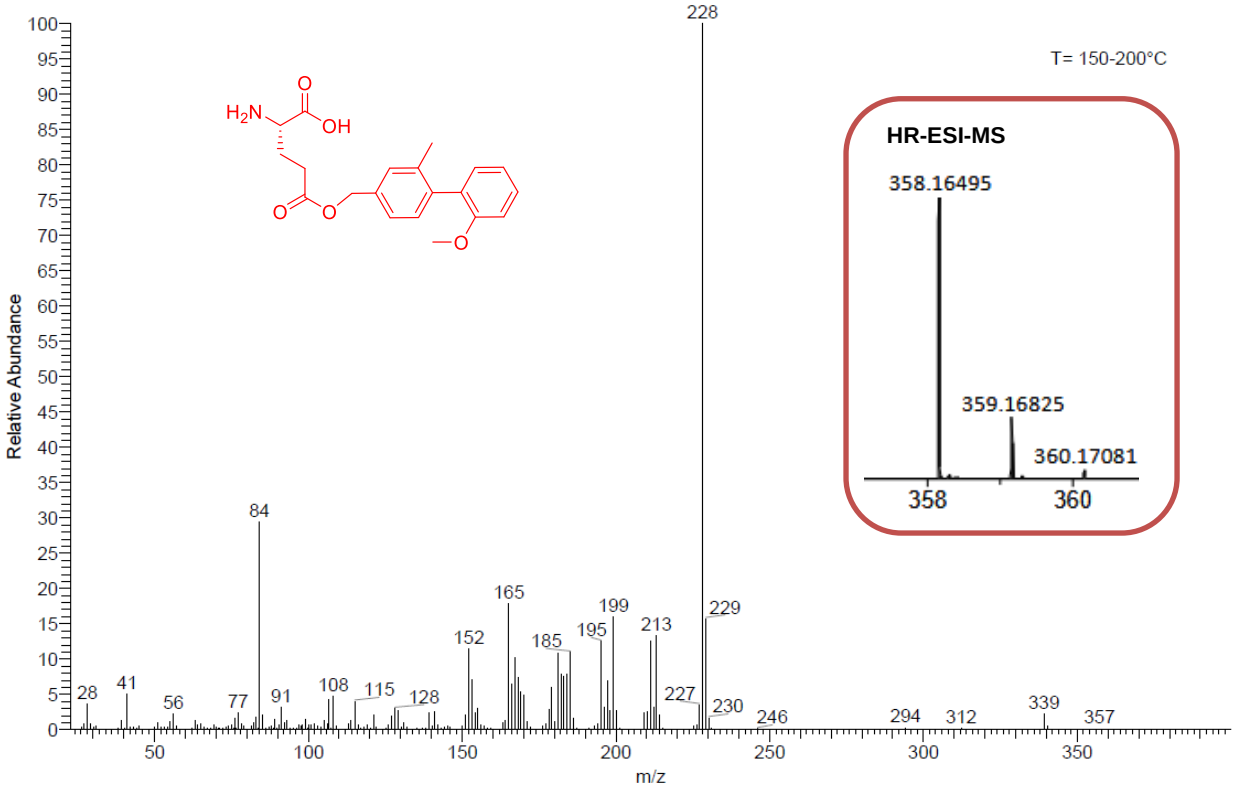


**IR** $\tilde{\nu}$ / $cm^{-1}$ 3225-2400 (br) -O-H stretching (acid / $-NH_3^+$ stretching amino acid hydrochloride)
1730 (s) -C=O stretching (acid)
750 (vs) =C-H bending (1,2 disubstituted benzene)

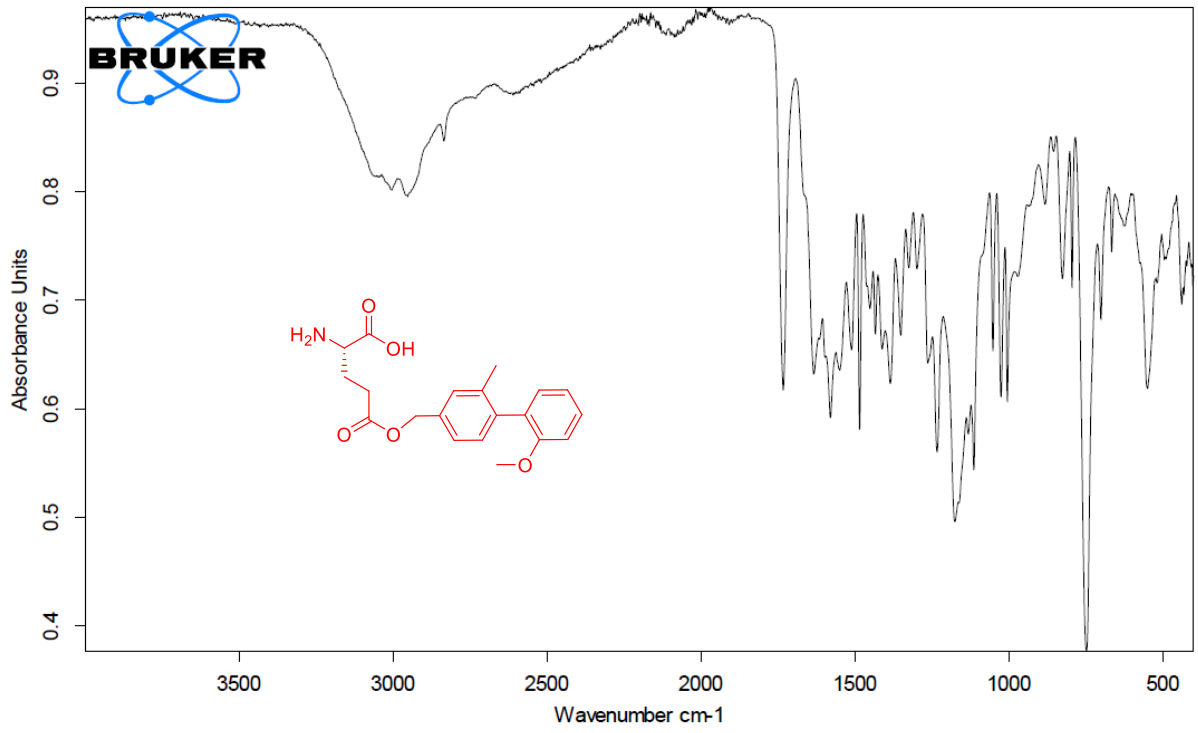


$[\alpha]_{589}^{20°C}$ 12.7° (β = 1.100·$10^{-3}$ g/mL, DMSO)

**Synthesis of L-glutamic acid γ-*p*-biphenylmethyl ester-*N*-carboxyanhydride (*m*-methyl-*p*-(*o*-methoxyphenyl) (11)**
IUPAC: (2'-methoxy-2-methyl-[1,1'-biphenyl]-4-yl)methyl (S)-3-(2,5-dioxooxazolidin-4-yl)propanoate

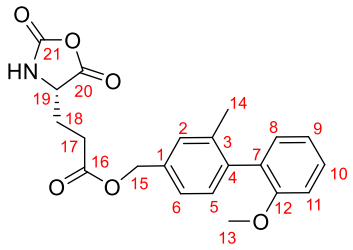

Based on a literature procedure[21, 6], 8.58 g (24 mmol, 1 equiv.) L-glutamic acid γ-p-biphenylmethyl ester **10** were suspended in 150 mL dry THF in a flame dried Schlenk flask under argon atmosphere. 15.4 mL (20% w/w in toluene, 29 mmol, 1.2 equiv.) phosgene were added and stirred at 40 °C for 2 hours until a clear solution was formed and stirred overnight at room temperature. The mixture was filtered through a syringe filter (0.45 µm PTFE) and concentrated under reduced pressure. Purification was carried out using column chromatography [V(ethyl acetate):V(*n*-hexane) = 1:1] under argon atmosphere.
**[DS-PG-01-09] [DS-PG-01-07]** [DS-02-64]

**Product yield, properties:** 6.7 g (73 %), colorless crystalline powder.

**$^{1}$H-NMR**(THF-$d_8$, 700 MHz, 300K): δ/ppm = 7.95 (s, NH), 7.30 (φtd, *J* = 8.3, 1.7 Hz, 1H$_{10}$), 7.21 (s, 1H$_2$), 7.16 (d, *J* = 7.7 Hz, 1H$_6$), 7.07 (d, *J* = 7.7 Hz, 1H$_5$), 7.05 (dd, *J* = 7.4, 1.7 Hz, 1H$_8$), 7.00 (d, *J* = 8.2 Hz, 1H$_{11}$), 6.95 (φtd, *J* = 7.4, 0.8 Hz, 1H$_9$), 5.10 (s, 2H$_{15}$), 4.40 (φt, *J* = 6.5 Hz, 1H$_{19}$), 3.70 (s, 3H$_{13}$), 2.54 (t, *J* = 7.5 Hz, 2H$_{17}$), 2.21 - 2.15 (m, 1H$_{18a}$), 2.09 (s, 3H$_{14}$). 2.10 - 2.00 (dφq, 14.3, 7.21 Hz, 1H$_{18b}$).

**$^{13}$C-NMR**(THF-$d_8$, 175 MHz, 300K): δ/ppm = 172.32 (C$_{16}$), 171.39 (C$_{20}$), 157.75 (C$_{12}$), 152.60 (C$_{21}$), 139.91 (C$_4$), 137.65 (C$_3$), 135.86 (C$_1$), 131.44 (C$_8$), 131.41 (C$_7$), 130.88 (C$_5$), 130.16 (C$_2$), 129.45 (C$_{10}$), 126.04 (C$_6$), 121.08 (C$_9$), 111.54 (C$_{11}$), 66.87 (C$_{15}$), 57.33 (C$_{19}$), 55.43 (C$_{13}$), 29.93 (C$_{17}$), 28.01 (C$_{18}$), 20.05 (C$_{14}$).

**$^{1}$H-NMR**

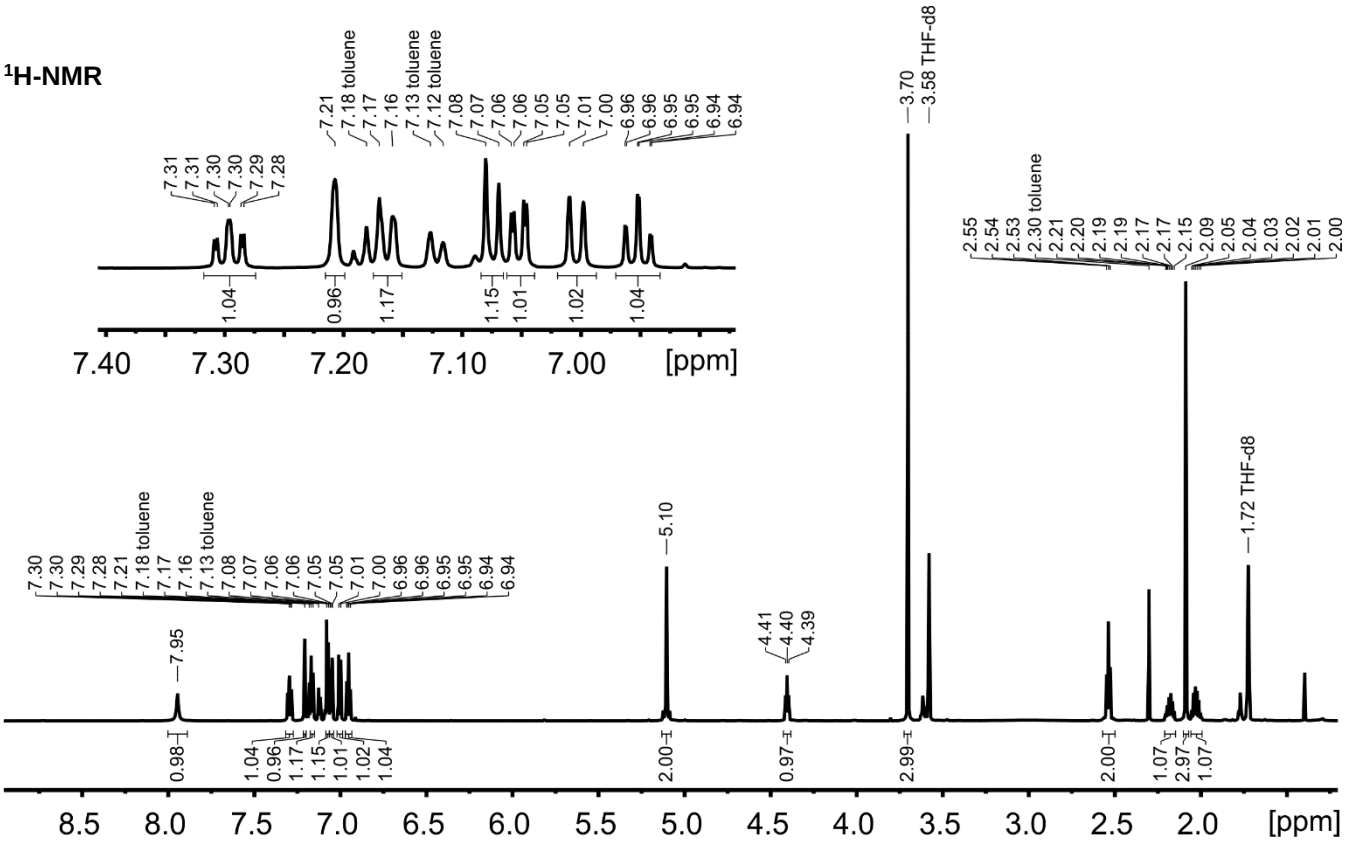

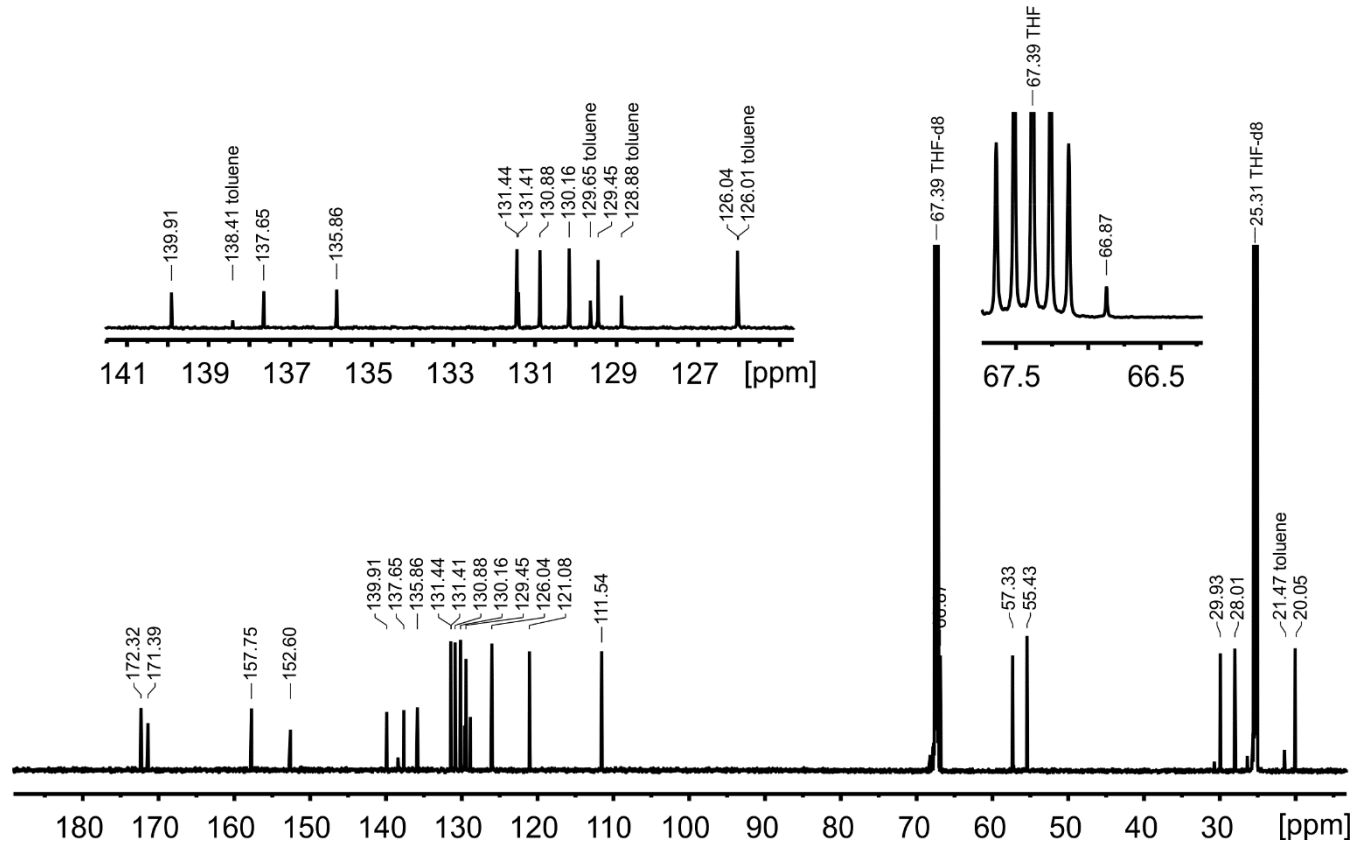


**IR** $\tilde{\nu}$ / $cm^{-1}$

| | |
|---|---|
| 3315 (w) | -N-H stretching (amide) |
| 1855 (m), | -C=O stretching (anhydride) |
| 1780 (vs) | -C=O stretching |
| 1730 (s) | -C=O stretching |
| 750 (vs) | =C-H bending (1,2 disubstituted benzene) |

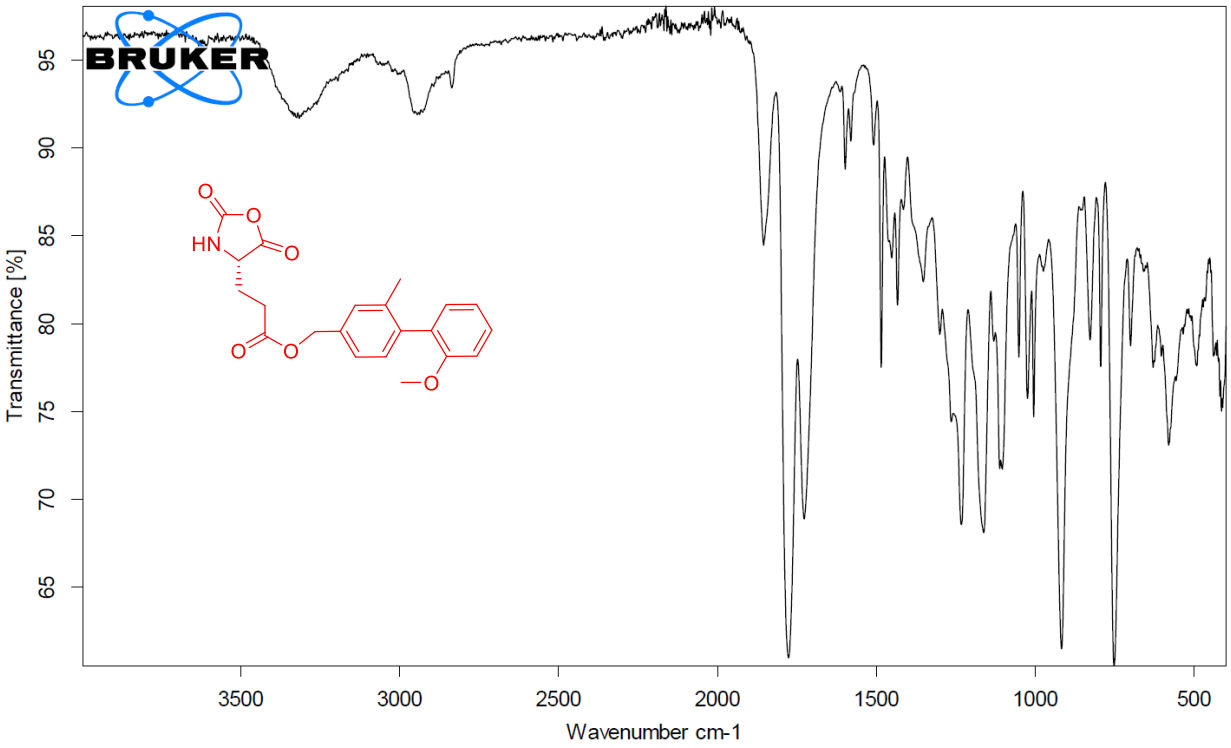

**PBPM$^3$LG (poly-*γ*-*p*-biphenyl(2'-methoxy-2-methyl)methyl-L-glutamate) (1)**

The syntheses of the polymers were performed under argon atmosphere with flame dried glassware. $THF_{abs.}$ was degassed via the freeze-pump-thaw procedure before dissolving the NCA monomer **11** with a concentration of 0.1 M in $THF_{abs}$ in a glovebox under argon atmosphere. The corresponding amount of the initiator triethylamine (TEA 10 μL) or diethylmethanolamine (DMEA M:I 400:1) was added quickly and the suspension was stirred at room temperature for several days. Polymerization progress was monitored via IR-spectroscopy (characteristic band of NCA at around 1800 $cm^{-1}$ decreases). The resulting polymer solution was added dropwise to acidic MeOH (1 % conc. HCl) and stirred for 30 minutes. The precipitate was filtrated, washed with MeOH and dried in high vacuum. After dissolving the dry polymer in $CHCl_3$, the resulting solution was once again added dropwise to *n*-hexane. Again, the precipitated polymer was filtrated and dried in high vacuum.[6]

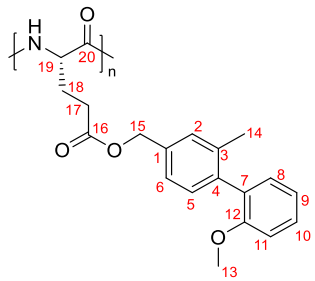

**$^1$H-NMR**($CDCl_3$ + TFA-$d_1$, 700MHz, 300K): δ/ppm = 7.31 (φtd, *J* = 7.8, 1.8 Hz, $H_{10}$), 7.13 (s, $H_2$), 7.09 (s, $2H_{5,6}$), 7.04 (dd, *J* = 7.4, 1.7 Hz, $H_8$), 6.98 (φt, *J* = 7.4 Hz, $H_9$), 6.95 (d, *J* = 8.3 Hz, $H_{11}$) 5.07 (2d, *J* = 12.0 Hz, $2H_{15a,15b}$), 4.65 (dd, *J* = 9.7, 4.8 Hz, $H_{19}$), 3.71 (s, $3H_{13}$), 2.53 - 2.51 (m, $2H_{17}$), 2.19 - 2.14 (m, $H_{18a}$), 2.05 (s, $3H_{14}$), 2.02 - 1.95 (m, $H_{18b}$).

**$^{13}$C-NMR**($CDCl_3$ + TFA-$d_1$, 175MHz, 300K): δ/ppm = 175.34 ($C_{16}$), 173.13 ($C_{20}$), 156.13 ($C_{12}$), 138.85 ($C_4$), 137.47 ($C_3$), 133.76 ($C_1$), 131.15 ($C_8$), 130.62 ($C_7$), 130.51 ($C_5$), 129.92 ($C_2$), 129.01 ($C_{10}$), 125.68 ($C_6$), 121.44 ($C_9$), 111.72 ($C_{11}$), 68.05 ($C_{15}$), 55.89 ($C_{13}$), 53.38 ($C_{19}$), 30.19 ($C_{17}$), 27.18 ($C_{18}$), 19.64 ($C_{14}$).

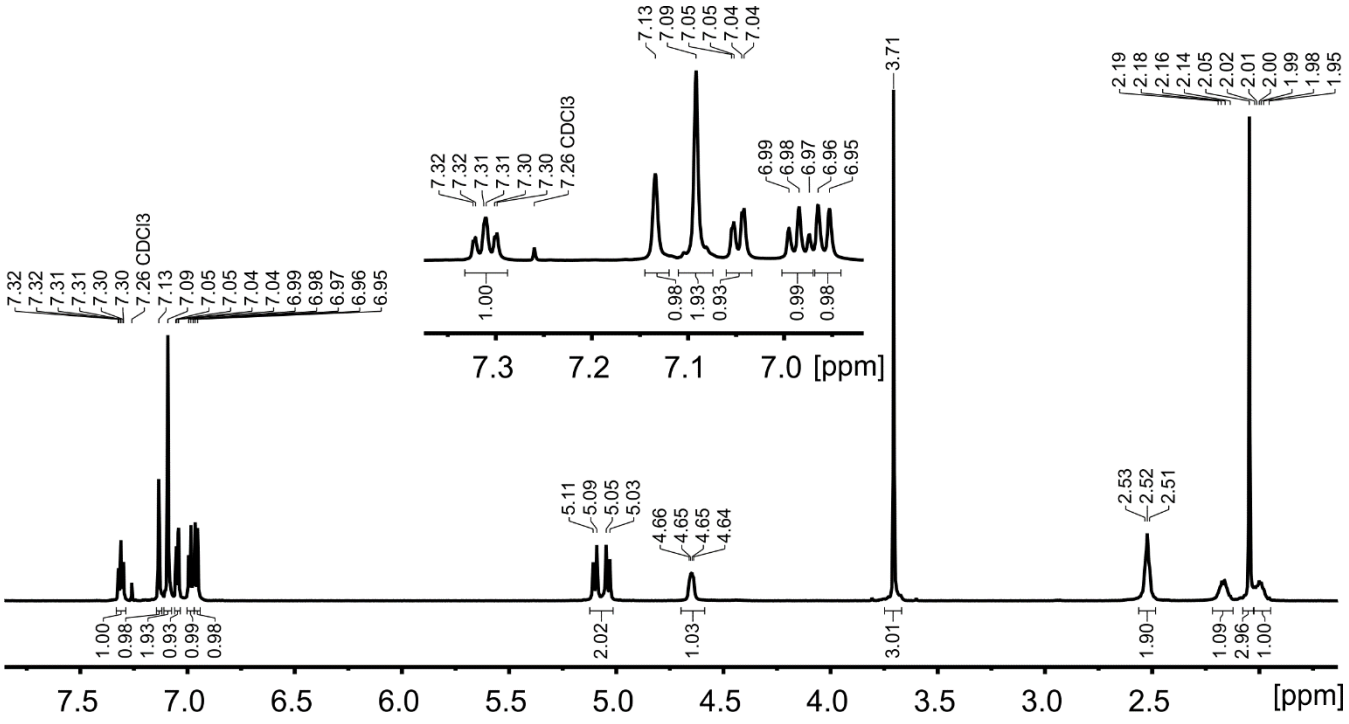

**$^{13}$C-NMR**

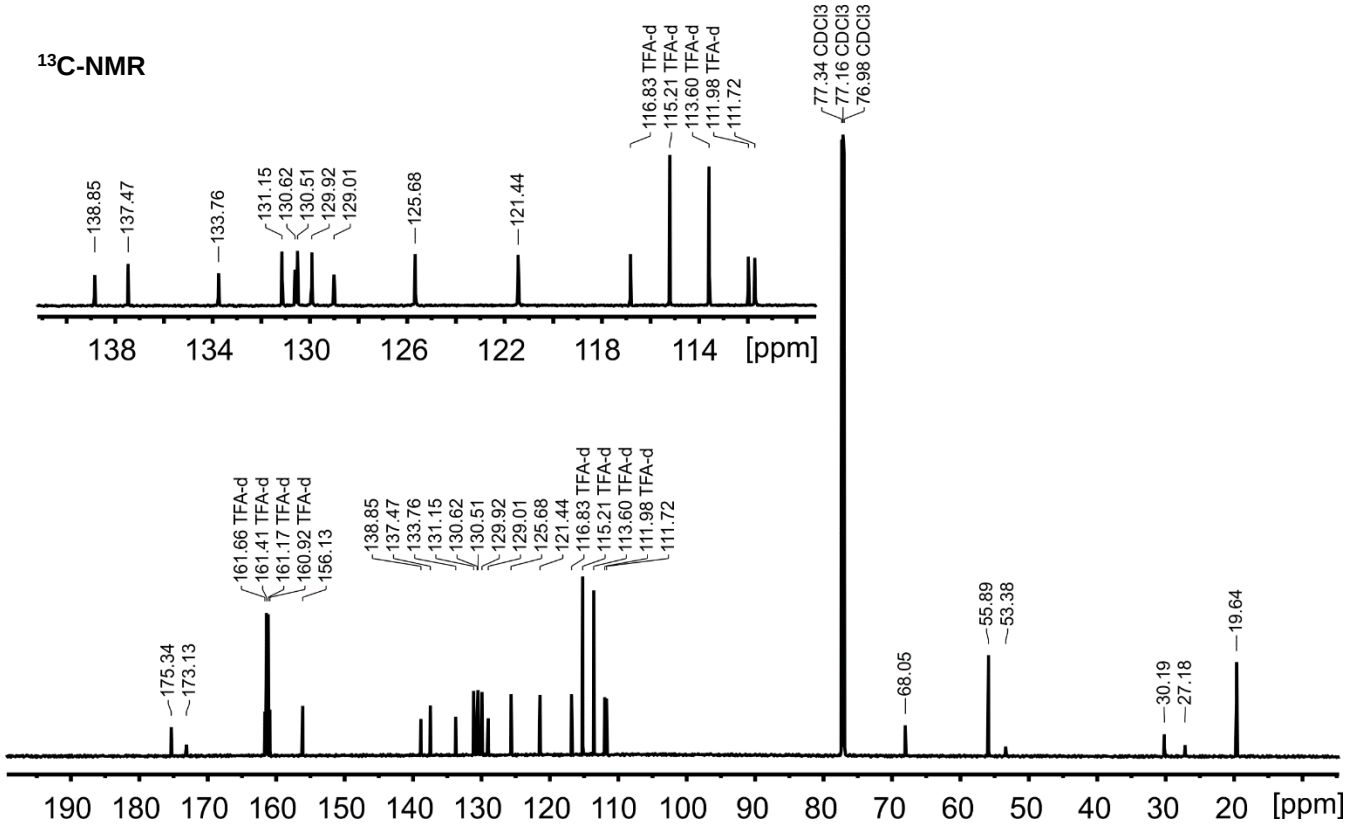


**IR** $\tilde{\nu}$ / cm$^{-1}$

| | |
|---|---|
| 3280 (br) | -N-H stretching (amide) |
| 1730 (m) | -C=O stretching (ester) |
| 1650 (s) | -C=O stretching (amide) |
| 750 (m) | =C-H bending (1,2 disubstituted benzene) |

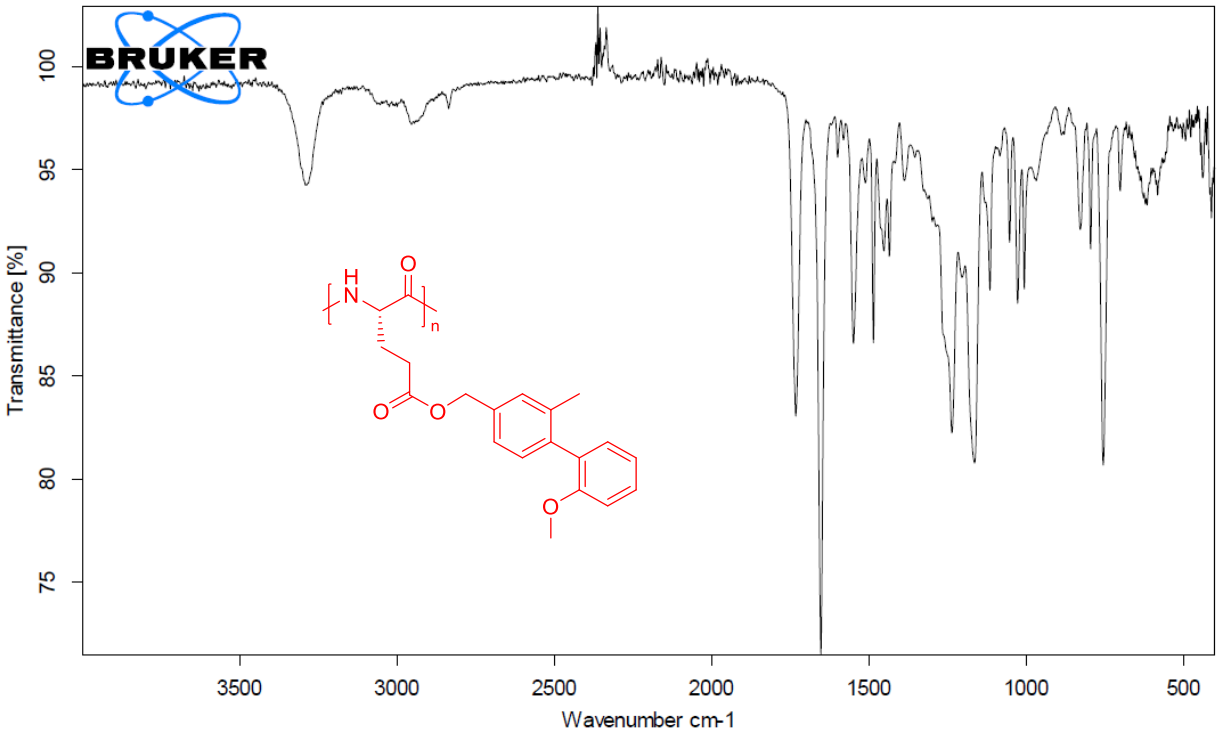

**MALDI-spectrum of PBPM$^3$LG (DMEA initiated)**
(DCTB (trans-2-[3-(4-tert-Butylphenyl)-2-methyl-2-propenylidene]malononitrile) matrix with Na-salt):

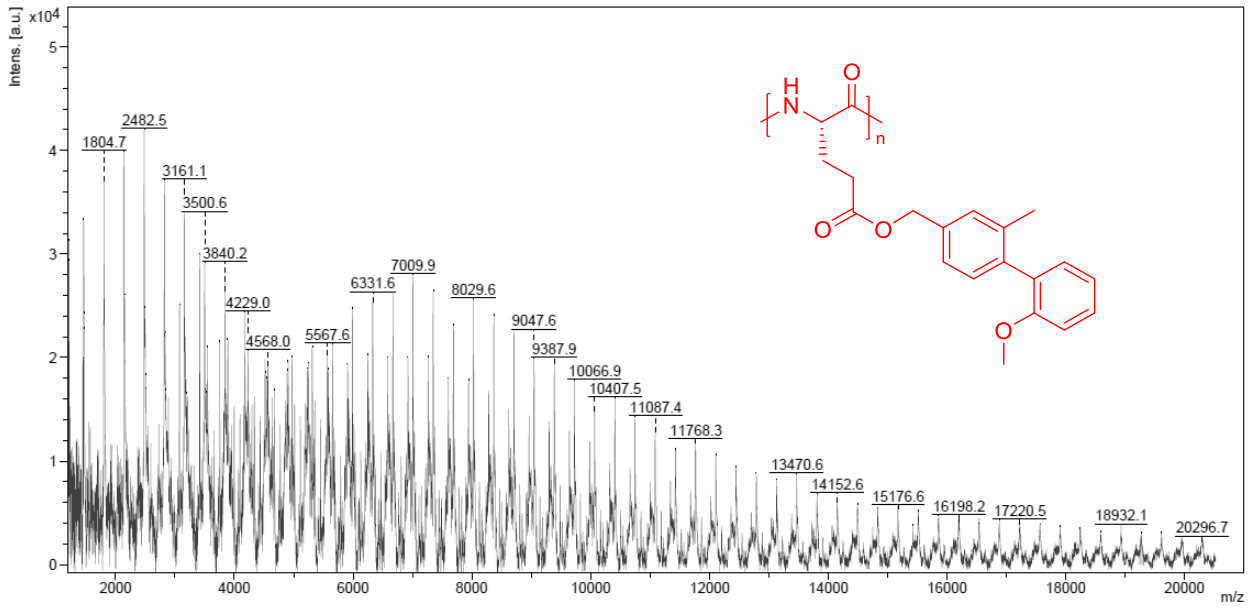


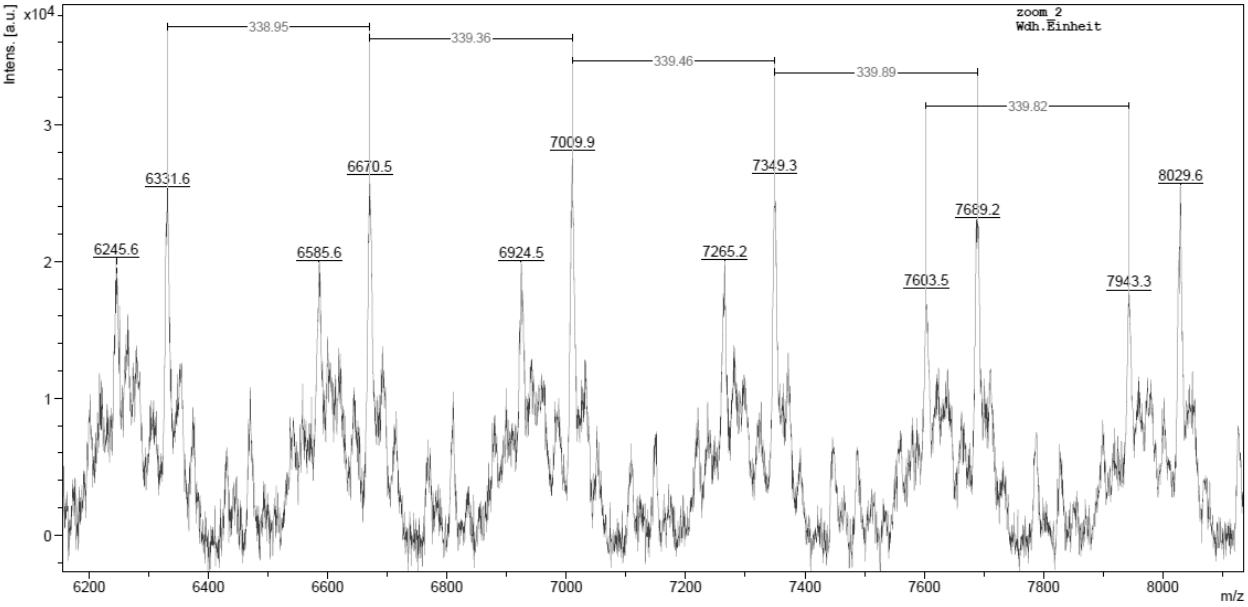


The mean molecular weight of the polymer could not be obtained, because the PDI was too high. Nonetheless, the fragmentation of the repeating unit is clearly visible and is as expected.

**SEC data of PBPM$^3$LG (DMEA initiated)**

$\bar{M}_n$ 8.40 $10^4$ g/mol

$\bar{M}_w$ 1.93 $10^5$ g/mol

$Đ_M$ 2.3

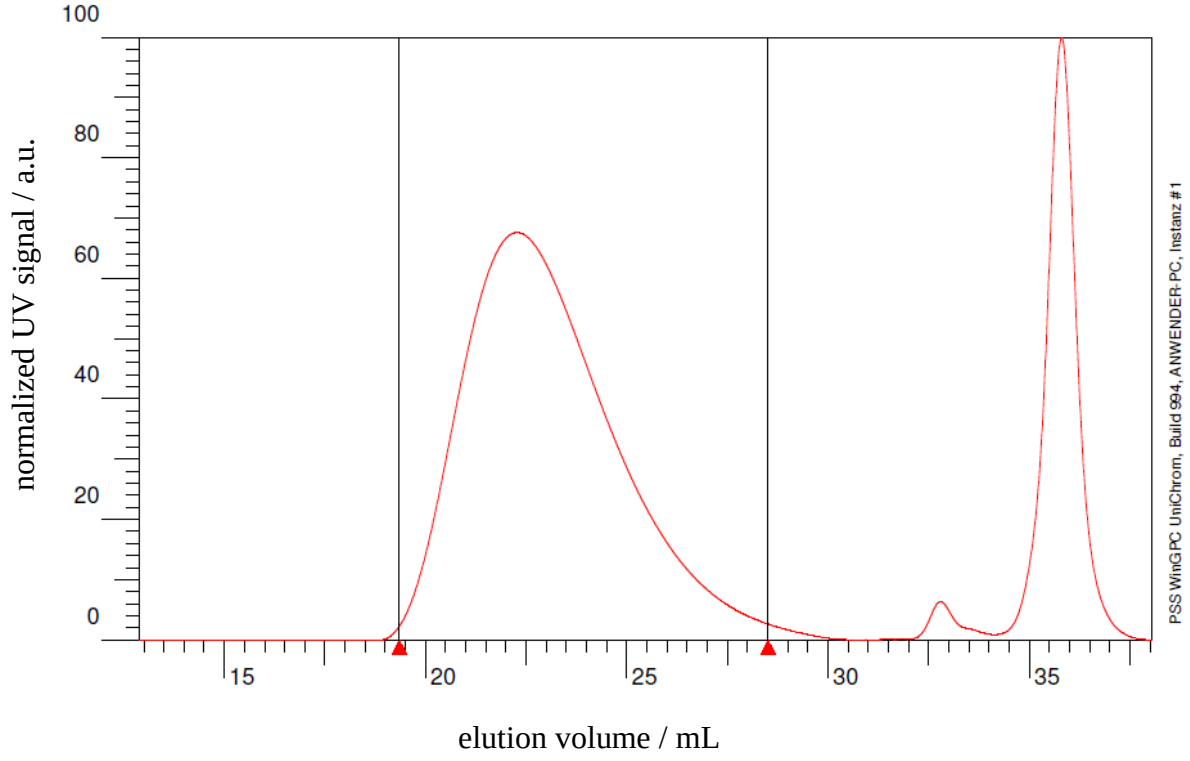


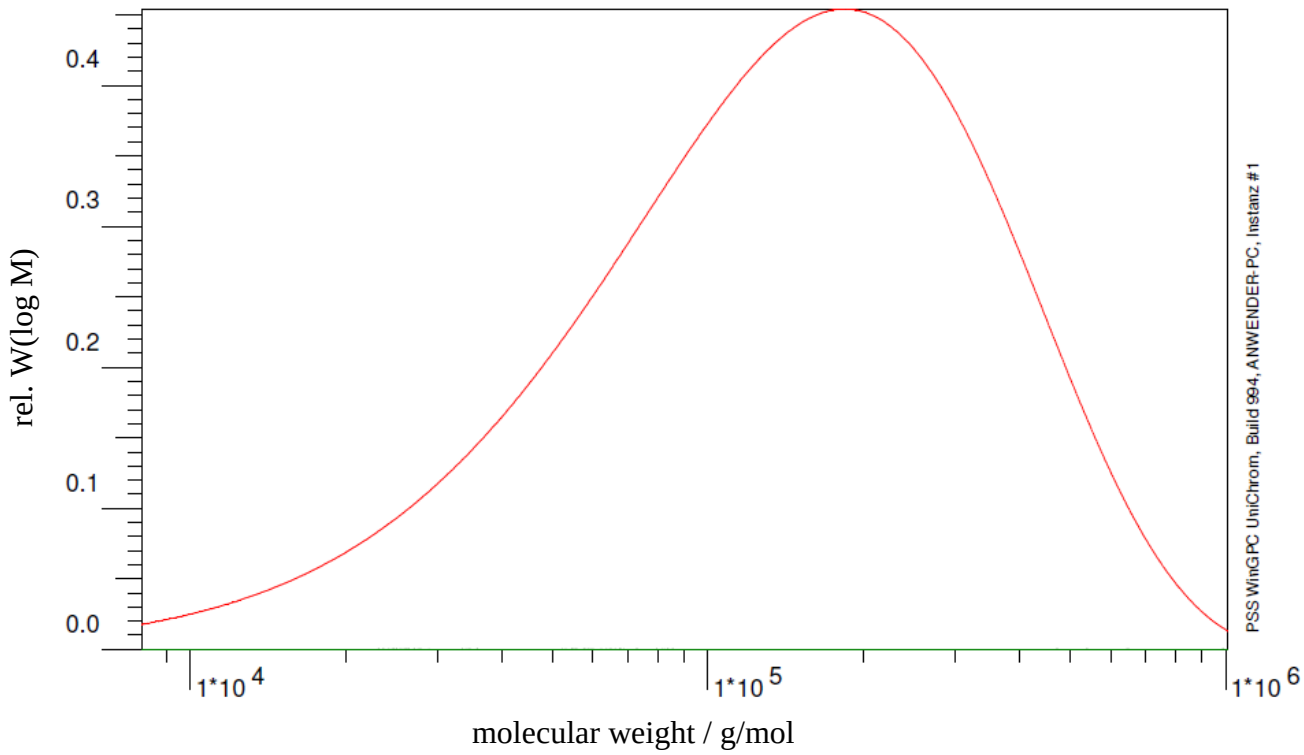

**MALDI-spectrum of PBPM$^3$LG (TEA initiated)**
(DCTB (trans-2-[3-(4-tert-Butylphenyl)-2-methyl-2-propenylidene]malononitrile) matrix with Na-salt):

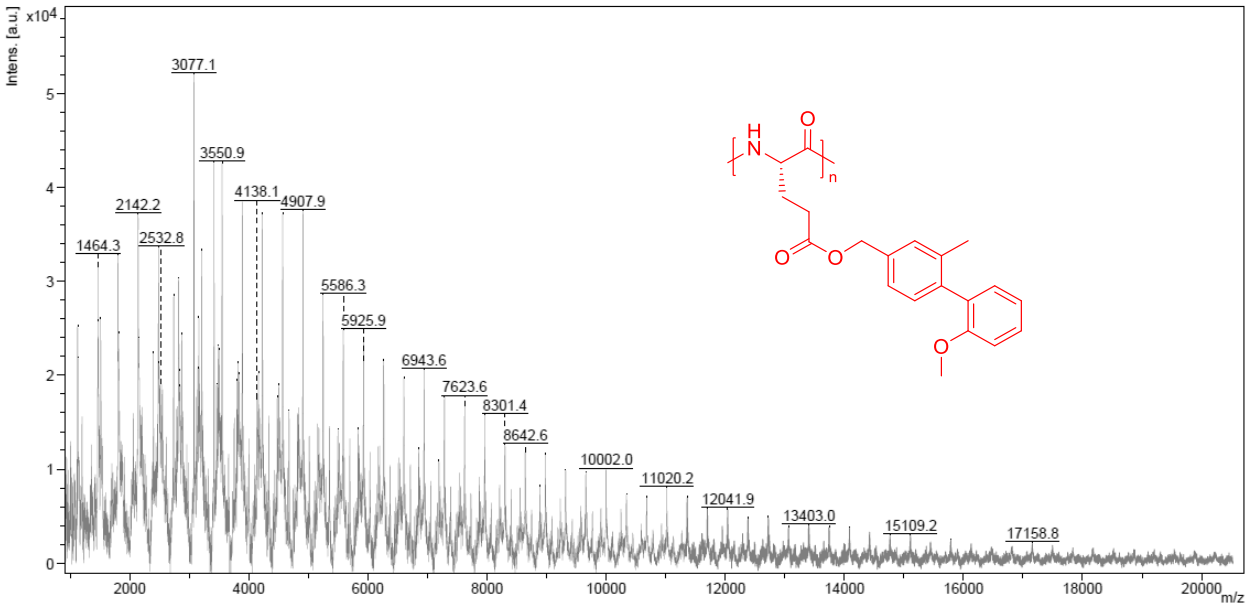


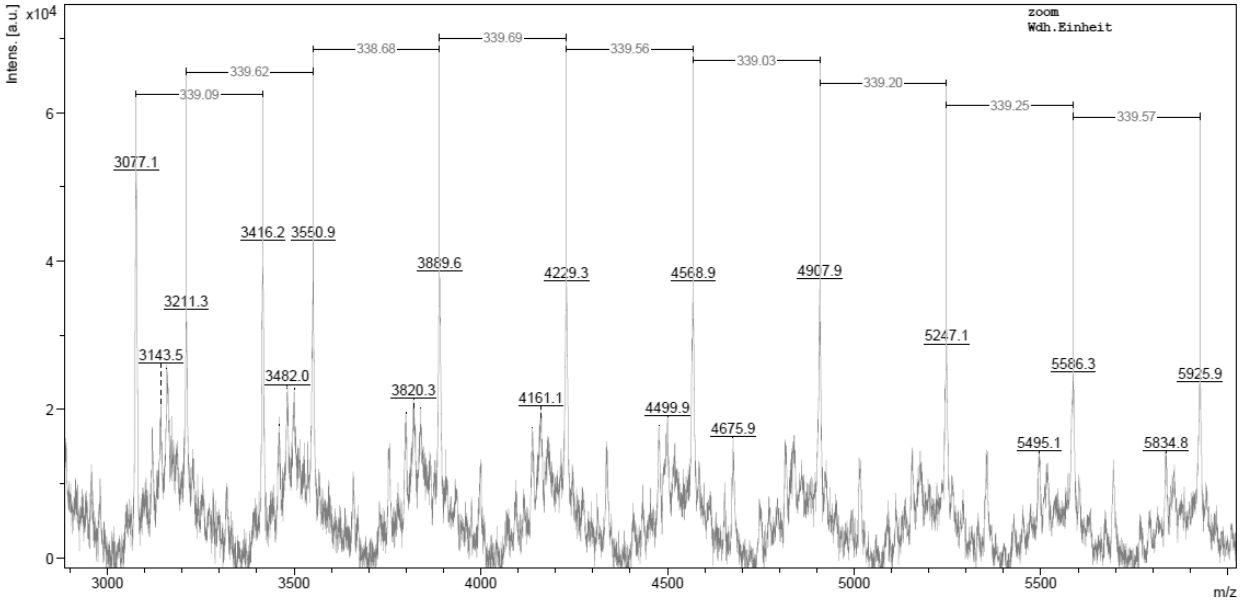


The mean molecular weight of the polymer could not be obtained, because the PDI was too high. Nonetheless, the fragmentation of the repeating unit is clearly visible and is as expected.

**SEC data of PBPM$^3$LG (TEA initiated)**

$\bar{M}_n$ 2.52 $10^4$ g/mol

$\bar{M}_w$ 1.07 $10^5$ g/mol

$Đ_M$ 4.3

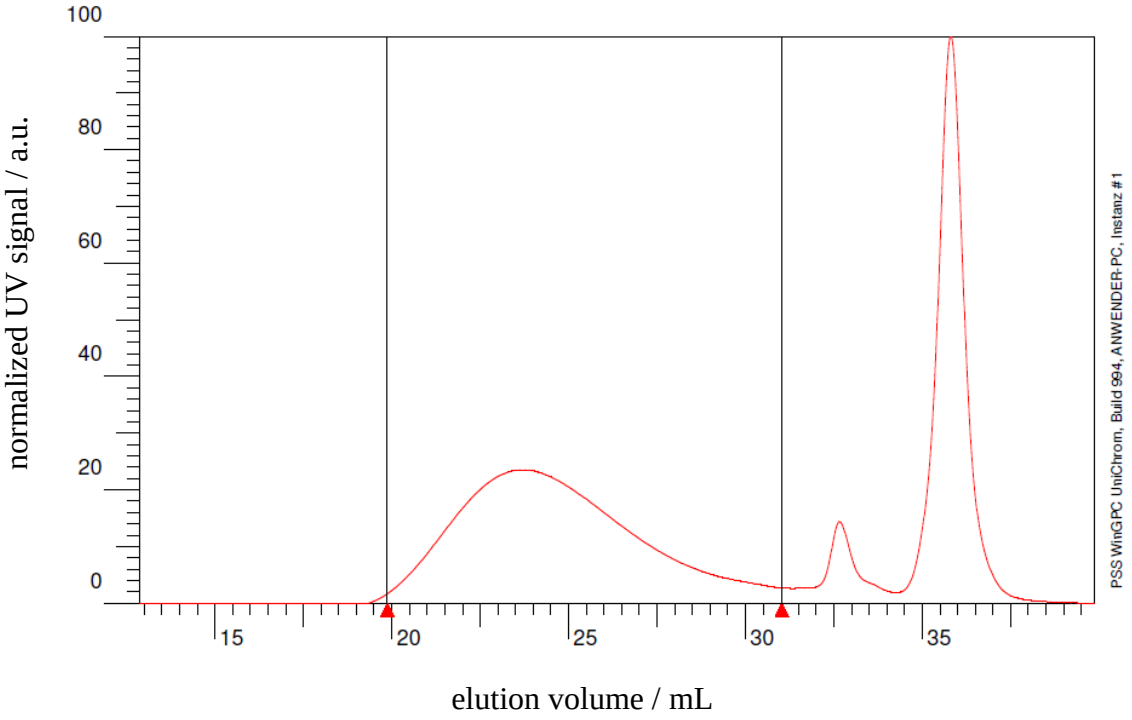


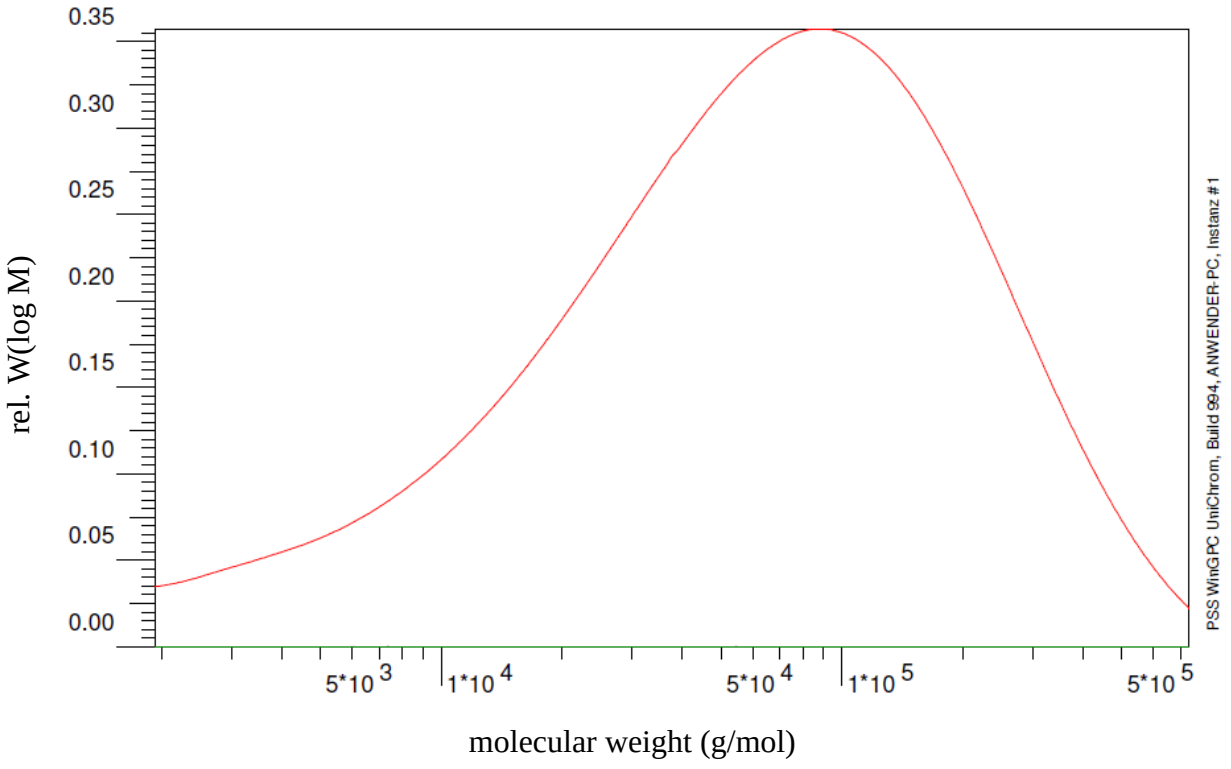

## Author Contributions

D.S.S. Conceptualization: Lead; Synthesis: Lead, Data acquisition (NMR): Lead, Data acquisition (POM): Lead, Data curation: Lead; Formal analysis: Lead; Data interpretation: Lead; Original Draft: Lead; Review & Editing: Lead
P.G: Synthesis: Supporting
M.L. Data acquisition (POM): Supporting, Data interpretation (POM): Supporting
C.M.T. Project administration: Lead; Conceptualization: Lead; Data interpretation: Supporting; Review & Editing: Supporting

## References


[1] L. Castañar, E. Sistaré, A. Virgili, R. T. Williamson, T. Parella, *Magn. Reson. Chem.* **2015**, *53*, 115-119.
[2] L. Verdier, P. Sakhaii, M. Zweckstetter, C. Griesinger, *J. Magn. Reson.* **2003**, *163*, 353-359.
[3] G. Kummerlöwe, S. Schmitt, B. Luy, *The Open Spectroscopy Journal* **2010**, *4*.
[4] a) R. Berger, C. Fischer, M. Klessinger, *J. Phys. Chem. A* **1998**, *102*, 7157-7167; b) V. Schmidts, PhD thesis: Technische Universität (Darmstadt), **2013**.
[5] a) J.-C. Hus, R. Brüschweiler, *J. Biomol. NMR* **2002**, *24*, 123-132; b) J.-C. Hus, W. Peti, C. Griesinger, R. Brüschweiler, *J. Am. Chem. Soc.* **2003**, *125*, 5596-5597.
[6] S. Jeziorowski, C. M. Thiele, *Chem. Eur. J.* **2018**, *24*, 15631-15637.
[7] D. S. Schirra, M. Hirschmann, I. A. Radulov, M. Lehmann, C. M. Thiele, *Angew. Chem. Int. Ed.* **2021**, *60*, 21040-21046.
[8] D. S. Schirra, S. Jeziorowski, M. Lehmann, C. M. Thiele, under consideration at *Macromolecules*.
[9] A. Marx, C. Thiele, *Chem. Eur. J.* **2009**, *15*, 254-260.
[10] a) B. M. Fung, T. H. Martin, *J. Chem. Phys.* **1974**, *61*, 1698-1702; b) M. Hirschmann, M. Schwab, C. M. Thiele, *Macromolecules* **2019**, *52*, 6025-6034.
[11] P. Tzvetkova, B. Luy, *Magn. Reson. Chem.* **2016**, *54*, 351-357.
[12] R. Duke, D. DuPré, E. Samulski, *J. Chem. Phys.* **1977**, *66*, 2748-2749.
[13] a) J. W C Johnson, *Annu. Rev. Biophys. Biophys. Chem.* **1988**, *17*, 145-166; b) S. M. Kelly, T. J. Jess, N. C. Price, *Biochim. Biophys. Acta* **2005**, *1751*, 119-139; c) N. J. Greenfield, *Nat. Protoc.* **2006**, *1*, 2876-2890.
[14] J. Xiang, Y. Li, Q. Li, D. A. Paterson, J. M. D. Storey, C. T. Imrie, O. D. Lavrentovich, *Adv. Mater.* **2015**, *27*, 3014-3018.
[15] a) J. Sass, F. Cordier, A. Hoffmann, M. Rogowski, A. Cousin, J. G. Omichinski, H. Löwen, S. Grzesiek, *J. Am. Chem. Soc.* **1999**, *121*, 2047-2055; b) F. Kramer, M. V. Deshmukh, H. Kessler, S. J. Glaser, *Concepts Magn. Reson. A* **2004**, *21A*, 10-21.
[16] M. J. Rashkin, R. M. Hughes, N. T. Calloway, M. L. Waters, *J. Am. Chem. Soc.* **2004**, *126*, 13320-13325.
[17] A. Del Zotto, F. Amoroso, W. Baratta, P. Rigo, *Eur. J. Org. Chem.* **2009**, *2009*, 110-116.
[18] S. M. M. Knapp, S. E. Shaner, D. Kim, D. Y. Shopov, J. A. Tendler, D. M. Pudalov, A. R. Chianese, *Organometallics* **2014**, *33*, 473-484.
[19] a) H. Yamamoto, Y. Kondo, T. Hayakawa, *Biopolymers* **2004**, *9*, 41-52; b) T. W. Baughman, J. C. Sworen, K. B. Wagener, *Tetrahedron* **2004**, *60*, 10943-10948.
[20] a) W. Heeswijk, M. Eenink, J. Feijen, *Synthesis* **1982**, *1982*, 744-747; b) W. Liu, M. Zhu, J. Xiao, Y. Ling, H. Tang, *J. Polym. Sci., Part A: Polym. Chem.* **2016**, *54*, 3425-3435.
[21] J. Feijen, W. L. Sederel, K. de Groot, A. C. de Visser, A. Bantjes, *Makromol. Chem.* **1974**, *175*, 3193-3206.
[22] a) W. Zhao, Y. Gnanou, N. Hadjichristidis, *Polym. Chem.* **2015**, *6*, 6193-6201; b) A. Rasines Mazo, S. Allison-Logan, F. Karimi, N. J.-A. Chan, W. Qiu, W. Duan, N. M. O'Brien-Simpson, G. G. Qiao, *Chem. Soc. Rev.* **2020**, *49*, 4737-4834.
[23] a) W. D. Fuller, M. S. Verlander, M. Goodman, *Biopolymers* **1976**, *15*, 1869-1871; b) N. Hadjichristidis, H. Iatrou, M. Pitsikalis, G. Sakellariou, *Chem. Rev.* **2009**, *109*, 5528-5578.
[24] J. R. Kramer, T. J. Deming, *Biomacromolecules* **2010**, *11*, 3668-3672.
[25] a) K. Harada, *Bull. Chem. Soc. Jpn.* **1965**, *38*, 1552-1555; b) G. V. Kalechits, N. G. Kozlov, *Chem. Nat. Compd.* **2008**, *44*, 446-449.